Journal of Medicinal Chemistry

Article

Structure-based design and pre-clinical characterization of selective and orally bioavailable Factor XIa inhibitors: Demonstrating the power of an integrated S1 protease family approach.

Edwige Lorthiois, James Roache, David Barnes-Seeman, Eva Altmann, Ulrich Hassiepen, Gordon Turner, Rohit Duvadie, Viktor Hornak, Rajeshri G. Karki, Nikolaus Schiering, Wilhelm A. Weihofen, Francesca Perruccio, Amy Calhoun, Tanzina Fazal, Darija Dedic, Corinne Durand, Solene Dussauge, Kamal Fettis, Fabien Tritsch, Celine Dentel, Adelaide Druet, Donglei Liu, Louise Kirman, Julie Lachal, Kenji Namoto, Douglas Bevan, Rose Mo, Gabriela Monnet, Lionel Muller, Richard Zessis, Xueming Huang, Loren Lindsley, Treeve Currie, Yu-Hsin Chiu, Cary Fridrich, Peter Delgado, Shuangxi Wang, Micah Hollis-Symynkywicz, Joerg Berghausen, Eric Williams, Hong Liu, Guiqing Liang, Hyungchul Kim, Peter Hoffmann, Andreas Hein, Paul Ramage, Allan D'Arcy, Stefanie Harlfinger, Martin Renatus, Simon Ruedisser, David Feldman, Jason Elliott, Richard C Sedrani, Jürgen Maibaum, and Christopher M. Adams

J. Med. Chem., **Just Accepted Manuscript** • DOI: 10.1021/acs.jmedchem.0c00279 • Publication Date (Web): 17 Jun 2020

Just Accepted

is published by the American Chemical Society. 1155 Sixteenth Street N.W., Washington, DC 20036

	RESEARCH EUROPE Namoto, Kenji; Novartis Institutes for BioMedical Research Basel, RESEARCH EUROPE Bevan, Douglas; Novartis Pharmaceuticals Corp Mo, Rose; Novartis Institutes for BioMedical Research Inc, Global Discovery Chemistry Monnet, Gabriela; Novartis Institutes for BioMedical Research Basel, RESEARCH EUROPE Muller, Lionel; Novartis Institutes for BioMedical Research Basel, RESEARCH EUROPE Zessis, Richard; Novartis Institutes for BioMedical Research Inc Huang, Xueming; Novartis Institutes for BioMedical Research Inc Lindsley, Loren; Novartis Institutes for BioMedical Research Inc Currie, Treeve; Novartis Institutes for BioMedical Research Inc Chiu, Yu-Hsin; Novartis Institutes for BioMedical Research Inc Fridrich, Cary; Relay Therapeutics Inc Delgado, Peter; Novartis Institutes for BioMedical Research Inc, Global Discovery Chemistry Wang, Shuangxi; Novartis Institutes for BioMedical Research Inc Hollis-Symynkywicz, Micah; Novartis Institutes for BioMedical Research Inc Berghausen, Joerg; Novartis Pharma AG, Williams, Eric; Molecular Templates Inc Liu, Hong; Novartis Institutes for BioMedical Research Inc Liang, Guiqing; Novartis Inst BioMed Res, Metabolism and Pharmacokinetics Kim, Hyungchul; Novartis Institutes for BioMedical Research Inc Hoffmann, Peter; Novartis Institutes for BioMedical Research Inc Hein, Andreas; Novartis Institutes for BioMedical Research Basel, Expertise Protease Platform Ramage, Paul; Novartis Institutes for BioMedical Research Basel D'Arcy, Allan ; Novartis Institutes for BioMedical Research Basel, RESEARCH EUROPE Harlfinger, Stefanie; AstraZeneca PLC, Oncology R&D, DMPK Renatus, Martin ; Novartis Institutes for BioMedical Research, RESEARCH EUROPE Ruedisser, Simon; ETH Zürich, BioNMR platform D- BIOL Feldman, David ; National Kidney Foundation Elliott, Jason; Novartis Institutes for BioMedical Research Inc Sedrani, Richard; Novartis Pharma AG, Novartis Inst. for BioMedical Research Maibaum, Jürgen; Novartis Pharma AG, Novartis Institutes of Biomedical Research Adams, Christopher; Novartis Institutes for BioMedical Research Inc, Global Discovery Chemistry

Structure-based design and pre-clinical characterization of selective and orally bioavailable Factor XIa inhibitors: Demonstrating the power of an integrated S1 protease family approach.

Edwige Lorthiois[‡], James Roache[†]*, David Barnes-Seeman[†], Eva Altmann[‡], Ulrich Hassiepen[‡], Gordon Turner[†], Rohit Duvadie[†], Viktor Hornak[†], Rajeshri G. Karki[†], Nikolaus Schiering[‡], Wilhelm A. Weihofen[†], Francesca Perruccio[‡], Amy Calhoun[†], Tanzina Fazal[†], Darija Dedic[‡], Corinne Durand[‡], Solene Dussauge[‡], Kamal Fettis[‡,¶], Fabien Tritsch[‡], Celine Dentel[‡], Adelaide Druet[‡], Donglei Liu[†], Louise Kirman[†,ʃ], Julie Lachal[‡], Kenji Namoto[‡], Douglas Bevan[†], Rose Mo[†], Gabriela Monnet[‡], Lionel Muller[‡], Richard Zessis[†], Xueming Huang[†], Loren Lindsley[†], Treeve Currie[†], Yu-Hsin Chiu[†], Cary Fridrich[†,t], Peter Delgado[†], Shuangxi Wang[†], Micah Hollis-Symynkywicz[†], Joerg Berghausen[‡], Eric Williams[†,l], Hong Liu[†], Guiqing Liang[†], Hyungchul Kim[†], Peter Hoffmann[†], Andreas Hein[‡], Paul Ramage[‡], Allan D'Arcy[‡], Stefanie Harlfinger[‡,$], Martin Renatus[‡], Simon Ruedisser[‡,%], David Feldman[&,!], Jason Elliott[†], Richard Sedrani[‡], Juergen Maibaum[‡], and Christopher M. Adams[†]*

[†]Novartis Institutes for BioMedical Research, Cambridge, Massachusetts 02139, USA

‡Novartis Institutes for BioMedical Research, Novartis Campus, CH-4056 Basel, Switzerland.

&Novartis Institutes for BioMedical Research, East Hanover, NJ 07396, USA.

KEYWORDS. *Coagulation, intrinsic pathway, factor XIa inhibitors, aPTT, PT, S1 protease, serine protease, structure-based drug design, Factor XI*.

ABSTRACT:

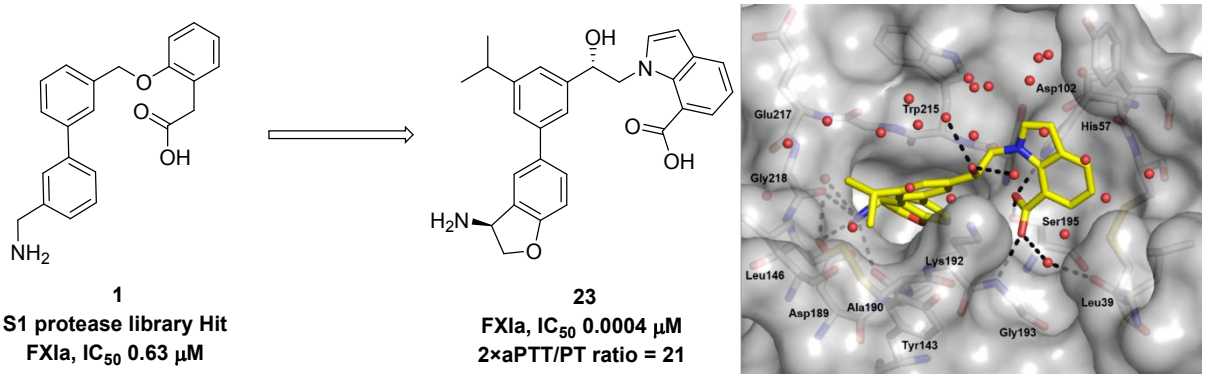

1
S1 protease library Hit
FXIa, IC_{50} 0.63 μM

23
FXIa, IC_{50} 0.0004 μM
2×aPTT/PT ratio = 21

The serine protease Factor XI (FXI) is a prominent drug target as it holds promise to deliver efficacious anti-coagulation without an enhanced risk of major bleeds. Several efforts have been described targeting the active form of the enzyme, FXIa. Herein we disclose our efforts to identify potent, selective, and orally bioavailable inhibitors of FXIa. Compound **1,** identified from a diverse library of internal serine protease inhibitors, was originally designed as a complement Factor D inhibitor and exhibited sub-micromolar

FXIa activity and an encouraging ADME profile while being devoid of peptidomimetic architecture. Optimization of interactions in the S1, S1β, and S1` pockets of FXIa through a combination of structure-based drug design and traditional medicinal chemistry led to the discovery of compound **23** with sub-nanomolar potency on FXIa, enhanced selectivity over other coagulation proteases, and a pre-clinical PK profile consistent with *bid* dosing in patients.

INTRODUCTION

The discovery of the anti-coagulant properties of dicoumarol in 1940, and subsequent development of warfarin, transformed the practice of medicine[1] offering patients at risk of thrombosis a prophylactic therapeutic option.[2] However, warfarin's clinical success is tempered by a narrow therapeutic index due to its mechanism of action (vitamin K antagonism), which poses a risk of major life threatening bleeding.[3] This is further compounded by drug-drug interactions and dietary interactions which require dose titration and frequent laboratory monitoring.[4] The advent of non-vitamin K anti-coagulants (NOACs) have offered patients an alternative to warfarin. Molecules selectively inhibiting the proteases Factor Xa (FXa) (e.g. rivaroxaban[5] and apixaban[6]) or thrombin (Factor II,

FII) (e.g. dabigatran[7]), which play a pivotal role in coagulation homeostasis, have gained clinical acceptance over the last decade, in part due to simpler dosing paradigms and a lower risk of bleeding.[8,9] However, NOACs are still associated with substantial risk of major bleeding events limiting their widespread use.[10,11]

More recently, the serine protease Factor XI (FXI) has come to prominence as a drug target offering the potential of providing efficacious anti-coagulation without an enhanced risk of major bleeds.[12] The activated form, FXIa, has a critical function in the amplification of thrombin generation in a low tissue-factor environment by directly activating FIX without intrinsic cascade activation.[13] This hypothesis is supported by human data, as individuals deficient in FXI activity have reduced risk of thromboembolic events without an increase in major bleeding events.[14] Furthermore, a recent clinical trial with an antisense oligonucleotide targeting FXI proved efficacious in preventing venous thrombosis in patients undergoing total knee arthroplasty.[15] Importantly, in this trial there was also a trend toward a reduction in bleeding events *versus* enoxaparin, a heparin mimetic. In light of this strong clinical rationale, several efforts have been disclosed targeting FXIa with low molecular weight compounds and biologics.[16,17,18,19] These efforts

have afforded several linear and macrocyclic scaffolds targeting the enzyme catalytic site and most recently culminated in the discovery of first clinical candidates.[20,21,22,23]

Herein we disclose our efforts to identify potent and selective inhibitors of FXIa by leveraging the power of a platform drug discovery approach to target serine proteases.[24] At the outset of this program, we decided to focus exclusively on demonstrating *in vitro* efficacy and selectivity in combination with high *in vivo* oral bioavailability for candidate FXIa inhibitors. These criteria included: 1) sufficient potency and pharmacokinetic properties to maintain >85% inhibition of FXIa, in line with genetic evidence that correlates ≥85% FXI deficiency to thromboprotection;[14] and 2) having sufficient selectivity over other proteases of the coagulation cascade to mitigate the potential risk of bleeding.[25] With regard to assessing FXI inhibition and selectivity, we chose to employ a combination of high throughput enzymatic assays and clinically translatable human plasma coagulation assays. The activated partial thromboplastin time (aPTT) and prothrombin time (PT) assays provided the primary means of assessing the functional potency/efficacy and functional selectivity, respectively, of our FXIa inhibitors.[26] These assays measure the

time it takes for plasma to coagulate when the intrinsic (aPTT assay) or extrinsic (PT assay) pathway is stimulated by an exogenous trigger (**Figure 1**). We relied exclusively on the *in vitro* assesments of efficacy since the translatability of FXIa inhibition from preclinical models to the clinic has not been established. Herein we show the results of our lead optimization efforts leading to a selective and orally bioavailable FXIa inhibitor that prolonged aPTT without a perturbation in the PT assay.

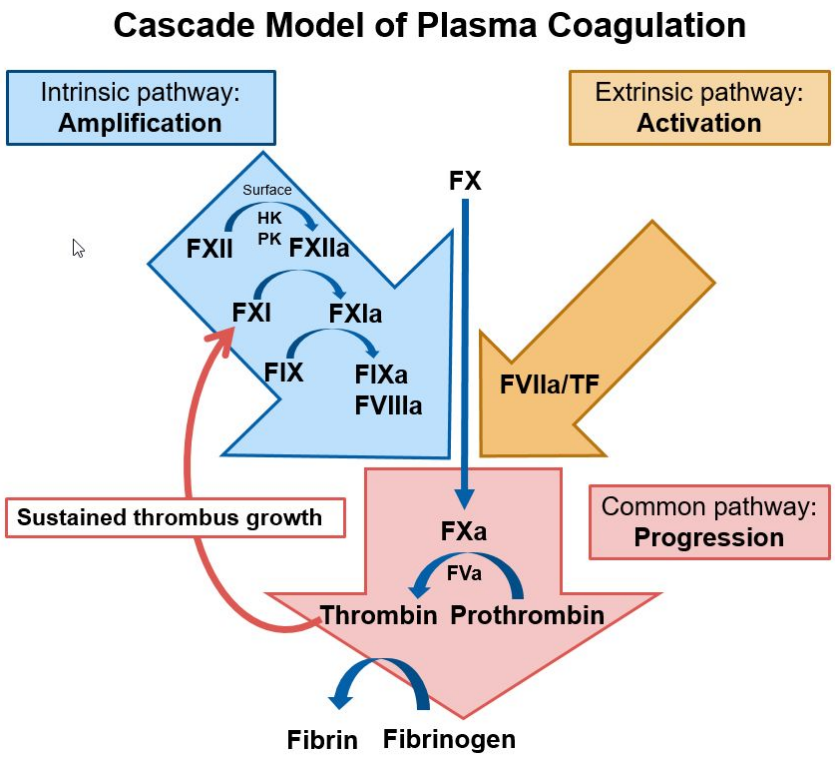

Figure 1: Schematic representation of the coagulation cascade. The aPTT assay assesses inhibition of the intrinsic (blue) and progression (red) components of the

pathway, while the PT assay assesses the extrinsic (orange) and progression components.

RESULTS AND DISCUSSION

Endeavoring for an accelerated hit finding campaign to identify promising starting points with a high potential for oral bioavailability, we took advantage of a combination of high throughput screening (HTS), virtual screening, and NMR-mediated fragment based screening (FBS) approaches. We also embarked on a more focused screen of a knowledge-based diversity library (~1750 compounds) of internal serine protease inhibitors and analogs thereof. This compound collection had been built as part of a protease drug discovery platform at Novartis.[24] While the HTS and FBS efforts delivered several hits that were initially taken forward for SAR exploration, we eventually became most intrigued by the activity of compound **1**[27] (**Figure 2**), which demonstrated an IC_{50} of 0.63 μM against human FXIa, and was structurally diverse from known FXIa inhibitors. This scaffold had originally been discovered as part of our efforts to identify inhibitors of complement Factor D (FD),[27,28,29] resulting from a dedicated structure-based design approach tackling a unique active-site architecture of an atypical trypsin-like S1 protease.

Compound **1** appeared to be particularly attractive due to its structural simplicity, low molecular weight, and a balanced lipophilicity/polarity ratio ($logD_{6.8}$ = 1.91). These properties translated into encouraging ADME properties and an excellent mouse pharmacokinetic profile.[27] Furthermore, the zwitterionic character of **1** provided a very low-affinity profile toward the hERG ion-channel with IC_{50} values >30 μM in both the dofetilide binding and the functional Q-patch assays. However, the potency of **1** against FD (IC_{50}: 0.008 μM) and the relatively moderate selectivity against other trypsin-like S1 proteases of the coagulation cascade (e.g. plasma kallikrein (PKL), IC_{50}: 3.1 μM; plasmin, IC_{50}: 2.2 μM; FVIIa, IC_{50}: 1.4 μM and urokinase, IC_{50}: 0.77 μM) needed to be addressed in addition to optimizing the potency against FXIa. Hence, the most prominent question raised was whether the design of a potent and highly selective FXIa inhibitor would be feasible at all by starting from a low-nanomolar FD inhibitor scaffold.

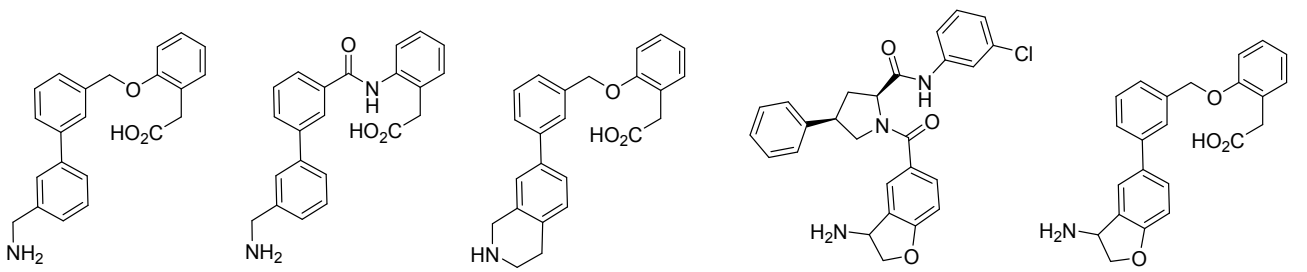

Figure 2. Chemical structures of early-stage S1-benzylamine-based FXIa inhibitors.

With the aim of developing a rational design concept toward improved FXIa selectivity, we resolved the co-crystal structure of a closely related analog, **2** (FXIa IC_{50}: 2.8 μM), bearing a carboxamide spacer instead of the ether linker in compound **1**. The overall binding mode of **2** in FXIa is similar to that observed in FD[27] (**Figure 3**) in that it spans the S1 and S1' pockets in a U-shape conformation. The basic primary amine is within H-bonding distance to the Ala_{190} backbone carbonyl and forms a salt bridge with the side-chain of Asp_{189}. The biphenyl portion of the molecule is sandwiched between the Lys_{192} side-chain and Trp_{215} backbone and the carboxylic acid moiety binds to the oxyanion hole making H-bonding interactions with the side-chain of His_{57} and the backbone NH of Gly_{193}. The H-bonding interactions with Ser_{195} are not visible in the X-ray structure as a FXIa active site mutant ($S_{195}A$ mutant; chymotrypsinogen numbering

has been used throughout this paper) was used to obtain this co-crystal structure. The absence of the OH in the mutant protein does not have an influence on the position of the carboxylic acid based on comparison to related compounds in Ser_{195} FXIa-containing crystals. The phenyl ring fits nicely in the S1' pocket and forms an edge-to-face interaction with His_{57}. Several X-ray structures of FXIa and inhibitor complexes, which were not available at the time of our work, have since been reported with a phenyl ring binding in a similar fashion in the S1' pocket of the FXIa active site.[16]

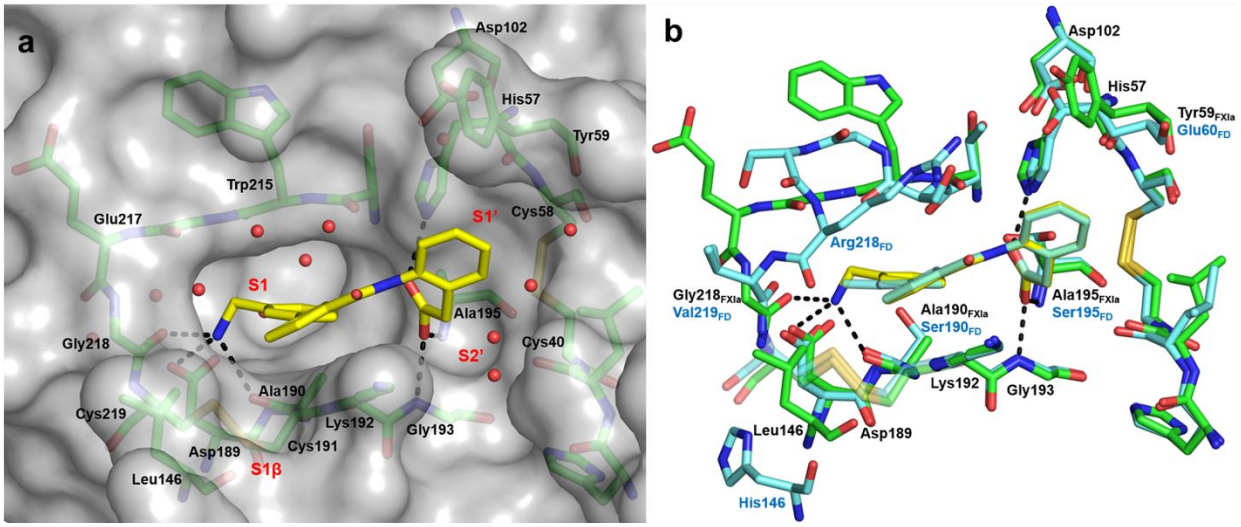

Figure 3. Binding mode of compound **2**: (**a**) Crystal structure of **2** (yellow, PDB code 6TS4) with FXIa $S_{195}A$ mutant (green). The surface of the protein is shown in gray and oxygen atoms of crystallographic water molecules are shown as red spheres. (**b**) Comparison of the crystal structures of compound **2** with FXIa (yellow and green carbons) and FD (pale blue, PDB code 6QMT).[27] Only selected residues in the ligand-binding pocket are shown.

FXIa and FD residues are labeled in black and in blue, respectively. H-bonding interactions are shown as black dotted lines.

Most importantly, the comparison between the FXIa[16] and the FD[30] inhibitor binding sites revealed several opportunities to concomitantly improve FXIa potency and FD selectivity by specifically targeting the deep S1 pocket, the S1β pocket and/or the prime site of FXIa. With regard to the S1 pocket, trypsin-like proteases can be differentiated based on the nature of the amino-acid 190 at the bottom of the S1 pocket, which dictates enzyme specificity. FXIa and thrombin display an alanine in position 190 while FD, urokinase and FVIIa bear the larger, more polar, serine residue at this position. As a consequence, the latter enzymes show substrate-specificity for the less sterically demanding P1 lysine residue, while FXIa prefers arginine.[31] This difference has been successfully exploited to enhance selectivity of various trypsin-like protease inhibitors.[32,33] Besides the S1 pocket, the small hydrophobic S1β pocket located on top of the Cys_{191}-Cys_{219} disulfide bridge was also considered to offer another opportunity for improving FXIa affinity and specificity, since the S1β pocket of FXIa is limited in size due to the side-chain of Leu_{146}. A literature survey of known inhibitors of serine proteases indicated that

binding in this region could contribute to improved ligand binding affinity.[29,34,35] Further extension into the S2' site, for which significant structural differences are observed between FXIa and off-target serine proteases, offers another option to enhance selectivity. In particular, FXIa exhibits a comparatively more open S1'-S2' binding region *versus* FD.[31] However, accessing the S2' pocket would require increasing the size of the molecule significantly, and therefore this strategy was initially deferred.[36]

A final key aspect defining our medicinal chemistry strategy related to the the nature of S1-S1' linker. At the outset of our work, it was argued that the basic amine of **1**, positioned in S1, and the carboxylic acid are engaged in key interactions with Asp_{189} and the canonical oxyanion hole (residues Gly_{193} and Ser_{195}), respectively, and therefore are unlikely to evoke differentiating binding interactions on their own for FXIa versus FD and other proteases.[37] However, the appropriate spacing and alignment of these two motifs might offer an opportunity to enhance potency and selectivity and to modulate ADME properties. Of equal importance was the notion that the zwitterionic motif of this scaffold provided an advantageous *in vitro* and *in vivo* ADME profile, in particular, when retaining the less polar ether linker of compound **1**.[27]

Our initial efforts focused on optimizing the binding interactions to the deep and solvent-shielded S1 specificity pocket, in particular, by growing toward Ala_{190} which was expected to enhance binding to FXIa and at the same time to be less well accommodated by the smaller S1 pocket of Ser_{190} S1 family serine proteases including FD. In order to

probe the impact of the larger FXIa S1 pocket, compound **3** (**Figure 2**) was prepared, in which the benzylamine motif was replaced by the rigid bicyclic tetrahydroisoquinoline, thereby mimicking the FXIa-bound conformation of the flexible aminomethyl group in **2**. Compound **3** displayed similar potency against FXIa as compound **1**, and the inhibitory activity toward FD was reduced by 100-fold (**Figure 2**). To confirm our design rationale, the X-ray crystal structure of **3** bound to FXIa with the native catalytic triad, was resolved (**Figure 4**). The binding mode spanning S1, S1' and the oxyanion hole is very similar as observed for FXIa-bound **2** (**Figure 3**). The basic NH motif makes H-bonding interactions with the Ala_{190} backbone carbonyl and the side-chain of Asp_{189} similar to that observed in the **2**-FXIa complex.

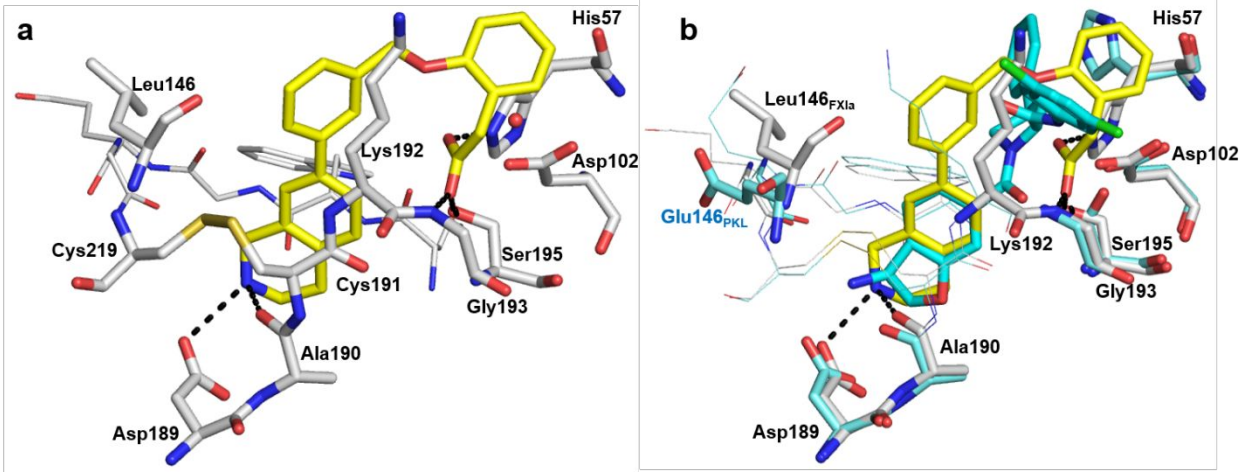

Figure 4. (**a**) Crystal structure of compound **3** (yellow) complexed with FXIa (white, PDB code 6TS7) (**b**) Overlay of the crystal structure of compound **3** (yellow) complexed with FXIa (white) on compound **4** (cyan) complexed with PKL (pale blue, PDB code 6T7P). Only selected residues in the ligand-binding pocket are shown. H-bonding interactions are shown as black dotted lines.

Encouraged by this result, we undertook a broad search of P1 moieties by close inspection of published and in-house co-crystal structures of S1-binding fragments and S1 protease inhibitors. Overlaying the FXIa-**2** and -**3** crystal structures with compound **4**, derived from our knowledge-based diversity library, bound to PKL,[38] a related trypsin-like Ala_{190} S1 protease, proved particularly fruitful. The aminodihydrobenzofuran of **4** (**Figure 2**) overlapped with the S1 binding phenyl and basic amine motifs from both inhibitors (**Figure 4b**). Compound **4** had been co-crystallized with PKL as a mixture of (*R*)- and (*S*)-2,3-dihydrobenzofuranyl-3-amine diastereoisomers. The electron density of the bound ligand was consistent with the absolute (*S*)-configuration of the 3-aminodihydrobenzofuran.[39] Racemic **5** (**Figure 2**), which combines the two key pharmacophores of **4** and **3**, was prepared and showed similar inhibitory affinity for both FXIa and FD as compared to **3**. Compound **5** was also found to be a weak inhibitor of PKL, albeit with a 5-fold lower IC_{50} value of 1.3 μM *versus* FXIa (IC_{50} of 0.2 μM). During

our continued optimization efforts, we preferred both the tetrahydroisoquinoline and the 3-aminodihydrobenzofuran S1 binding motifs as more tractable replacements of the benzylamine moiety of the screening hit **1,** as these scaffolds offered the benefit of a lower risk for semicarbazide-sensitive amine oxidase (SSAO) mediated metabolism[40] and potential toxicity.[41]

Next we focused our attention on targeting the S1β pocket in FXIa. SAR exploration of a representative selection of compound **1** analogs from the FD inhibitor program[27,42] in the FXIa biochemical assay indicated a preference for small and branched aliphatic substituents. This finding was in line with the limited size of the FXIa S1β pocket due to the conformational fold of the Leu_{146} side-chain. Intriguingly, incorporation of an isopropyl substituent into the *meta*-position of the middle phenyl ring at the edge of the S1β site resulted in a significant 65-fold potency increase for compound **6** bearing the P1 (*S*)-2,3-dihydrobenzofuranyl-3-amine moiety as single stereoisomer.[43] Inhibitor **6** displayed single-digit nanomolar potency toward FXIa with an IC_{50} value of 0.003 μM in the biochemical assay (**Table 1**), however a 40-fold drop in potency was observed for **6**

when measured in the presence of 50% human plasma (cd-FXIa IC_{50}: 0.12 μM; **Table 1**).[44] The potency of **6** against FD was also increased, leading to a 10-fold selectivity for FXIa over FD. There was no improvement in PKL selectivity due to the high homology between FXIa and PKL. In previous reports,[17] achieving selectivity toward PKL has proven to be difficult and, to our knowledge, only the large FXIa inhibitor BMS-962212 lacking oral bioavailability has demonstrated a significant selectivity against PKL (~400-fold).[20] Among S1 proteases PKL is an exceptionally close homolog of FXI, indicating a recent divergence from a common ancestor.[45] Selectivity over PKL was not considered a necessary attribute as human congenital deficiency in prekallikrein (PK), the inactive precursor of PKL, or PK-deficient mice do not encounter an increase in clinically relevant bleeding.[46]

Table 1. *In vitro* FXIa potency (IC_{50}), selectivity data *versus* FD and PKL and *in vitro* profiles.

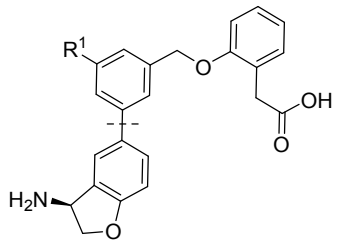

6 (R^1= $CH(CH_3)_2$)
7 (R^1= $C(CH_3)_2CN$)
8 (R^1= $C(CH_3)_2OH$)
9 (R^1= $C(CH_3)_2CONH_2$)

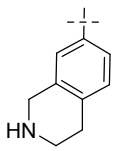

10 (R^1= $C(CH_3)_2OH$)

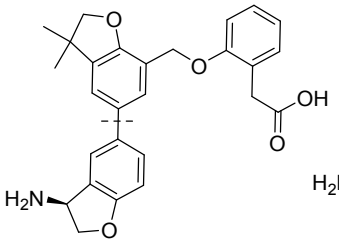

11

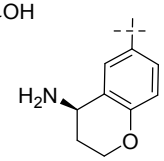

12

Compounds	FXIa IC_{50} [µM][a]	cdFXIa plasma IC_{50} [µM][b]	FD IC_{50} [µM][c]	PKL IC_{50} [µM][d]	Caco-2 P_{app}(AB)/(BA) x10^{-6} (cm/s) (ratio (BA)/(AB))	HT-eq solubility pH 6.8 (mM)[e]
6	0.003	0.12	0.04	0.003	7/ 17 (2.3)	0.008
7	0.004	0.05	0.04	0.002	1.4/ 41 (30)	0.06
8	0.004	0.17	0.32	0.006	BLQ[f]/ 19 (-)	>1
9	0.009	0.067	0.32	0.011	BLQ[f]/ 4 (-)	0.78
10	0.10	0.43	0.23	0.33	ND[g]	ND[g]
11	0.003	0.085	0.05	0.007	12/ 12 (1)	<0.004
12	0.006	0.26	15	0.004	ND[g]	ND[g]

Half-maximal inhibition of [a]purified human FXIa and [b] recombinant catalytic domain of human FXIa as determined in a fluorogenic rhodamine-110 based peptide cleavage assay. [c]Half-maximal inhibition of recombinant human complement FD as determined in a TR-FRET assay. [d]Half-maximal inhibition of PKL as determined in a fluorogenic rhodamine-110-based peptide cleavage assay. Data represent geometric mean values of multiple measurements (n≥2). [e]Equilibrium high throughput solubility in aqueous buffer (pH 6.8). [f]BLQ = below limit of quantitation. [g]ND = not determined.

The improvement in biochemical potency and selectivity against FD demonstrated by **6** warranted assessment in the aPTT and PT coagulation assays. In our hands, a two-fold increase in aPTT coagulation time correlated with ~95% inhibition of FXIa activity in plasma, surpassing our threshold of 85%.[47] Hence, we evaluated **6** and subsequent analogs on the concentration necessary to effect a doubling of coagulation time assessed by aPTT (2×aPTT). For comparison, we also evaluated the inhibitor concentration required to double prothrombin time (2×PT) as a measure of selectivity.[48] We aimed for compounds that could achieve 2×aPTT at total plasma concentrations ≤1.5 μM. These criteria were based on the assumption that identifying a compound with a pharmacokinetic profile enabling C_{trough} concentrations of >1.5 μM would be exceedingly difficult. For the PT selectivity assessment, we aimed for a ≥20-fold difference between aPTT and PT doubling concentrations with the assumption that such a margin should enable functional selectivity at both peak and trough plasma concentrations when paired with a suitable PK profile. Inhibitor **6** afforded a 2×aPTT value of 2.2 μM and a 2×PT value of 9.9 μM resulting in a 2×aPTT/PT ratio of only about 4-fold. Notably, the significant PT activity of this compound suggested that off-target activity against other coagulation

cascade proteases was likely influencing the aPTT assessment as well resulting in an overestimation of FXIa-driven potency in the latter assay (*vide infra*; **Table 3**).

Despite the suboptimal functional selectivity observed with **6**, we wanted to investigate how these structural changes relative to compound **1**[27] impacted ADME and PK properties (**Table 2**). Gratifyingly, the favorable ADME properties of compound **1** were retained and translated to low clearance and excellent oral bioavailability in mice.

Table 2. *In vivo* mouse pharmacokinetic profiles for compounds **1**,[27] **6**, **7**, **8** and **11**.

Compounds	1[a]	6[a]	7[a]	8[a]	11[a]
CL ($mL \cdot min^{-1} \cdot kg^{-1}$)	14[b]	1 ± 0	55 ± 4	19 ± 2	4 ± 1
V_{SS} (L/kg)	0.7[b]	0.4 ± 0.1	0.7 ± 0.1	0.4 ± 0.1	1 ± 0.1
$t_{1/2term}$ (h)	1.6[b]	5.5 ± 0.2	0.3 ± 0.0	1.7 ± 0.2	6.4 ± 3.4
AUC p.o. d.n. (nM·h)	3284 ± 138	48927[b]	171 ± 146	186 ± 26	6525 ± 1508
%F	100 ± 17	100[b]	25 ± 21	3 ± 0	61 ± 14
C_{max} d.n. (nM)	2591 ± 36	5263[b]	137 ± 111	99 ± 10	1126 ± 320

[a]Discrete PK profiles, male mice (C57BL/6), dose i.v. 1.0 $mg \cdot kg^{-1}$, dose p.o. 3.0 $mg \cdot kg^{-1}$, except for compound **1** dosed po at 10 $mg \cdot kg^{-1}$; [b]No SD calculated as one animal was excluded from the dosing group due to experimental issues.

We next explored the interactions to the S1β pocket with the additional aim to improve solubility and to reduce the potency shift observed with compound **6** in the presence of plasma (**Table 1**). To that end, we investigated substitution of the P1β isopropyl group by various polar residues. Introduction of a nitrile (**7**), hydroxyl (**8**), or a

primary carboxamide (**9**) retained the high biochemical potency for FXIa and PKL. For compound **7**, a slight improvement in potency in the 50% plasma assay was observed (**Table 1**). Interestingly, biochemical selectivity against FD was also substantially improved for **8** (40-fold) and **9** (80-fold) but not for **7** (**Table 1**). Introduction of S1β-binding residues to the P1 tetrahydroisoquinoline scaffold, as exemplified by compound **10**, afforded only a minor 4-fold improvement in potency for FXIa, while inhibitory activity toward FD was retained as compared to compound **3** (**Table 1**).

The X-ray crystal structure of **7** in complex with FXIa (**Figure 5a**) revealed a binding pose very similar to that observed for compound **3** with a perfect overlap of the respective biphenyl scaffolds, the ether linkers, and the arylacetic acid motifs of both inhibitors. The isopropyl nitrile moiety was nicely accommodated by the hydrophobic S1β pocket formed by the side-chains of Leu_{146}, Tyr_{143}, and Lys_{192}. The 2,3-dihydrobenzofuran-3(*S*)-amine moiety closely filled the S1 pocket, with the amine H-bonding with the side-chain of Asp_{189} and the backbone carbonyl of Ala_{190} and Gly_{218}.

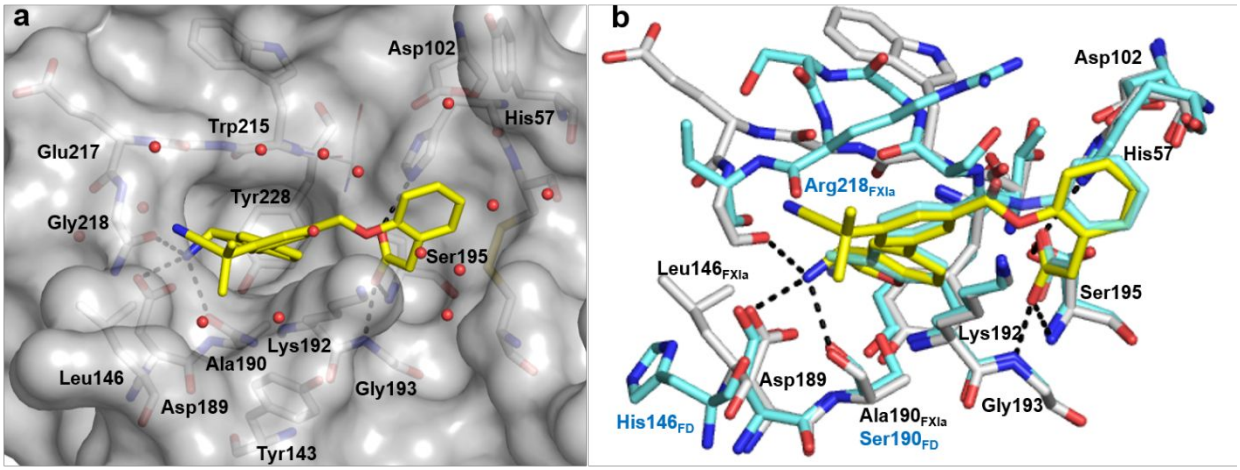

Figure 5. (**a**) Crystal structure of compound **7** (yellow, PDB code 6TS6) in complex with FXIa (white). The surface of the protein is shown in gray and oxygen atoms of crystallographic water molecules are shown as red spheres. (**b**) Comparison of the co-crystal structure of compound **7** (yellow) complexed with FXIa (white) and compound **2** (pale blue) complexed with FD (pale blue, PDB code 6QMT).[27] Only selected residues in the ligand-binding pocket are shown. H-bonding interactions are shown as black dotted lines. FXIa residues are labeled in black and FD residues are labeled in blue.

We also noted that terminal polar P1β residues, as exemplified by compounds **7** to **9**, had a beneficial impact on solubility, but they also proved detrimental to cell permeability and induced efflux as measured by a Caco-2 assay (**Table 1**). In addition, *in vivo* mouse PK profiles for compounds **7** and **8** indicated increased clearance and reduced oral bioavailability relative to compound **6** (**Table 2**). This prompted us to explore the introduction of locally masked or shielded polarity as part of an additional heterocycle attached to the upper phenyl ring while keeping the beneficial hydrophobic van der Waals

interactions to the S1β pocket. To this end, we synthesized the 3,3-dimethyl-dihydrobenzofuran analog **11** which exhibited similar low-nanomolar potency toward FXIa in both the biochemical and in the plasma assay, and also showed a ~17-fold selectivity over FD (**Table 1**). This compound demonstrated an improved mouse PK profile, as compared with **7** and **8**, characterized by low clearance and good bioavailability (**Table 2**). However, a 2×PT value of 19.8 μM in relation to a 2×aPTT value of 2.5 μM (aPTT/PT ratio of ~8) needed further improvement (*vide infra,* **Table 3**). We then explored modifications of the aliphatic portion of the P1 pharmacophore, which is deeply buried at the bottom of the S1 recognition site upon binding to FXIa. We reasoned that filling more tightly the unoccupied space near Ala_{190} could further improve selectivity versus FD and other Ser_{190} proteases. As an example, enlargement of the (*S*)-2,3-dihydrobenzofuranyl-3-amine of **11** to the 6-membered ring provided the sterically more demanding (*R*)-chromanyl amine **12** (**Table 1**). Relative to compound **11**, compound **12** showed similar potency toward FXIa in the biochemical assay, but with a 3-fold drop in potency in the FXIa plasma assay. Despite the insufficient FXIa plasma potency, **12** demonstrated

exquisite 2,500-fold selectivity against FD, which was attributed to a steric clash with Ser_{190} present in FD.

In order to assess the selectivity profile of our emerging lead FXIa inhibitors, we tested them against a panel of serine proteases of the coagulation cascade and serine proteases, which play a role in fibrinolysis, i.e. in breaking down blood clots (e.g. tPa, urokinase, plasmin). Inhibitors **6** and **11** exhibited acceptable selectivity over FVIIa and plasmin, but also showed sub-micromolar affinity for FIXa, FXa, thrombin, tissue plasminogen activator (tPa) and urokinase (**Table 3**). Compound **12** bearing a larger S1-binding motif demonstrated improved selectivity against serine proteases FVIIa, urokinase, FXa and thrombin, and also versus FIXa. However, we considered the moderate selectivity across the off-target protease panel for these 3 compounds still to be insufficient, as inhibition of either one specific enzyme, or the additive effect of partial inhibition of several of these proteases, may negatively affect the risk of bleeding, as evidenced by the poor 2×aPTT/PT ratios for compounds **6** and **11**.

Table 3. *In vitro* S1 protease selectivity data for selected FXIa inhibitors.

Compounds	6	11	12

FVIIa IC_{50} (μM)[a]	5.10	7.1	75
FIXa IC_{50} (μM)[a]	0.17	0.21	1.6
FXa IC_{50} (μM)[a]	0.50	0.84	4.3
Thrombin IC_{50} (μM)[a]	0.090	0.13	0.86
tPa IC_{50} (μM)[a]	0.090	0.10	0.19
Plasmin IC_{50} (μM)[a]	2.60	6.3	14
Urokinase IC_{50} (μM)[a]	0.047	0.016	0.95

[a]Half-maximal inhibition of selected proteases as determined in biochemical activity assays using quenched fluorescent peptide substrates. Data represent mean values of duplicate measurements.

FXIa inhibitor **6** comprising a very lean zwitterionic structure of low molecular weight and demonstrating a high inhibitory ligand efficiency for FXIa (BEI[49] of 20, LLE[50] of 5.4, $logD_{7.4}$ of 3.1) provided a better understanding of the foundational SAR as it relates to FXIa and FD activity. Compound **6** also demonstrated a low risk of DDI and hERG inhibition (CYPs 3A4, 2C9, 2D6: all IC_{50} >20 μM; hERG Qpatch IC_{50}: 24 μM) and afforded good selectivity against a panel of 69 enzymes, receptors and ion channels (all IC_{50}'s >30 μM except: Cox1 IC_{50}: 3.3 μM; PDE4d IC_{50}: 7.2 μM; and VMAT2 IC_{50}: 5.2 μM). Furthermore, **6** afforded an excellent mouse pharmacokinetic profile (**Table 2**). Therefore,

we chose compound **6** as a minimal pharmacophore, maintaining the key 3-amino-dihydrobenzofuran moiety at S1 and the iPr group at S1β for further optimization.

With our primary pharmacophore set, we turned our attention toward addressing protease selectivity. To this end, we explored optimizing the spacing between the 3-amino-dihydrobenzofuran and the carboxylic acid making the critical interaction in the oxyanion hole. We reasoned that rigidifying the structure to enforce a conformation that would better position the carboxylic acid in the oxyanion hole would improve both FXIa affinity and potentially enhance selectivity against other serine proteases. Molecular modeling suggested that a fused ring system would provide such an opportunity. A fused 3,4-dihydro-2H-benzo[b][1,4]oxazine, that essentially ties the aryl acetic acid back into the linker as in **13**, appeared particularly promising (**Figure 6**). In addition, the added polarity of this linker offered the potential to reduce the plasma IC_{50} shift associated with compound **6**. Synthesized as a mixture of diastereomers at the 2 position of the 3,4-dihydro-2H-benzo[b][1,4]oxazine and subsequently separated, the more potent (*R)*-isomer, **13**,[51] exhibited exquisite potency that was at the limit of the biochemical assay

(<0.7 nM). This increase in biochemical potency also translated to a 10-fold shift in potency relative to compound **6** in the presence of plasma (**Table 4**). In addition, the concentration necessary to elicit a doubling in aPTT time was only 0.4 μM (~5-fold more potent than compound **6**). Unfortunately, the 2×aPTT/PT ratio was low (5.1x) indicating very little selectivity between the intrinsic and extrinsic coagulation pathways and suggesting that the observed potency in the aPTT assay was not entirely due to FXIa inhibition.

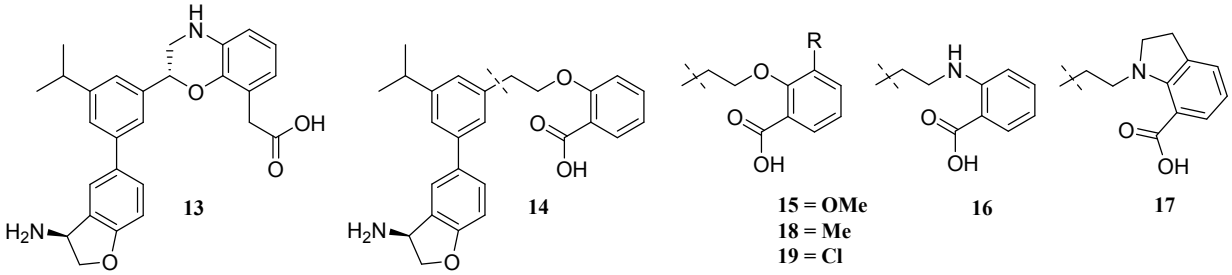

Figure 6. Structure of the fused 3,4-dihydro-2H-benzo[b][1,4]oxazine (**13**) and benzoic acids (**14**-**19**).

With selectivity remaining a significant challenge, we next explored more substantial changes in the spacing between the 3-amino-dihydrobenzofuran and the carboxylic acid. Up to this point, we had focused on aryl acetic acids as a means of spanning the six-atom distance between the S1β moiety and the carboxylic acid of our

pharmacophore. It was reasoned that pushing the P1' phenyl ring further toward the oxyanion hole by converting the aryl acetic acid to a benzoic acid and by extending the linker by one atom to maintain the requisite spacing might offer new SAR to aid in addressing the selectivity challenge. To this end, an introductory set of benzoic acid compounds exemplified by **14**, **15**, **16**, and **17** were synthesized (**Figure 6**). The inclusion of indoline **17** was inspired by the exquisite potency offered by the fused ring system of **13**. The ether-linked benzoic acid, **14**, proved to be 5-fold less potent than **6** against FXIa and exhibited a larger plasma shift (**Table 4**). In addition, **14** did not demonstrate a significant improvement in selectivity over other serine proteases. Surprisingly, addition of a *m*-methoxy group to the benzoic acid, **15**, demonstrated a substantial increase in selectivity over most of the coagulation factors and fibrinolysis proteases, although FXIa potency, especially in the presence of plasma, did not improve compared to compound **6** (**Table 4**). Exchanging the ether oxygen in the linker for a nitrogen, **16**, resulted in a significant loss of FXIa potency (IC_{50} 2.52 μM). However, the indoline **17** provided biochemical potency on par with compound **6** and, like **15**, also afforded an increase in selectivity against the coagulation proteases (**Table 4**). In addition, indoline **17**

demonstrated an encouraging *in vivo* mouse PK profile with a long $t_{1/2}$ (9 h), and promising oral bioavailability (36%) (**Table 5**).

Table 4. *In vitro* potency and selectivity data: IC_{50} (μM)[a]:

Compound	6	13	14	15	16	17	18	19	20*	21*	22*	23
FXIa	0.003	<0.0007	0.012	0.003	2.52	0.006	0.017	0.015	0.04	0.002	<0.0007	0.0004
cd-FXIa plasma	0.12	0.01	1.19	0.24	ND[b]	0.22	6.62	5.49	8.11	0.17	0.045	0.01
FVIIa	5.10	2.00	3.27	28.3	ND[b]	6.23	45.1	20.5	12.5	8.75	16.7	3.65
FIXa	0.17	0.03	0.04	10.2	ND[b]	3.30	11.3	9.60	15.5	7.86	13.4	1.92
FXa	0.50	0.22	0.24	6.21	ND[b]	1.83	12.5	11.1	16.3	1.71	11.2	1.05
Thrombin	0.090	0.03	0.05	9.09	ND[b]	3.08	9.82	6.22	7.43	6.14	7.21	2.57
PKL	0.003	0.001	0.025	0.009	ND[b]	0.058	0.041	0.021	0.16	0.002	0.016	0.001
tPA	0.090	0.05	0.09	2.20	ND[b]	0.66	4.13	3.67	6.68	0.49	3.70	0.25
Plasmin	2.60	0.69	0.59	30.8	ND[b]	2.56	>100	34.0	46.2	9.58	17.4	1.89
uPA	0.047	0.02	0.02	0.40	ND[b]	0.52	2.48	0.93	1.13	0.25	1.42	0.17
FD	0.04	0.06	1.32	17.5	ND[b]	4.41	>100	34.2	27.2	73.6	8.92	ND[b]

[a]All values are geometric means of ≥2 replicates; *Diastereomeric mixture. [b]ND = not determined.

From the introductory set of compounds, **15** and **17** emerged as frontrunners being equipotent with compound **6**, but with improved selectivity in the coagulation pathway. However, further attempts to expand the SAR around **15** to improve FXIa potency,

especially in the presence of 50% plasma, while maintaining selectivity proved non-productive. The *m*-methyl and *m*-chloro derivatives, **18** and **19** (**Figure 6**), were 5-fold less potent against FXIa than **15**, and showed a greater than 300-fold IC_{50} plasma shift (**Table 4**).

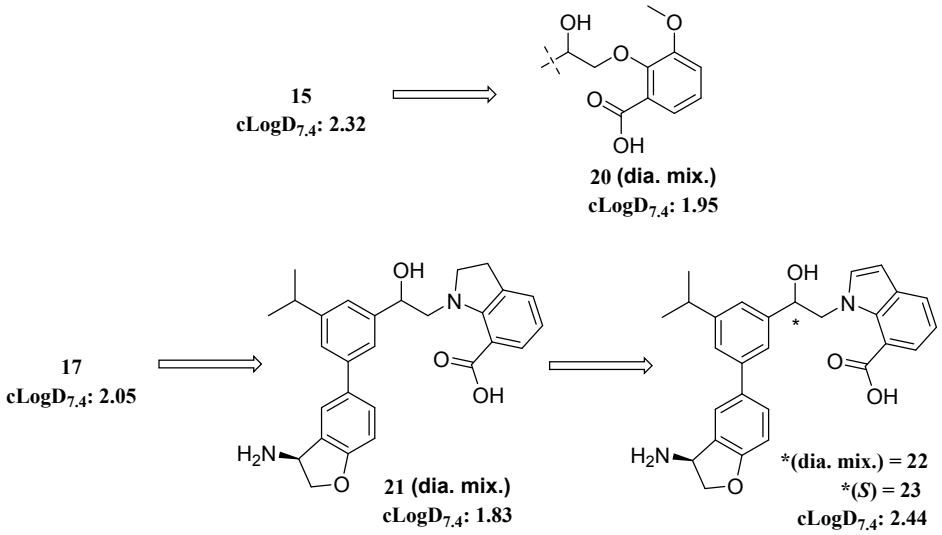

Figure 7. Exploration of addition of a hydroxyl to the linker between the S1β and S1' sites.

We then focused on the linker between the S1β and prime site with an aim to enhance biochemical potency and reduce plasma IC_{50} shift. We hypothesized that installation of a polar moiety could introduce additional conformational bias in the linker and lower the $LogD_{7.4}$. To this end, **20** and **21** were synthesized as diastereomeric mixtures with a hydroxyl group appended to the benzylic position of the linker (**Figure 7**).

This modification lowered the calculated $LogD_{7.4}$ for each of these compounds compared to **15** and **17**. Unfortunately, this change was not productive in the context of **20** which resulted in 10-fold loss in potency against FXIa in the biochemical assay and a 200-fold plasma IC_{50} shift (**Table 4**). Conversely **21**, the hydroxyl analog of **17**, maintained encouraging FXIa activity even as a mixture of diastereomers and appeared to improve selectivity on all relevant coagulation factors (FIXa, FXa, FVIIa, thrombin, and plasmin). In addition to the coagulation factors, an impressive improvement in FD selectivity from 700-fold for **17** to over 30,000-fold for **21** was observed (**Table 4**). While the indoline afforded a promising selectivity and potency profile, it had a propensity to oxidize, thus the corresponding indole, **22**, was synthesized as a diastereomeric mixture (**Figure 7**). Interestingly, **22** increased FXIa potency 4-fold over the diastereomeric indoline and, despite an increase in $cLogD_{7.4}$, maintained a reasonable plasma IC_{50} shift. Furthermore, the change to the indole appeared to suggest an improvement in selectivity versus all of the coagulation factors as well as the fibrinolysis proteases uPA and tPA (**Table 4**). When the diastereomeric mixture was separated, the (*S*)-isomer, **23**, proved to be the more active isomer[52] with sub-nanomolar activity against FXIa and an IC_{50} of 10 nM in the

presence of 50% plasma. Furthermore, the overall improvement in selectivity profile seen with **22** was maintained.[53] **23** also preserved the high inhibitory ligand efficiency for FXIa of compound **6** (BEI[49] of 20) and demonstrated an improved LLE[50] of 5.4 ($logD_{7.4}$ of 2.2).

In an effort to better rationalize the enhanced FXIa potency and selectivity of **23** we obtained a co-crystal structure of **23** with FXIa. Similar to earlier co-crystal structures, **23** binds to FXIa with the biphenyl portion of the inhibitor sitting in the S1 pocket and the basic amino group making H-bonding interactions with the backbone carbonyl from Ala_{190} and the side-chain of Asp_{189} (**Figure 8a**). The carboxylic acid moiety binds in the oxyanion hole and has H-bonding contacts with the backbone NH of Gly_{193} and the side-chains of His_{57} and Ser_{195}. A water mediated H-bonding interaction is also seen with the backbone carbonyl of Leu_{39}. The binding interactions of **23** with FXIa gave no direct evidence to rationalize the increased selectivity. However, a superposition of the structures of compound **1** complexed with FD and **23** complexed with FXIa suggests that the carboxylic acid of **23** does not sit as deep in the oxyanion hole as for compound **1** (**Figure 8b**). Interestingly, when a comparable overlay with one of the observed binding poses of the

selective benzoic acid **15** is performed, a similar arrangement in the oxyanion hole is observed as with **23**. This weaker interaction in the oxyanion hole may be responsible for the increased selectivity of both **15** and **23** over the other coagulation factors.

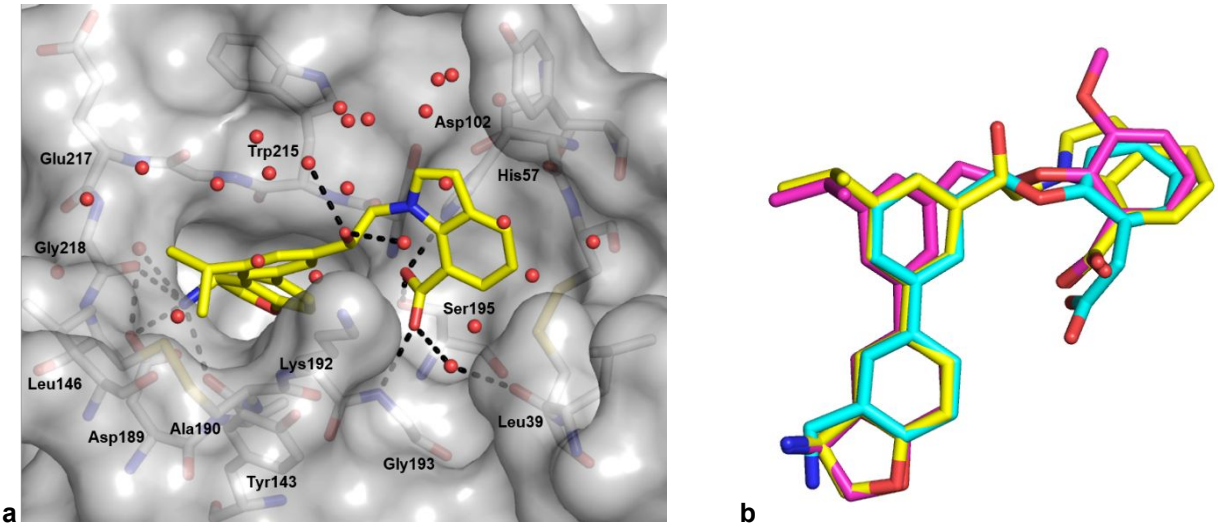

Figure 8. (a) Crystal structure of **23** (yellow) in complex with FXIa (white, PDB code 6USY). The surface of the protein is shown in gray and oxygen atoms of crystallographic water molecules are shown as red spheres. Only selected residues in the ligand-binding pocket are shown. H-bonding interactions are shown as black dotted lines. **(b)** Overlay of compound **1** (cyan) bound to FD, **15** bound to FXIa (magenta, PDB code 6TS5), and **23** (yellow) bound to FXIa.

The enhanced FXIa potency of **23** translated to requiring a concentration of 1.3 μM to effect a doubling in aPTT clotting time. More importantly, the enhancement in biochemical selectivity resulted in a PT value of 28.7 μM to afford a functional selectivity ratio (2×aPTT/PT) of ~21-fold, thus **23** met our functional potency and selectivity

requirements for advancement (*vide supra*). However, a low dose mouse PK (3 mg/kg) study with **23** afforded only 16 % bioavailability despite exhibiting relatively low clearance (11 mL·min^{-1}·kg^{-1}) (**Table 5**).

Table 5. *In vivo* mouse pharmacokinetic profiles of indoline and indole FXIa inhibitors.

	17	**23**	**23**
Dose [i.v. / p.o.] (mg/kg)	0.4 / 3.0	1.0 / 3.0	100 (p.o.)
CL (mL·min^{-1}·kg^{-1})	1	11.01	-
V_{SS} (L/kg)	0.4	0.57	-
$t_{1/2term}$ (h)	9.2	3.73	-
AUC i.v. d.n. (nM·h)	38652	3264 ± 35	-
AUC p.o. d.n. (nM·h)	14041 ± 1090	1297 ± 112	260215 ± 8503
%F	36 ± 3	16	100%
C_{max} d.n. (nM)	1'495 ± 158	494 ± 52	26795 ± 144
T_{max} (h)	0.7 ± 0.3	1	4.0

Assessment of **23** in an *in vitro* MDCK-MDR1 assay demonstrated low permeability (Papp (AB) 0.4 x 10^{-6} cm/s) and a high efflux ratio (21.5). Speculating that transporter mediated efflux might be contributing to the low oral bioavailability observed in mice, we examined the impact of higher oral doses to explore the possibility of saturating the efflux mechanism. When increasing the dose to 100 mg/kg, the oral bioavailability increased substantially to ~100% (**Table 5**). This phenomenon of over proportionality was also

observed in PK studies conducted in both rats and dogs, albeit to a lesser extent, as increasing the dose to 100 mg/kg in rats afforded a bioavailability of ~45% and in dogs 21% for a dose of 75 mg/kg (**Figure 9**). We postulate, based on preliminary mechanistic studies, that the non-linear oral PK profile observed in rats and dogs is likely due to saturation of intestinal metabolism and/or efflux transporters. While the precise cause of the observed dose over-proportionality has not yet been identified, it was encouraging to see that across all preclinical species tested, improved bioavailability was observed at higher doses. Furthermore, as in the mouse, **23** demonstrated low clearance in both dogs and rats and a low volume of distribution providing additional confidence in the overall ADME profile in the context of an anticoagulant agent.[54]

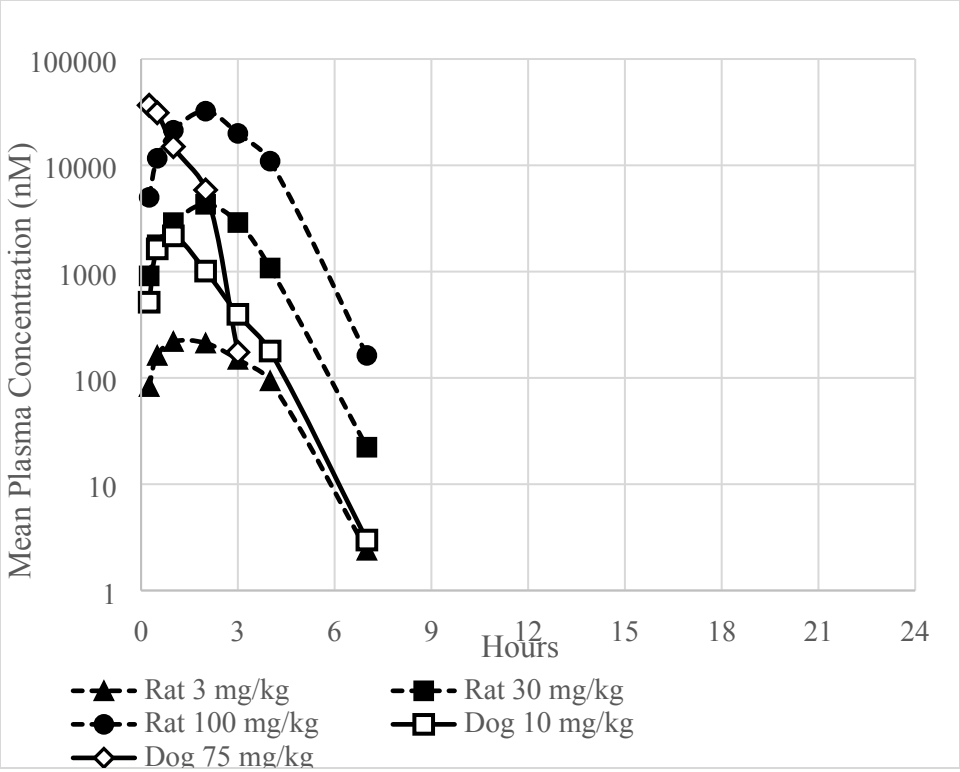

Species	PO Dose (mg/kg)	D.N. Cmax (nM)	D.N. AUC_{0-t} (nM*h)	%F
Rat	3	77 ± 4	382 ± 71	10 ± 2
	30	143 ± 39	621 ± 169	19 ± 5
	100	323 ± 64	1770 ± 439	45 ± 11
Dog	10	217 ± 57	560 ± 254	5 ± 2
	75	504 ± 171	2200 ± 620	21 ± 6
IV parameters (1mg/kg)	Cl (ml/min/kg)	AUC0-t (nM*h)	Vdss (L/kg)	T½ (h)
Rat	9.4 ± 1.0	3330 ± 370	1.3 ± 0.2	6.4 ± 0.1
Dog	4.4 ± 0.4	10660 ± 960	0.3 ± 0.0	2.8 ± 0.1

Figure 9. *In Vivo* Rat and Dog mean plasma pharmacokinetic parameters for **23**. D.N. = dose normalized.

Combining the rat and dog PK profiles with our desire to maintain plasma C_{trough} concentrations of ~1.3 μM (the 2×aPTT value for **23** in human plasma) permitted preliminary physiologically based pharmacokinetic (PBPK) modeling (GastroPlus™;

version 9.5; Simulations Plus Inc., Lancaster, CA, USA).[55] The modeling suggested that a 535 mg to 2000 mg dose administered *bid* should afford plasma concentrations above the 1.3 μM threshold at trough, with the low end of this range more likely. Furthermore, plasma exposure was predicted to stay below the 28.7 μM 2×PT value for **23** (predicted human Cmax = 7.9 μM). Compound **23** was then further profiled against a panel of ~115 enzymes, receptors, and ion channels to assess potential safety liabilities, wherein all IC_{50} values were ≥ 30 μM except for: COX1 IC_{50}: 4.3 μM; PDE4d IC_{50}: 2.4 μM; BSEP IC_{50}: 28 μM; and PPARγ, 65% binding at 10 μM. The favorable aPTT and PT values, relatively clean *in vitro* safety profile, and a preclinical PK profile suggesting a high, but tractable, anticipated human dose, led to the selection of **23** for advanced DMPK and preclinical safety profiling, which will be reported in due course.

CHEMISTRY

The compounds described herein were generally constructed unless otherwise noted following the synthetic route depicted in **Scheme 1** using either commercially available building blocks or readily synthesized building blocks as described in the

Supporting Information. In the first step, a Mitsunobu reaction is performed between aliphatic alcohols (**24**-**29**) and phenols (**30**-**35**). The resulting aryl bromide intermediates (**36**-**44**) were then either transformed into the corresponding boronic ester and reacted with aryl bromide **49** or **45** or reacted with aryl bromides (**45** and **46**) using the two-step, one-pot palladium catalyzed borylation/Suzuki cross-coupling reaction protocol developed by Molander[56] or reacted with the corresponding boronic acid/ester (**47**, **48**, **50**) using Suzuki coupling conditions. Finally, acidic deprotection of the Boc protected amine when necessary with concomittent *t*Bu ester deprotection, when present, or subsequent saponification of the methyl ester, when present, lead to the desired amino acid final compounds **3**, **5**-**12**, **15**, **18**. For the synthesis of **14** and **19**, steps 1 and 2 were inverted, i.e., aryl bromide **28** was first engaged in the Suzuki reaction with the boronic acid **47**, followed by the Mitsunobu reaction with phenols **32** and **35**, respectively. For the synthesis of compounds **8** and **10**, modifications were made to the R_1 group of intermediate **40** (R_1=CH_2OH) to generate intermediate **41** (R_1 = $C(CH_3)_2OH$) prior to the Suzuki coupling and deprotection steps as described in the Experimental Section. While compound **9** was obtained following the same sequence as for compound **7** except that

after completion of the cross-coupling reaction the reaction mixture was heated with sodium hydroxide, water and *tert*-butanol to hydrolyze the nitrile group into the corresponding amide (R_1 = $CONH_2$).

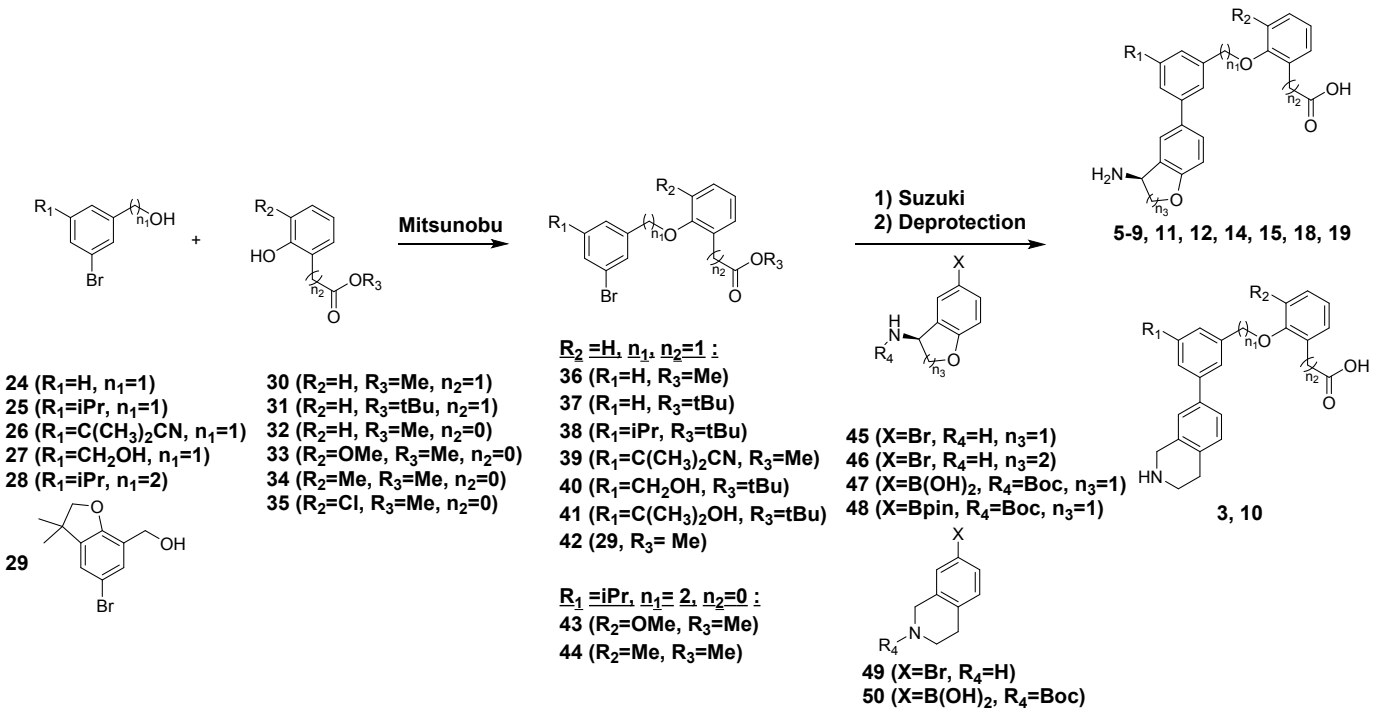

Scheme 1. General synthetic route to aryl acetic acid and benzoic acid FXIa inhibitors.

Compounds **20-22** containing a benzylic alcohol were prepared either from the appropriate α-bromo ketone or epoxide intermediate and are described in the Experimental Section as are the synthesis of compounds **13, 16** and **17**. For the synthesis of compound **23**, the optically pure epoxide **54** was first synthesized in three steps. Asymmetric dihydroxylation of 1-bromo-3-isopropyl-5-vinylbenzene (**51**) using AD-mix-α afforded diol **52** in

moderate yield, activation of the primary alcohol with mesityl sulfonyl chloride followed by intramolecular S_N2 reaction produced the desired chiral epoxide **54** (**Scheme 2**).

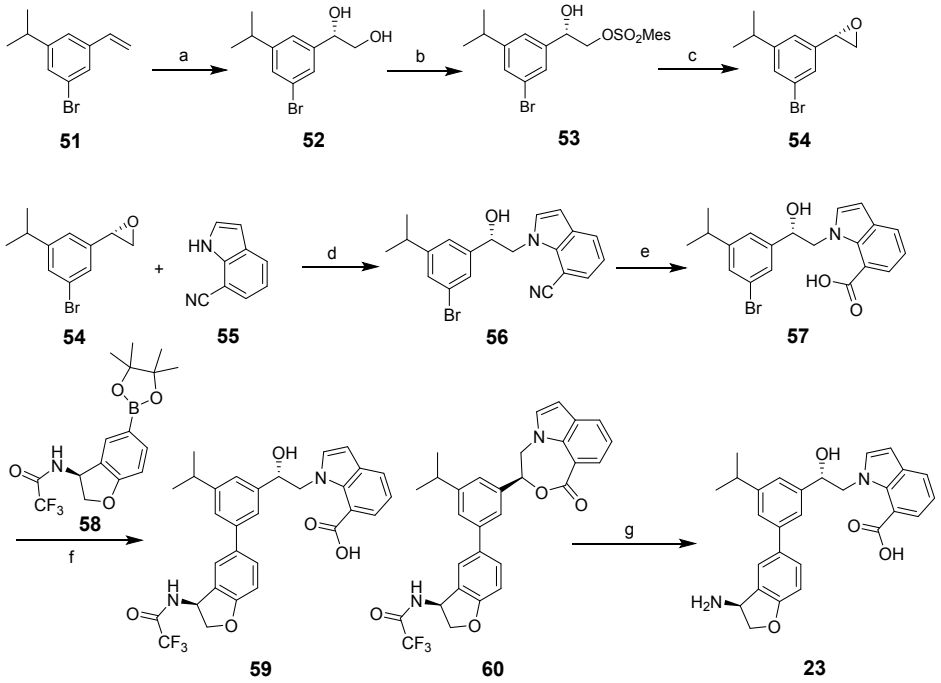

Scheme 2. a) AD-mix-α, tBuOH/H_2O, -10°C-25°C, 38%; b) mesityl-Cl, pyridine, DMAP, CH_2Cl_2, 72%; c) Cs_2CO_3, DMF, 82%; d) K_2CO_3, DMF, 80°C, 86%; e) KOH, EtOH, 0-100°C, 100%; f) $PdCl_2(dppf)\cdot CH_2Cl_2$, 2M Na_2CO_3, 1,4-dioxane, 70°C; g) 3N NaOH, MeOH, 60°C, 32%.

We then tried to open the epoxide with methyl 1H-indole-7-carboxylate but this resulted in only a ~10% yield of the desired hydroxy ethyl indole (not shown). We reasoned that sterics might play a significant role in this reaction, thus we explored a less hindered nucleophile. When 1H-indole-7-carbonitrile (**55**) was used instead, the desired product **56** was obtained in 86% yield. Hydrolysis of the nitrile to the corresponding carboxylic acid provided aryl bromide **57** in excellent yield. However, **57** proved troublesome to work with due to its tendency to lactonize in both in the subsequent Suzuki reaction when boronic ester **48** was used, and in the following Boc deprotection step. By switching to the trifluoroacetamide protected boronic ester **58**, a single basic

hydrolysis step at the end of the synthesis deprotected the amine and hydrolyzed lactone **60** present in the reaction mixture thereby affording compound **23**.

CONCLUSION

Evaluating a knowledge-based small diversity library (~1750 compounds) of internal serine proteases inhibitors enabled the rapid identification of a micromolar FXIa inhibitor with a non-peptidomimetic scaffold originating from a historical FD program. Compound **1** demonstrated good ADME and PK properties, and initial SAR demonstrated the possibility to increase potency for FXIa while improving selectivity against FD. Optimization of interactions in the S1 pocket led to the identification of compound **5** with a 3-amino-dihydrobenzofuran moiety conferring increased FXIa potency and reduced activity toward FD. Filling the small hydrophobic S1β pocket with an isopropyl group (compound **6**) further increased FXIa potency and FD selectivity. Finally, linker modifications and incorporation of a 6,5-fused indole moiety dramatically improved the selectivity over serine proteases from both the intrinsic and extrinsic coagulation pathways. Eventually, compound **23** emerged with sub-nanomolar potency on FXIa, excellent selectivity over coagulation proteases, and an acceptable pharmacokinetic

profile in preclinical species. Based on the overall excellent *in vitro* and *in vivo* characteristics, **23** was selected for advanced preclinical evaluation.

EXPERIMENTAL SECTION

1. Experimental procedures and compound characterization for novel compounds (3, 5-23)

1.1. General Chemistry Information

Unless otherwise specified, all solvents and reagents were obtained from commercial suppliers and used without further drying or purification. KOAc and K_2CO_3 were dried in an oven at 40 °C for 4 h; EtOH and aqueous K_2CO_3 solution were thoroughly degassed by bubbling nitrogen prior to use in the two-step, one-pot palladium catalyzed borylation/Suzuki cross-coupling reaction protocol. Phase separator were obtained from Biotage: Isolute Phase separator (Part Nr: 120-1908-F for 70 mL and Part Nr: 120-1909-J for 150 mL). Normal-phase flash chromatography was performed using Merck silica gel 60 (230-400 mesh), Merck Darmstadt, Germany. R_f values for thin layer chromatography (TLC) were determined using 5 x 10 cm TLC plates, silica gel F254, Merck, Darmstadt, Germany. ^{1}H NMR and ^{13}C spectra were recorded on a Bruker 600 MHz AVANCE III spectrometer equipped with a 5 mm BBO probe with a z-gradient system and a Bruker

600 MHz AVANCE II spectrometer equipped with a 5 mm dual $^{13}C\{^{1}H\}$ CryoProbe™ with a z-gradient system. High-resolution mass spectra (HRMS) measurements by using electrospray ionization in positive ion mode after separation by liquid chromatography (Vanquish, Thermo). The elemental composition was derived from the mass spectra acquired at the high resolution of about 240'000 on an Orbitrap Fusion Lumos mass spectrometer (Thermo Scientific). The high mass accuracy below <1 ppm was obtained by using a Internal Calibrant (IC). Liquid chromatography mass spectra (LC−MS) were determined by using electrospray ionization in positive and negative ion modus using a Waters Acquity UPLC instrument. Purity was determined by analytical HPLC using an Agilent 1100 series instrument and by integration of the area under the UV absorption curve at λ =254 nm or 214 nm and ^{1}H NMR, all final compounds reported were ≥95%, pure unless otherwise stated. t_R refers to retention time. The following conditions (a to k) were used for analytical HPLC, UPLC or preparative HPLC, if not indicated otherwise: HPLC conditions: (a) Waters XBridge C18; particle size: 2.5 µm; column size: 3 x 30 mm; eluent/gradient: 10-98% CH_3CN/H_2O/3 min, 98% CH_3CN/0.5 min (CH_3CN and H_2O containing 0.1% TFA); flow rate: 1.4 mL/min; column temperature: 40 °C. (b) Waters

XBridge C18; particle size: 2.5 µm; column size: 3 x 50 mm; eluent/gradient: 10-98% CH_3CN/H_2O/8.6 min, 98% CH_3CN/1.4 min (CH_3CN and H_2O containing 0.1% TFA); flow rate: 1.4 mL/min; column temperature: 40 °C. UPLC/MS conditions: (c) Acquity HSS T3; particle size: 1.8 µm; column size: 2.1 x 50 mm; eluent A: H_2O + 0.05% HCOOH + 3.75 mM ammonium acetate; eluent B: CH_3CN + 0.04% HCOOH; gradient: 10 to 95% B in 1.5 min; flow rate: 1 mL/min; column temperature: 60 °C. (d) Acquity HSS T3; particle size: 1.8 µm; column size: 2.1 x 50 mm; eluent A: H_2O + 0.05% HCOOH + 3.75 mM ammonium acetate; eluent B: CH_3CN + 0.04% HCOOH; gradient: 5 to 98% B in 9.4 min; flow rate: 1 mL/min; column temperature: 60 °C. (e) Acquity UPLC BEH C18; particle size: 1.7 µm; column size: 2.1 x 50 mm; eluent A: H_2O with 0.1% Formic Acid; eluent B: acetonitrile with 0.1% Formic Acid; gradient: 2 to 98% B in 4.40 min, 98% B for 0.75 min; flow rate: 1 mL/min; column temperature: 50 °C. (f) Acquity UPLC BEH C18; particle size: 1.7 µm; column size: 2.1 x 50 mm; eluent A: H_2O with 5 mM NH_4OH; eluent B: acetonitrile with 5 mM NH_4OH; gradient: 2 to 98% B in 4.40 min, 98% B for 0.75 min; flow rate: 1 mL/min; column temperature: 50 °C. Preparative HPLC conditions: (g) Waters X-Bridge C18 OBD; particle size: 5 µm; column size: 30 x 100 mm; eluent A: H_2O with 7.3 mM NH_4OH; eluent

B: CH_3CN with 7.3 mM NH_4OH; gradient: 10 to 99% B in 12.5 min, 99% B for 2.5 min; flow rate: 45 mL/min; column temperature: RT. (h) HPLC-MS Waters X-Bridge C18 OBD; particle size: 5 µm; column size: 30 x 100 mm; eluent A: H_2O with 7.3 mM NH_4OH; eluent B: CH_3CN with 7.3 mM NH_4OH; gradient: 5 to 99% B in 12.5 min, 99% B for 2.5 min; flow rate: 45 mL/min; column temperature: RT. (i) Waters X-Bridge® BEH C18 OBD Prep; particle size: 5 µm; column size: 30 x 50 mm; eluent A: H_2O containing 10 mM NH_4OH; eluent B: Acetonitrile containing 10 mM NH_4OH; gradient: variable; flow rate: 75 mL/min. (j) Shimadzu Preparative Liquid Chromatograph LC- Phenomenex Gemini-NX C18; particle size: 5 µm; column size: 30 x 100 mm; eluent A: H_2O containing 0.1% NH_4OH; eluent B: Acetonitrile; gradient variable; flow rate: 40 mL/min. (k) Shimadzu Preparative Liquid Chromatograph LC-8A Sunfire Prep C18; particle size: 5 µm; column size: 30 x 100 mm; eluent A: H_2O containing 0.1% TFA; eluent B: Acetonitrile; gradient variable; flow rate: 42 mL/min.

1.2. Experimentals

2-(2-((3-(1,2,3,4-Tetrahydroisoquinolin-7-yl)benzyl)oxy)phenyl)acetic acid (3): In a microwave vial with stir bar was placed methyl 2-(2-((3-(4,4,5,5-tetramethyl-1,3,2-dioxaborolan-2-yl)benzyl)oxy)phenyl)acetate (125 mg, 0.33 mmol) and 7-bromo-1,2,3,4-tetrahydroisoquinoline (**49**) (83 mg, 0.39 mmol) in DMF (2.94 mL) and H_2O (0.33 mL). Then, K_3PO_4 (aqueous 2M, 654 µl, 1.31 mmol) and $PdCl_2(dppf).CH_2Cl_2$ adduct (13.35 mg, 0.016 mmol) was added. The vial was sealed and the reaction was heated at 110 °C for 60 min to complete the reaction. NaOH (2N, 818 µl, 1.64 mmol) was added and the mixture heated at 55°C overnight. The reaction mixture was concentrated, filtered and purified by preparative HPLC (Gemini® NX 5 µm C18 110A; column size 100 x 30 mm; gradient: MeCN / water containing 0.1% (ammonium hydroxide 28%) to give after lyophilization of the product containing fractions the title compound (42 mg, 34% yield). HPLC (Acquity BEHC18; particle size: 1.7 µm; column size: 2.1 x 50 mm; eluent/gradient: 0.2-98% CH_3CN/H_2O/7.5 min (CH_3CN containing 0.04% formic acid and 3.75 mM ammonium acetate); flow rate: 1.0 mL/min; temperature 50 °C), t_R: 2.68 min, purity 100%; 1H NMR (400 MHz, DMSO-d_6) δ ppm 7.83-7.72 (m, 1H), 7.55 (m, 1H), 7.48-7.33 (m, 4H), 7.22-7.10 (m, 2H), 7.07-6.99 (m, 1H), 6.94-6.88 (m, 1H), 6.80 (td, J = 7.3, 0.85 Hz, 1H), 5.12 (d, J = 6.85 Hz, 2H), 4.50 (s, 1H), 3.91 (s, 1H), 3.50 (t, J = 5.4 Hz, 1H), 3.26 (s, 1H), 3.20 (s, 1H), 2.96 (t, J = 5.7 Hz, 1H), 2.73-2.63 (m, 2H).

Methyl 2-(2-((3-(4,4,5,5-tetramethyl-1,3,2-dioxaborolan-2-yl)benzyl)oxy)phenyl)acetate: A degassed mixture of methyl 2-(2-((3-bromobenzyl)oxy)phenyl)acetate (**36**) (0.8 g, 2.39 mmol), 4,4,4',4',5,5,5',5'-octamethyl-2,2'-bi(1,3,2-dioxaborolane) (1.51 g, 5.97 mmol),

potassium acetate (586 mg, 5.97 mmol) and $PdCl_2$(dppf) (0.11 g, 0.14 mmol) in dichloroethane (12 mL) was heated at 80 °C for 2.5 h. The reaction mixture was cooled to room temperature and directly loaded onto a silica column and purified by flash chromatography (eluent: 0-50% EtOAc in heptane) to give the title compound (866 mg, 78% yield, purity 80%). HPLC (Acquity HSS T3; particle size: 1.8 µm; column size: 2.1 x 50 mm; eluent A: H_2O + 0.05% HCOOH + 3.75 mM ammonium acetate; eluent B: CH_3CN + 0.04% HCOOH; gradient: 5 to 95% B in 1.4 min; flow rate: 1.2 mL/min; column temperature: 80 °C), t_R: 1.33 min, purity 80%; ^{1}H NMR (400 MHz, DMSO-d_6) δ 7.75-7.69 (m, 1H), 7.63 (dt, J = 7.3, 1.3 Hz, 1H), 7.54 (dt, J = 7.9, 1.5 Hz, 1H), 7.45-7.37 (m, 1H), 7.29-7.18 (m, 2H), 7.05 (dd, J = 8.2, 1.1 Hz, 1H), 6.91 (td, J = 7.4, 1.1 Hz, 1H), 5.11 (s, 2H), 3.62 (s, 2H), 3.57 (s, 3H), 1.30 (s, 12H).

Methyl 2-(2-((3-bromobenzyl)oxy)phenyl)acetate (**36**): To a solution of (3-bromophenyl)methanol (**24**) (3 g, 16.0 mmol) in anhydrous THF (50 mL) under argon atmosphere was added PPh_3 (5.05 g, 19.25 mmol) followed by methyl 2-(2-hydroxyphenyl)acetate (**30**) (3.20 g, 19.25 mmol). The mixture was cooled to 0°C and DIAD (3.74 mL, 19.25 mmol) was added dropwise. The reaction mixture was allowed to reach RT. After completion of the reaction, the mixture was diluted with EtOAc and washed with a saturated solution of $NaHCO_3$. The organic layer was separated, dried (Na_2SO_4), filtered and concentrated to dryness. The crude residue was purified by flash chromatography (Isolera Four system, column: 100 g, eluent: EtOAc in c-hexane from 0% to 55% in 55 min) to give the title compound as a yellow oil (4.58 g, 82% yield).

UPLC/MS (conditions c), t_R: 1.29 min, purity 96%; 352.0/354.0 [M+H]+; ^{1}H NMR (400 MHz, DMSO-d_6): δ 7.63 (br.s, 1H), 7.53 (br.d, J = 7.8 Hz, 1H), 7.53 (br.d, J = 7.8 Hz, 1H), 7.37 (t, J = 7.7 Hz, 1H), 7.28-7.24 (m, 2H), 7.04 (d, J = 8.2 Hz, 1H), 6.93 (t, J = 7.4 Hz, 1H), 5.13 (s, 2H), 3.67 (s, 2H), 3.60 (s, 3H).

Methyl 2-(2-hydroxyphenyl)acetate (**30**): To an ice-cooled, yellow solution of 2-(2-hydroxyphenyl)acetic acid (10 g, 65.7 mmol) in MeOH (143 mL) was added dropwise under a nitrogen atmosphere thionyl chloride (9.59 mL, 131 mmol). The reaction mixture was stirred at RT for 1 h. The reaction mixture was evaporated to dryness to give the title compound as a brown solid (10.9 g, 95 %) which was used without purification in the next step. TLC, Rf (EtOAc) = 0.43; UPLC/MS (ESI$^+$) *m/z* 167.0 (M+1); HPLC (conditions b), t_R: 1.93 min, purity 100%; ^{1}H NMR (400 MHz, DMSO-d_6): δ 9.50 (s, 1H), 7.12-7.06 (m, 2H), 6.80 (d, J = 8.1 Hz, 1H), 6.74 (t, J = 7.4 Hz, 1H), 3.59 (s, 3H), 3.5 (s, 2H).

2-(2-((3-(3-Amino-2,3-dihydrobenzofuran-5-yl)benzyl)oxy)phenyl)acetic acid (5): To a yellow solution of *tert*-butyl 2-(2-((3-(3-amino-2,3-dihydrobenzofuran-5-yl)benzyl)oxy)phenyl)acetate (purity ~85%, 113 mg, 0.22 mmol) in dioxane (3.1 mL) was added HCl (4N in dioxane, 1.67 mL, 6.68 mmol) and the solution was stirred at RT for 2.5 d. The reaction mixture was concentrated and the crude residue was purified by preparative HPLC-MS (conditions h) to give, after lyophilization of the compound containing fractions to give the title compound as a beige solid (47 mg, 55%). HPLC (conditions a), t_R: 1.66 min, purity 98%; HPLC (conditions b), t_R: 3.14 min, purity 98%;

UPLC/MS (ESI+) *m/z* 376.2 (M+1); ^{1}H NMR (400 MHz, DMSO-d_6): δ 7.91 (s, 1H), 7.80 (s, 1H), 7.55 (d, *J* = 7.7 Hz, 2H), 7.42 (t, *J* = 7.6 Hz, 1H), 7.34 (d, *J* = 7.6 Hz, 1H), 7.21-7.16 (m, 2H), 7.00 (d, *J* = 8.2 Hz, 1H), 6.88 (m, 2H), 5.22 (s, 2H), 4.79 (m, 1H), 4.71 (t, *J* = 8.8 Hz, 1H), 4.23 (dd, *J* = 9.7, 5.2 Hz, 1H), 3.59 (d, *J* = 15.8 Hz, 1H), 3.52 (d, *J* = 15.8 Hz, 1H).

tert-Butyl 2-(2-((3-(3-amino-2,3-dihydrobenzofuran-5-yl)benzyl)oxy)phenyl)acetate: A microwave vial was charged with *tert*-butyl 2-(2-((3-(4,4,5,5-tetramethyl-1,3,2-dioxaborolan-2-yl)benzyl)oxy)phenyl)acetate (120 mg, 0.27 mmol), 5-bromo-2,3-dihydro-benzofuran-3-ylamine (HCl salt, 82 mg, 0.33 mmol), K_3PO_4 (2N in water, 543 µL, 1.09 mmol) and $PdCl_2$(dppf).CH_2Cl_2 adduct (11.1 mg, 0.014 mmol) in acetonitrile (4 mL). The reaction mixture was purged with nitrogen and heated under microwave irradiations at 120 °C for 40 min. The reaction mixture was allowed to cool to RT and filtered through a pad of celite. The solvents were evaporated, the residue was taken up in THF (3 mL) and SiliaMetS®Thiol (particle size: 40-63 µm; loading 1.39 mmol/g; 0.054 mmol, 39 mg) was added. The mixture was swirled for 1 h at 40 °C, filtered, rinsed with THF and concentrated under reduced pressure. The crude residue was purified by flash chromatography on silica gel (Isco companion; column: 12 g, eluent: CH_2Cl_2 to CH_2Cl_2/MeOH 97-3 in 9 min, then hold for 5 min) to give the title compound (115 mg, 83%, purity 85%). TLC, Rf (EtOAc) = 0.2; HPLC (conditions a), t_R: 2.11 min, purity 85%; UPLC/MS (ESI+) *m/z* 432.3 (M+1); ^{1}H NMR (400 MHz, DMSO-d_6): δ 7.68 (br s, 2H), 7.55 (d, *J* = 7.7 Hz, 2H), 7.48-7.43 (m, 2H), 7.39 (d, *J* = 7.6 Hz, 1H), 7.29-7.20 (m, 2H), 7.06

(d, *J* = 8.2 Hz, 1H), 6.91 (t, *J* = 7.4 Hz, 1H), 6.86 (d, *J* = 8.6 Hz, 1H), 5.18 (s, 2H), 4.67-4.60 (m, 2H), 4.09 (m, 1H), 3.57 (s, 2H), 2.19 (m, 2H), 1.30 (s, 9H),

tert-Butyl 2-(2-((3-(4,4,5,5-tetramethyl-1,3,2-dioxaborolan-2-yl)benzyl)oxy)phenyl)acetate: To *tert*-butyl 2-(2-((3-bromobenzyl)oxy)phenyl)acetate (**37**) (1.50 g, 3.98 mmol) in dioxane (45 mL) was added bis(pinacolato)diboron (1.41 g, 5.57 mmol), potassium acetate (1.17 g, 11.9 mmol) and $PdCl_2$(dppf).CH_2Cl_2 adduct (162 mg, 0.20 mmol). The reaction mixture was evacuated under vaccum and nitrogen was added (this operation was repeated 3 times) and the mixture was stirred at 100 °C overnight. The reaction mixture was diluted with EtOAc, water was added and the layers were separated. The aqueous layer was back-extracted with EtOAc and the combined organic extracts were dried (phase separator) and concentrated. The crude residue was purified by flash chromatography (c-hexane to c-hexane/EtOAc 9:1 in 50 min) to give the title compound as a colorless oil (836 mg, 48%). TLC, Rf (c-hexane/EtOAc 9:1): 0.23; HPLC (conditions a), t_R: 3.02 min, purity 96%; UPLC/MS (ESI$^+$) *m/z* 442.3 (M+18); ^{1}H NMR (400 MHz, DMSO-d_6): δ 7.76 (s, 1H), 7.64 (d, *J* = 7.3 Hz, 1H), 7.60 (d, *J* = 7.7 Hz, 1H), 7.41 (t, *J* = 7.5 Hz, 1H), 7.25 (t, *J* = 7.8 Hz, 1H), 7.20 (d, *J* = 7.4 Hz, 1H), 7.05 (d, *J* = 8.1 Hz, 1H), 6.91 (t, *J* = 7.4 Hz, 1H), 5.12 (s, 2H), 3.53 (s, 2H), 1.32 (s, 21H).

tert-Butyl 2-(2-((3-bromobenzyl)oxy)phenyl)acetate (**37**): To a solution of *tert*-butyl 2-(2-hydroxyphenyl)acetate (**31**) (3.28 g, 15.75 mmol) in THF (90 mL) were successively added under a nitrogen atmosphere triphenylphosphine (4.54 g, 17.3 mmol) and 3-bromobenzyl alcohol (**24**) (3.24 g, 17.3 mmol). The solution was cooled at 0 °C and

diisopropyl azodicarboxylate (3.37 mL, 17.3 mmol) was added dropwise. The yellow solution was stirred at 0 °C and slowly allowed to reach RT. The reaction mixture was poured into a saturated aqueous solution of $NaHCO_3$ and extracted with EtOAc (2x). The combined organic layers were dried (phase separator) and concentrated. The crude residue was purified by flash chromatography (c-hexane to c-hexane/EtOAc 7:3 in 45 min) to give the tile compound as a pale yellow solid (5.16 g, 87 %). TLC, Rf (c-hexane/EtOAc 7:3): 0.82; HPLC (conditions a), t_R: 2.87 min, purity 100%; MS (ESI^+) *m/z* 377.1/379.1 (M+1); ^1H NMR (400 MHz, DMSO-d_6): δ 7.66 (s, 1H), 7.54 (br d, *J* = 7.9 Hz, 1H), 7.46 (d, *J* = 7.9 Hz, 1H), 7.37 (t, *J* = 7.8 Hz, 1H), 7.25 (td, *J* = 7.8, 1.8 Hz, 1H), 7.22 (dd, *J* = 7.4, 1.7 Hz, 1H), 7.02 (d, *J* = 8.3 Hz, 1H), 6.9 (td, *J* = 7.4, 1.1 Hz, 1H), 5.13 (s, 2H), 3.56 (s, 2H), 1.34 (s, 9H).

tert-Butyl 2-(2-hydroxyphenyl)acetate (**31**): The title compound was prepared as described in WO15009977. To a suspension of (2-hydroxybenzyl)-triphenylphosphonium bromide (10.1 g, 22.5 mmol) in CH_2Cl_2 (75 mL) was added Et_3N (9.35 mL, 67.4 mmol) followed by slow addition of Boc_2O (5.22 mL, 22.5 mmol). The reaction mixture was stirred at 40 °C for 7 days. A saturated aqueous solution of $NaHCO_3$ was added, the layers were separated and the aqueous one back-extracted twice with CH_2Cl_2. The combined organic layers were dried (phase separator) and concentrated. The crude residue was purified by flash column chromatography (c-hexane to c-hexane/EtOAc 8:2 in 50 min) to give the title compound as a pale yellow oil (3.28 g, 70%). TLC, Rf (c-hexane/EtOAc 1:1): 0.85; HPLC (conditions a), t_R: 1.94 min, purity 100%; UPLC/MS (ESI^+) *m/z* 209.1 (M+1); ^1H NMR

(400 MHz, DMSO-d_6): δ 9.43 (s, 1H), 7.09-7.04 (m, 2H), 7.79 (d, J = 7.4 Hz, 1H), 7.73 (td, J = 7.4, 1.2 Hz, 1H), 3.44 (s, 2H), 1.41 (s, 9H).

(*S*)-2-(2-((3-(3-Amino-2,3-dihydrobenzofuran-5-yl)-5-isopropylbenzyl)oxy)phenyl)acetic acid (6): To a solution of (*S*)-*tert*-butyl 2-(2-((3-(3-amino-2,3-dihydrobenzofuran-5-yl)-5-isopropylbenzyl)oxy)phenyl)acetate (154 mg, 0.29 mmol, purity 90%) in dioxane (3 mL) was added a 4 N solution of HCl in dioxane (1.46 mL, 5.85 mmol). The reaction mixture was stirred at RT until completion and then was concentrated under reduced pressure. The crude residue was purified by preparative HPLC (conditions g) and the combined purified fractions were lyophilized to give the title compound (60 mg, 45%). UPLC/MS (ESI$^+$) *m/z* 418.2 (M+1); HPLC (conditions a), t_R: 1.94 min, purity 100%; HPLC (conditions b), t_R: 3.94 min, purity 100%; ^{1}H NMR (600 MHz, DMSO-d_6) δ 7.90 (s, 1H), 7.59 (s, 1H), 7.54 (dd, J = 8.2, 2.0 Hz, 1H), 7.40 (s, 1H), 7.22 (s, 1H), 7.20-7.16 (m, 2H), 7.00 (d, J = 8.1 Hz, 1H), 6.87 (m, 2H), 5.17 (s, 2H), 4.79 (dd, J = 8.4, 5.4 Hz, 1H), 4.70 (t, J = 9.0 Hz, 1H), 4.23 (dd, J = 9.6, 5.4 Hz, 1H), 3.58 (d, J = 15.9 Hz, 1H), 3.50 (d, J = 15.9 Hz, 1H), 2.96 (hept., J = 6.9 Hz, 1H), 1.27 (d, J = 6.9 Hz, 6H); HRMS *m/z* (ESI) calcd for $C_{26}H_{27}NO_4$ [M+H]+ 418.20129; found, 418.20120.

(*S*)-*tert*-Butyl 2-(2-((3-(3-amino-2,3-dihydrobenzofuran-5-yl)-5-isopropylbenzyl)oxy)-phenyl)acetate: To an oven-dried glass vial charged with a stirring bar were subsequently added *tert*-butyl 2-(2-((3-bromo-5-isopropylbenzyl)oxy)phenyl)acetate (**38**) (170 mg, 0.32 mmol), X-Phos-Pd-G2 (2.55 mg, 3.24 μmol), X-Phos (3.09 mg, 6.49 μmol),

tetrahydroxydiboron (87 mg, 0.97 mmol) and KOAc (95 mg, 0.97 mmol). The vessel was sealed, then evacuated and back-filled with argon (x4). EtOH (2.1 mL) was added via syringe and the reaction mixture was heated at 80 °C for 1 h. After completion of the formation of the boronic intermediate, 1.8 M aqueous K_2CO_3 (0.72 mL, 1.30 mmol) was added, followed by the addition of (*S*)-5-bromo-2,3-dihydro-benzofuran-3-ylamine hydrochloride (**45**) (J&W Pharmlab, 81 mg, 0.32 mmol) dissolved in EtOH (2.1 mL). The reaction mixture was heated at 80 °C until completion of the reaction. After cooling to RT, the mixture was diluted with EtOAc, water was added and the layers were separated. The aqueous phase was extracted with EtOAc (x2) and the combined organics were dried (phase separator) and concentrated in vacuo. SiliaMetS®Thiol (particle size: 40-63 μm; loading 1.39 mmol/g; 0.026 mmol, 19 mg) was added to the residue in THF (3 mL) and the mixture was swirled for 1 h at 40 °C, filtered, rinsed with THF and concentrated under reduced pressure. The residue was purified by flash column chromatography on silica gel (CH_2Cl_2 to CH_2Cl_2/MeOH 9:1 in 35 min) to give the title compound (154 mg, 90%). TLC, Rf (CH_2Cl_2/MeOH 9:1): 0.50; UPLC/MS (ESI^+) *m/z* 474.3 (M+1); HPLC (conditions a), t_R: 2.37 min, purity 90%; ^{1}H NMR (400 MHz, DMSO-d_6) δ 7.66 (d, *J* = 2.0 Hz, 1H), 7.48 (s, 1H), 7.46 (dd, *J* = 8.3, 2.0 Hz, 1H), 7.40 (s, 1H), 7.27 (s, 1H), 7.25 (td, *J* = 7.7, 1.8 Hz, 1H), 7.20 (dd, *J* = 7.4, 1.7 Hz, 1H), 7.06 (d, *J* = 8.2 Hz, 1H), 6.91 (t, *J* = 7.9 Hz, 1H), 6.85 (d, *J* = 8.3 Hz, 1H), 5.14 (s, 2H), 4.67-4.60 (m, 2H), 4.09 (dd, *J* = 7.5, 4.3 Hz, 1H), 3.56 (s, 2H), 2.97 (m, 1H), 2.28 (s, 9H), 1.27 (d, *J* = 6.9 Hz, 6H).

tert-Butyl 2-(2-((3-bromo-5-isopropylbenzyl)oxy)phenyl)acetate (**38**): To a solution of *tert*-butyl 2-(2-hydroxyphenyl)acetate (**31**) (0.91 g, 4.36 mmol) in dry THF (35 mL) under a nitrogen atmosphere were subsequently added triphenylphosphine (1.37 g, 5.24 mmol) and (3-bromo-5-isopropylphenyl)methanol (**25**, Supp. Info.) (1.00 g, 4.36 mmol). The solution was cooled to 0 °C and DIAD (1.02 mL, 5.24 mmol) was added dropwise. The yellow solution was allowed to slowly warm up to RT and stirring was continued overnight. The reaction mixture was poured into a saturated aqueous $NaHCO_3$ solution and was extracted with EtOAc (2x). The combined organics were dried (phase separator), concentrated in vacuo, and the residue was purified by flash column chromatography (c-hexane to c-hexane/EtOAc 9:1) to give the title compound (1.40 g, 61%, purity 80%). TLC, Rf (c-hexane/EtOAc 9:1): 0.75; UPLC/MS (ESI^+) *m/z* 419.1/421.1 (M+1); HPLC (conditions a), t_R: 3.16 min, purity 80%; ^1H NMR (400 MHz, DMSO-d_6) δ 7.46 (s, 1H), 7.40 (s, 1H), 7.34 (s, 1H), 7.28-7.20 (m, 2H), 7.02 (d, *J* = 8.3 Hz, 1H), 6.92 (t, *J* = 7.3 Hz, 1H), 5.10 (s, 2H), 3.56 (s, 2H), 2.91 (m, 1H), 1.33 (s, 9H), 1.21 (d, *J* = 6.9 Hz, 6H).

(*S*)-2-(2-((3-(3-Amino-2,3-dihydrobenzofuran-5-yl)-5-(2-cyanopropan-2-yl)benzyl)-oxy)phenyl)acetic acid (7): A round-bottomed flask was charged with methyl 2-(2-((3-bromo-5-(2-cyanopropan-2-yl)benzyl)oxy)phenyl)acetate (**39**) (300 mg, 0.75 mmol), X-Phos-Pd-G2 (5.87 mg, 7.46 µmol), X-Phos (7.11 mg, 0.02 mmol), tetrahydroxydiboron (201 mg, 2.24 mmol) and KOAc (220 mg, 2.24 mmol). The flask was evacuated and back-filled with argon (3x). Then, EtOH (6 mL) was added via syringe and the reaction mixture

was heated at 80 °C for 1 h. After completion of the formation of the boronic intermediate, a 1.8 M aqueous solution of K_2CO_3 (2.07 mL, 3.73 mmol) was added via syringe, followed by the addition of (*S*)-5-bromo-2,3-dihydrobenzofuran-3-amine hydrochloride (**45**) (187 mg, 0.75 mmol). The reaction mixture was stirred at 80 °C until completion (17 h). Volatiles were removed under reduced pressure and the residue was dissolved in THF (6 mL), MeOH (2 mL) and water (0.6 mL), followed by addition of 1 M aqueous NaOH (6.24 mL, 6.24 mmol) and the mixture was stirred at RT for 16 h. Volatiles were removed under reduced pressure and the aqueous layer was acidified by the addition of 1 N aqueous HCl, followed by lyophilization. To the residue dissolved in THF (2 mL) was added SiliaMetS®Thiol (30 μmol, 21 mg) and the mixture was swirled for 1 h at 40 °C, filtered, washed with THF and the filtrate was concentrated under reduced pressure. The residue was purified by preparative HPLC (conditions g). The fractions containing the product were combined and lyophilized to give the title compound as a white powder (121 mg, 37%). UPLC/MS (conditions c), t_R: 0.82 min, purity 99.5%; UPLC/MS (conditions d), t_R: 3.07 min, purity 100%, UPLC/MS (ESI$^+$) *m/z* 443.2 (M+1); ^{1}H NMR (600 MHz, DMSO-d_6) δ 7.94 (s, 1H), 7.77 (s, 1H), 7.65 (s, 1H), 7.60 (dd, *J* = 8.3, 2.0 Hz, 1H), 7.50 (s, 1H), 7.21-7.17 (m, 2H), 7.01 (d, *J* = 8.1 Hz, 1H), 6.91 (d, *J* = 8.3 Hz, 1H), 6.88 (t, *J* = 7.3 Hz, 1H), 5.24 (s, 2H), 4.81 (m, 1H), 4.72 (t, *J* = 9.0 Hz, 1H), 4.25 (dd, *J* = 9.6, 5.3 Hz, 1H), 3.59 (d, *J* = 15.8 Hz, 1H), 3.50 (d, *J* = 15.8 Hz, 1H), 1.77 (s, 3H), 1.76 (s, 3H); HRMS *m/z* (ESI) calcd for $C_{27}H_{26}N_2O_4$ [M+H]+ 443.19653; found, 443.19635.

Methyl 2-(2-((3-bromo-5-(2-cyanopropan-2-yl)benzyl)oxy)phenyl)acetate (**39**): To a solution of methyl 2-(2-hydroxyphenyl)acetate (**30**) (301 mg, 1.81 mmol), triphenylphosphine (570 mg, 2.17 mmol) and 2-(3-bromo-5-(hydroxylmethyl)phenyl)-2-methylpropanenitrile (**26**, Supp. Info.) (460 mg, 1.81 mmol) in dry THF (18 mL) under nitrogen atmosphere, cooled to 0 °C, was added DIAD (422 µL, 2.17 mmol). The ice bath was removed and the mixture was stirred at RT for 3 h. The reaction mixture was poured into a saturated aqueous solution of $NaHCO_3$ and extracted with EtOAc (2x). The combined organic extracts were dried (phase separator) and concentrated under reduced pressure. The residue was purified by flash column chromatography on silica gel (c-hexane to c-hexane/EtOAc 7:3) to give the title compound as a colorless oil (428 mg, 59%). TLC Rf (c-hexane/EtOAc 7:3) = 0.57; UPLC/MS (conditions c), t_R: 1.37 min, purity 100%; UPLC/MS (ESI^+) *m/z* 402.1/404.1 (M+1); ^1H NMR (400 MHz, DMSO-d_6) δ 7.66 (br. s, 1H), 7.61 (br. s, 2H), 7.30-7.24 (m, 2H), 7.06 (d, *J* = 8.1 Hz, 1H), 6.95 (t, *J* = 7.5 Hz, 1H), 5.17 (s, 2H), 3.68 (s, 2H), 3.59 (s, 3H), 1.72 (s, 6H).

(*S*)-2-(2-((3-(3-Amino-2,3-dihydrobenzofuran-5-yl)-5-(2-hydroxypropan-2-yl)benzyl)oxy)phenyl)acetic acid (8): To a solution of (*S*)-tert-butyl 2-(2-((3-(3-amino-2,3-dihydrobenzofuran-5-yl)-5-(2-hydroxypropan-2-yl)benzyl)oxy)phenyl)acetate (55 mg, 0.11 mmol) in dioxane (1 mL) was added HCl (4N in dioxane, 0.56 mL, 2.25 mmol) and the reaction mixture was stirred at RT for 16 h. The reaction mixture was concentrated and the residue was purified by preparative HPLC (conditions g) to give after lyophilization

of the compound containing fractions the title compound (19 mg, 39 %). UPLC/MS (ESI^+) *m/z* 434.3 (M+1); HPLC (conditions a) t_R: 1.59 min, purity 100%; HPLC (conditions b) t_R: 2.96 min, purity 100%; ^1H NMR (600 MHz, DMSO-d_6) δ 7.90 (s, 1H), 7.65 (s, 1H), 7.62 (s, H), 7.53 (dd, *J* = 8.4, 2.0 Hz, 1H), 7.42 (s, 1H), 7.20-7.16 (m, 2H), 7.00 (d, *J* = 8.1 Hz, 1H), 6.89- 6.86 (m, 2H), 5.18 (s, 2H), 4.80 (dd, *J* = 8.4, 5.5 Hz, 1H), 4.70 (t, *J* = 9.0 Hz, 1H), 4.23 (dd, *J* = 9.6, 5.3 Hz, 1H), 3.58 (d, *J* = 15.8 Hz, 1H), 3.50 (d, *J* = 15.8 Hz, 1H), 1.49 (s, 3H), 1.48 (s, 3H); HRMS *m/z* (ESI) calcd for $C_{26}H_{27}NO_5$ [M+H]+ 434.1962; found, 434.19611.

(*S*)-*tert*-Butyl 2-(2-((3-(3-amino-2,3-dihydrobenzofuran-5-yl)-5-(2-hydroxypropan-2-yl): In an oven dried glass vessel was added *tert*-butyl 2-(2-((3-bromo-5-(2-hydroxypropan-2-yl)benzyl)oxy)phenyl)acetate (**41**, Supp. Info.) (85 mg, 0.18 mmol), X-Phos-Pd-G2 (1.41 mg, 1.79 µmol), X-Phos (1.71 mg, 3.59 µmol), tetrahydroxydiboron (48.3 mg, 0.54 mmol) and KOAc (52.9 mg, 0.54 mmol). The vessel was sealed and then evacuated and backfilled with argon (x4). EtOH 1.2 mL (degassed during 10 minutes) was added via syringe. The reaction mixture was then heated to 80 °C for 1 h. UPLC indicates formation of the boronic intermediate. Then K_2CO_3 (1.8M aqueous, 0.40 mL, 0.72 mmol) degassed was added followed by the addition of (*S*)-5-bromo-2,3-dihydro-benzofuran-3-ylamine hydrochloride (**45**) (45.0 mg, 0.18 mmol) in a solution in degassed EtOH (1.2 mL). The reaction mixture was heated at 80 °C for 60 h. The reaction mixture was filtered through a pad of celite, and the solvents were evaporated. The residue was taken up in THF (3 mL) and SiliaMetS®Thiol (Particle Size: 40-63 µm, loading 1.39 mmol/g, 0.007 mmol, 5

mg) was added and the mixture swirled at 40°C for 1h, then filtered, and the filtrate was concentrated. The crude residue was purified by flash chromatography (eluent: CH_2Cl_2 to CH_2Cl_2/MeOH 9:1 in 35 min) to give the title compound as a pale beige oil (55 mg, 63%). TLC, Rf (CH_2Cl_2/MeOH 9:1): 0.50; HPLC (conditions a), t_R: 2.03 min; purity 100%; UPLC/MS (ESI$^+$) *m/z* 490.3 (M+1); ^{1}H NMR (400 MHz, DMSO-d_6) δ 7.66 (br. s, 2H), 7.50-7.44 (m, 3H), 7.25 (td, *J* = 7.9, 1.8 Hz, 1H), 7.20 (dd, *J* = 7.4, 1.7 Hz, 1H), 7.07 (d, *J* = 8.1 Hz, 1H), 6.91 (t, *J* = 7.3 Hz, 1H), 6.85 (d, *J* = 8.3 Hz, 1H), 5.16 (s, 2H), 5.09 (s, 1H), 4.67-4.60 (m, 2H), 4.09 (dd, *J* = 7.5, 4.2 Hz, 1H), 3.56 (s, 2H), 1.49 (s, 6H), 1.27 (s, 9H).

(*S*)-2-(2-((3-(3-Amino-2,3-dihydrobenzofuran-5-yl)-5-(1-amino-2-methyl-1-oxopropan-2-yl)benzyl)oxy)phenyl)acetic acid trifluoroacetate (9): A round bottom flask was charged with methyl 2-(2-((3-bromo-5-(2-cyanopropan-2-yl)benzyl)oxy)phenyl)acetate (**39**) (178 mg, 0.44 mmol), X-Phos-Pd-G2 (3.48 mg, 4.42 µmol), X-Phos (4.22 mg, 8.85 µmol), tetrahydroxydiboron (119 mg, 1.33 mmol) and KOAc (130 mg, 1.33 mmol). The flask was evacuated under vacuum and backfilled with argon (3x). EtOH (4.5 mL) was added via syringe and the reaction mixture was heated at 80 °C for 1.5 h. After conversion of the starting material into the corresponding boronic acid, K_2CO_3 (1.8 M in water; 0.98 mL, 1.77 mmol) and (*S*)-5-bromo-2,3-dihydrobenzofuran-3-amine hydrochloride (**45**) (111 mg, 0.44 mmol) were added and the reaction mixture was stirred at 80 °C for 18 h. Volatiles were removed under reduced pressure, the residue was dissolved in t-BuOH (2 mL) and water (0.1 mL) and a 1 M aqueous NaOH solution (4.42 mL, 4.42 mmol) was added. The

mixture was stirred at 120 °C for 5 h and subsequently at 80 °C for 17 h. The reaction mixture was concentrated under reduced pressure; the residual aqueous layer was acidified by addition of 4 M aqueous HCl and then lyophilized. The residue was taken up in THF (5 mL), SiliaMetS®Thiol (18 μmol, 4.5 mg (particle size: 40-63 μm; loading 1.39 mmol/g) was added and the mixture was swirled at 40 °C for 1 h, filtered, washed with THF and the filtrate was concentrated. The residue was purified by preparative HPLC (condition j) to give after lyophilization the title compound as a TFA salt as a white solid (68 mg, 27%), the corresponding nitrile precursor was also isolated (45 mg, 18%). UPLC/MS (conditions c), t_R: 0.70 min, purity 100%; UPLC/MS (conditions d), t_R: 2.55 min, purity 100%, UPLC/MS (ESI$^+$) *m/z* 461.3 (M+1); ^{1}H NMR (600 MHz, DMSO-d_6) δ 12.2 (br.s, 1H), 8.43 (br.s, 3H), 7.83 (s, 1H), 7.64 (dd, *J* = 8.5, 2.0 Hz, 1H), 7.54 (s, 1H), 7.46 (s, 1H), 7.44 (s, 1H), 7.27-7.23 (m, 2H), 7.09 (d, *J* = 8.2 Hz, 1H), 7.05 (d, *J* = 8.4 Hz, 1H), 6.98 (br. s, 1H), 6.94-9.91 (m, 2H), 5.17 (s, 2H), 5.13 (dd, *J* = 8.2, 3.5 Hz, 1H), 4.77 (dd, *J* = 10.9, 8.2 Hz, 1H), 4.54 (dd, *J* = 10.9, 3.5 Hz, 1H), 3.60 (s, 2H), 1.52 (s, 3H), 1.51 (s, 3H); HRMS *m/z* (ESI) calcd for $C_{27}H_{28}N_2O_5$ [M+H]+ 461.20710; found, 461.20700.

2-(2-((3-(2-Hydroxypropan-2-yl)-5-(1,2,3,4-tetrahydroisoquinolin-7-yl)benzyl)oxy)phenyl)acetic acid (10): To a solution of *tert*-butyl 7-(3-((2-(2-(tert-butoxy)-2-oxoethyl)phenoxy)methyl)-5-(2-hydroxypropan-2-yl)phenyl)-3,4-dihydroisoquinoline-2(1H)-carboxylate (35 mg, 0.06 mmol) in dioxane (0.8 mL) was added HCl (4N in dioxane, 447 μL, 1.79 mmol). The solution was stirred at RT for 15 h. HCl (4N in dioxane, 149 μL,

0.60 mmol) was again added and the reaction mixture was further stirred at RT for 3 h, then heated at 60 °C for 1 h. The reaction mixture was concentrated and the crude residue was purified by preparative HPLC (conditions h) to give the title compound as a white solid (3 mg, 20%). HPLC (conditions a), t_R: 1.60 min, purity 97%; HPLC (conditions b), t_R: 3.0 min, purity 97%; UPLC/MS (ESI$^+$) *m/z* 432.3 (M+1); ^{1}H NMR (400 MHz, DMSO-d_6) δ 7.69 (br. s, 1H), 7.66 (br. s, 1H), 7.50 (br. s, 1H), 7.45 (dd, *J* = 7.9, 2.0 Hz, 1H), 7.37 (br. s, 1H), 7.27-7.22 (m, 2H), 7.18 (d, *J* = 8.0 Hz, 1H), 7.09 (d, *J* = 8.0 Hz, 1H), 6.92 (t, *J* = 7.3 Hz, 1H), 5.17 (s, 2H), 3.99 (s, 2H), 3.60 (s, 2H), 3.04 (t, *J* = 5.8 Hz, 1H), 2.77 (t, *J* = 5.9 Hz, 1H), 4.47 (m, 2H), 1.49 (s, 6H).

tert-Butyl 7-(3-((2-(2-(tert-butoxy)-2-oxoethyl)phenoxy)methyl)-5-(2-hydroxypropan-2-yl)phenyl)-3,4-dihydroisoquinoline-2(1H)-carboxylate: A microwave vial was charged with tert-butyl 2-(2-((3-bromo-5-(2-hydroxypropan-2-yl)benzyl)oxy)phenyl)acetate (**41**, Supp. Info.) (62 mg, 0.14 mmol), 2-boc-1,2,3,4-tetrahydroisoquinolin-7-ylboronic acid (**50**) (43.2 mg, 0.16 mmol), K_3PO_4 (2N in water, 0.21 mL, 0.43 mmol) and $PdCl_2$(dppf).CH_2Cl_2 adduct (5.8 mg, 7.09 µmol) in acetonitrile (1.9 mL). The reaction mixture was heated at 120 °C for 40 min under microwave irradiations. The reaction mixture was filtrated through a pad of celite, the solvents were evaporated and the residue was taken up in THF (2 mL), SiliaMetS®Thiol (Particle Size: 40-63 µm, loading 1.39 mmol/g, 0.028 mmol, 20 mg) was added and the mixture was swirled at 40°C for 1 h, filtered, washed with THF and the filtrate was concentrated. The crude residue was purified by flash chromatography (Isco companion, column 12 g, flow: 25 mL/min, eluent: c-hexane to c-hexane/EtOAc 4-1 in 25

min, then hold 10 min) to give the title compound as a white foam (36 mg, 43 %). HPLC (conditions a), t_R: 2.99 min, purity 100%; UPLC/MS (ESI+) *m/z* 588.3 (M+1); ^{1}H NMR (400 MHz, DMSO-d_6) δ 7.70 (br. s, 1H), 7.57 (br. s, 1H), 7.51-7.48 (m, 3H), 7.27-7.20 (m, 3H), 7.03 (d, *J* = 8.3 Hz, 1H), 6.91 (t, *J* = 7.6 Hz, 1H), 5.17 (s, 2H), 5.11 (s, 1H), 4.59 (m, 2H), 3.59 (m, 2H), 3.56 (s, 2H), 2.82 (m, 2H), 1.52 (s, 6H), 1.45 (s, 9H).

(*S*)-2-(2-((3'-Amino-3,3-dimethyl-2,2',3,3'-tetrahydro-[5,5'-bibenzofuran]-7-yl)methoxy)phenyl)acetic acid (11): The title compound (592 mg, 53%) was prepared from methyl 2-(2-((5-bromo-3,3-dimethyl-2,3-dihydrobenzofuran-7-yl)methoxy)phenyl)acetate (**42**) (1.00 g, 2.47 mmol) and (*S*)-5-bromo-2,3-dihydro-benzofuran-3-ylamine hydrochloride (**45**) (618 mg, 2.47 mmol) in a similar manner as described for the preparation of (*S*)-2-(2-((3-(3-amino-2,3-dihydrobenzofuran-5-yl)-5-(2-cyanopropan-2-yl)benzyl)oxy)phenyl)acetic acid (**7**). The title compound was purified by preparative HPLC (conditions h). UPLC/MS (conditions c), t_R: 0.90 min, purity 100%; UPLC/MS (conditions d), t_R: 3.47 min, purity 100%, UPLC/MS (ESI+) *m/z* 446.3 (M+1); ^{1}H NMR (600 MHz, DMSO-d_6) δ 7.88 (s, 1H), 7.57 (s, 1H), 7.50 (d, *J* = 8.3 Hz, 1H), 7.41 (s, 1H), 7.19-7.14 (m, 2H), 6.97 (d, *J* = 8.1 Hz, 1H), 6.87-6.84 (m, 2H), 5.13 (d, *J* = 13.1 Hz, 1H), 5.09 (d, *J* = 13.1 Hz, 1H), 4.81 (m, 1H), 4.70 (t, *J* = 9.0 Hz, 1H), 4.33 (s, 2H), 4.24 (dd, *J* = 9.8, 5.2 Hz, 1H), 3.57 (d, *J* = 15.7 Hz, 1H), 3.46 (d, *J* = 15.7 Hz, 1H), 1.37 (s, 3H), 1.35 (s, 3H). HRMS *m/z* (ESI) calcd for $C_{27}H_{27}NO_5$ [M+H]+ 446.1962; found, 446.19614.

Methyl 2-(2-((5-bromo-3,3-dimethyl-2,3-dihydrobenzofuran-7-yl)methoxy)phenyl)acetate (**42**): The title compound (1.42 g, 67%) was prepared from (5-bromo-3,3-dimethyl-2,3-dihydrobenzofuran-7-yl)methanol (**29**, Supp. Info.) (1.34 g, 5.21 mmol) and methyl 2-(2-hydroxyphenyl)acetate (**30**) (0.87 g, 5.21 mmol) in a similar manner as described for the preparation of *tert*-butyl 2-(2-((3-bromo-5-isopropylbenzyl)oxy)phenyl)acetate (**38**). TLC, Rf (c-hexane/EtOAc 9:1): 0.50; UPLC/MS (conditions c), t_R: 1.51 min, purity 98%; UPLC/MS (ESI^+) *m/z* 405.1/407.1 (M+1); ^1H NMR (400 MHz, DMSO-d_6) δ 7.41 (d, *J* = 2.1 Hz, 1H), 7.33 (d, *J* = 2.1 Hz, 1H), 7.29-7.22 (m, 2H), 7.06 (d, *J* = 8.3 Hz, 1H), 6.94 (t, *J* = 7.4 Hz, 1H), 5.01 (s, 2H), 4.31 (s, 2H), 3.64 (s, 2H), 3.59 (s, 3H), 1.32 (s, 6H).

(*R*)-2-(2-((5-(4-Aminochroman-6-yl)-3,3-dimethyl-2,3-dihydrobenzofuran-7-yl)methoxy)phenyl)acetic acid trifluoroacetate (12): The title compound (14.5 mg, 21%) was prepared from methyl 2-(2-((5-bromo-3,3-dimethyl-2,3-dihydrobenzofuran-7-yl)methoxy)phenyl)acetate (**42**) (50 mg, 0.12 mmol) and (*R*)-6-bromochroman-4-amine hydrochloride (**46**) (32.6 mg, 0.12 mmol) in a similar manner as described for the preparation of (*S*)-2-(2-((3-(3-amino-2,3-dihydrobenzofuran-5-yl)-5-(2-cyanopropan-2-yl)benzyl)oxy)phenyl)acetic acid (**7**). The title compound was purified by preparative HPLC (conditions g) then again by preparative HPLC (column: Waters Sunfire C18 OBD; particle size: 5 µm; column size: 30 x 100 mm; eluent: 5-100% CH_3CN/H_2O in 20 min, 100% CH_3CN/3 min (CH_3CN and H_2O containing 0.1% TFA); flow rate: 40 mL/min; column temperature: RT) and the compound containing fractions were lyophilized to give

the title compound as a trifluoroacetate salt. UPLC/MS (conditions c), t_R: 0.96 min, purity 100%; UPLC/MS (conditions d), t_R: 3.71 min, purity 100%; UPLC/MS (ESI$^+$) *m/z* 460.3 (M+1); ^{1}H NMR (400 MHz, DMSO-d_6) δ 7.75 (br. s, 1H), 7.56 (dd, *J* = 8.6, 2.3 Hz, 1H), 7.51 (br. s, 1H), 7.43 (d, *J* = 2.0 Hz, 1H), 7.26-7.20 (m, 2H), 7.07 (d, *J* = 8.1 Hz, 1H), 6.92 (d, *J* = 8.3 Hz, 1H), 6.91 (t, *J* = 7.3 Hz, 1H), 5.09 (s, 2H), 4.58 (m, 1H), 4.35 (s, 2H), 4.28 (m, 2H), 3.58 (s, 2H), 2.29 (m, 1H), 2.10 (m, 1H), 1.38 (s, 6H).

2-((*R*)-2-(3-((S)-3-Amino-2,3-dihydrobenzofuran-5-yl)-5-isopropylphenyl)-3,4-dihydro-2H-benzo[b][1,4]oxazin-8-yl)acetic acid (13): To a solution of 2-(2-(3-((S)-3-((*tert*-butoxycarbonyl)amino)-2,3-dihydrobenzofuran-5-yl)-5-isopropylphenyl)-3,4-dihydro-2H-benzo[b][1,4]oxazin-8-yl)acetic acid (84 mg, 0.15 mmol) in dioxane (0.8 mL) was added 4N HCl in dioxane (0.77 mL, 3.08 mmol). The reaction mixture was shaken at RT for 18 h. The volatiles were removed under reduced pressure, and the residue was taken up in CH_3CN, the solvent removed under reduced pressure, and the residue was purified by reversed phase column chromatography (RediSep Rf GOLD 50 g C18 column; Eluent A: H_2O+0.1% TFA, B: CH_3CN, Gradient: 10% to 100% B in 13 min, flow 40 mL/min) to afford 2-(2-(3-((S)-3-amino-2,3-dihydrobenzofuran-5-yl)-5-isopropylphenyl)-3,4-dihydro-2H-benzo[b][1,4]oxazin-8-yl)acetic acid as a trifluoroacetate salt (55 mg, 63%). UPLC/MS (ESI$^+$) *m/z* 445 (M+1), t_R: 3.33 min, purity 99% (conditions d). ^{1}H NMR (400 MHz, DMSO-d_6) δ 8.38 (s, 3H), 7.86 (s, 1H), 7.69 (d, *J* = 8.7 Hz, 1H), 7.47 (s, 1H), 7.41 (s, 1H), 7.34 (s, 1H), 7.05 (d, *J* = 8.4 Hz, 1H), 6.67 (t, *J* = 7.6 Hz, 1H), 6.61-6.55 (m, 1H), 6.48 (d, J =

6.9 Hz, 1H), 5.98 (m, 1H), 5.13 (m, 1H), 5.06 (d, *J* = 8.3 Hz, 1H), 4.78 (t, *J* = 10.1 Hz, 1H), 4.55 (dd, *J* = 10.9, 3.5 Hz, 1H), 3.59 (d, *J* = 10.9 Hz, 1H), 3.50 (s, 1H), 3.22-3.13 (m, 1H), 3.03-2.95 (m, 2H), 1.29 (d, *J* = 6.9 Hz, 6H). The diastereomers (50 mg, 0.11 mmol) were separated by preparative HPLC (Sepiatec ASAP HPLC System; column: Chiralpak ID 250 x 20 mm 5µm; eluent: n-Heptan:CH_2Cl_2:MeOH 85:7.5:7.5 (v:v:v + 0.05% Et_2NH); flow: 10 mL/min; temperature: RT; detection at 270 nm). The title compound eluted as the first peak from the column (t_R = 55 min) (5.7 mg, 11%, > 99% chiral purity). UPLC/MS (conditions d), t_R: 3.33 min, purity 100%; MS (ESI$^+$) *m/z* 445 (M+1). ^{1}H NMR (400 MHz, DMSO-d_6) δ 7.91 (s, 1H), 7.57 (s, 1H), 7.51 (dd, *J* = 8.4, 2.0 Hz, 1H), 7.39 (s, 1H), 7.22 (s, 1H), 6.86 (d, *J* = 8.3 Hz, 1H), 6.58 (t, *J* = 7.6 Hz, 1H), 6.51-6.44 (m, 2H), 5.78 (s, 1H), 5.17 (dd, *J* = 7.7, 2.7 Hz, 1H), 4.77 (dd, *J* = 8.3, 5.2 Hz, 1H), 4.69 (t, *J* = 8.9 Hz, 1H), 4.21 (dd, *J* = 9.5, 5.2 Hz, 1H), 3.58-3.51 (m, 3H), 3.05 (dd, *J* = 11.8, 8.0 Hz, 1H), 3.00-2.91 (m, 1H), 1.26 (dd, *J* = 7.0, 1.7 Hz, 6H).

2-(2-(3-((*S*)-3-((*tert*-Butoxycarbonyl)amino)-2,3-dihydrobenzofuran-5-yl)-5-isopropylphenyl)-3,4-dihydro-2H-benzo[b][1,4]oxazin-8-yl)acetic acid: To a solution of ethyl 2-(2-(3-((*S*)-3-((*tert*-butoxycarbonyl)amino)-2,3-dihydrobenzofuran-5-yl)-5-isopropylphenyl)-3,4-dihydro-2H-benzo[b][1,4]oxazin-8-yl)acetate (95 mg, 0.154 mmol) in THF/water/MeOH (1:0.1:0.5, 3 2 mL) was added 1M NaOH aqueous solution (1.54 mL, 1.54 mmol). The reaction mixture was stirred at RT for 18 h. The volatiles were removed under reduced pressure, and the residual aqueous layer was acidified with 1N hydrochloric acid followed by extraction with CH_2Cl_2 (2x). The combined organic layers

were dried (phase separator) and evaporated to afford the title compound, which was used without purification (108 mg, quant.). MS (ESI+) *m/z* 545 (M+1); ^{1}H NMR (400 MHz, DMSO-d_6) δ 7.79-7.73 (m, 1H), 7.63-7.61 (m, 1H), 7.52 (t, *J* = 7.1Hz, 1H), 7.46 (s, 1H), 7.36 (s, 1H), 7.27 (s, 1H), 6.88 (d, *J* = 6.9Hz, 1H), 6.53 (dd, *J* = 8.3, 6.8Hz, 1H), 6.49-6.44 (m, 1H), 6.40 (d, *J* = 7.7Hz, 1H), 5.69 (s, 1H), 5.34-5.25 (m, 1H), 5.03-4.95 (m, 1H), 4.76-4.66 (m, 1H), 4.27-4.21 (m, 1H), 3.50 (m, 1H), 3.18-3.11 (m, 2H), 3.01-2.92 (m, 1H), 2.56-2.54 (m, 1H), 1.41 (s, 9H), 1.26 (d, *J* = 6.9Hz, 6H).

Ethyl 2-(2-(3-((*S*)-3-((*tert*-butoxycarbonyl)amino)-2,3-dihydrobenzofuran-5-yl)-5-isopropylphenyl)-3,4-dihydro-2H-benzo[b][1,4]oxazin-8-yl)acetate: To a solution of ethyl 2-(2-(3-bromo-5-isopropylphenyl)-3,4-dihydro-2H-benzo[b][1,4]oxazin-8-yl)acetate (95 mg, 0.23 mmol) in CH_3CN (4.5 mL) were added (*S*)-(3-((*tert*-butoxycarbonyl)amino)-2,3-dihydrobenzofuran-5-yl)boronic acid (**47,** Supp. Info.) (63.4 mg, 0.23 mmol) and 2M K_3PO_4 aqueous solution (0.34 mL, 0.68 mmol). The reaction was degassed with argon for 2 min and then $PdCl_2$(dppf).CH_2Cl_2 adduct (9.27 mg, 0.011 mmol) was added. The reaction was stirred at 125 °C for 30 min under microwave irradiation. The reaction mixture was diluted with EtOAc and washed with water and brine. The organic layer was dried (Na_2SO_4), filtered and concentrated under reduced pressure. The crude residue was purified by flash column chromatography (100% c-hexane to c-hexane/EtOAc (7:3) in 15 min) to afford the title compound (95 mg, 68%). MS (ESI+) *m/z* 573 (M+1); ^{1}H NMR (400 MHz, DMSO-d_6) δ 7.57 (m, 2H), 7.50 (d, *J* = 8.4 Hz, 1H), 7.40 (s, 1H), 7.37 (s, 1H), 7.23 (s, 1H), 6.89 (d, *J* = 8.1 Hz, 1H), 6.65 (t, *J* = 7.6 Hz, 1H), 6.57 (d, *J* = 8.2 Hz, 1H),

6.45 (d, *J* = 7.3 Hz, 1H), 5.98 (s, 1H), 5.31 (m, 1H), 5.02-4.95 (m, 1H), 4.70 (t, *J* = 9.1 Hz, 1H), 4.26 (m, 1H), 3.95 (m, 2H), 3.56 (m, 1H), 3.52 (s, 2H), 3.15 (t, *J* = 10.3 Hz, 1H), 2.95 (m, 1H), 1.40 (s, 9H), 1.25 (d, *J* = 6.9 Hz, 6H), 1.01 (td, *J* = 7.0, 2.3 Hz, 3H).

Ethyl 2-(2-(3-bromo-5-isopropylphenyl)-3,4-dihydro-2H-benzo[b][1,4]oxazin-8-yl)acetate: To a solution of 2-(2-(3-bromo-5-isopropylphenyl)-3-oxo-3,4-dihydro-2H-benzo[b][1,4]oxazin-8-yl)acetate (138 mg, 0.319 mmol) in THF (3 mL) at 0°C was added $BH_3.Me_2S$ (61 μL, 0.638 mmol). The reaction mixture was stirred at RT for 4 h, then was cooled to 0 °C, quenched with water and extracted with EtOAc (2x). The combined organic layer was washed with brine, dried (phase separator), the solvent evaporated under reduced pressure and the residue was purified by flash column chromatography (eluent: 100% c-hexane to c-hexane/EtOAc (1:1) in 20 min) to afford the title compoud (95.7 mg, 72% yield). MS (ESI^+) *m/z* 418/420 (M+1); ^1H NMR (400 MHz, DMSO-d_6) δ 7.42 – 7.37 (m, 2H), 7.31 (s, 1H), 6.65 (t, *J* = 7.6 Hz, 1H), 6.56 (dd, *J* = 7.9, 1.6 Hz, 1H), 6.45 (dd, *J* = 7.3, 1.6 Hz, 1H), 5.98 (d, *J* = 3.5 Hz, 1H), 4.98 (dd, *J* = 8.5, 2.5 Hz, 1H), 4.03 (q, *J* = 7.1 Hz, 2H), 3.57 – 3.46 (m, 3H), 3.07 (dd, *J* = 11.4, 8.0 Hz, 1H), 2.90 (p, *J* = 6.8 Hz, 1H), 1.20 (d, *J* = 6.9 Hz, 6H), 1.09 (t, *J* = 7.1 Hz, 3H).

Ethyl 2-(2-(3-Bromo-5-isopropylphenyl)-3-oxo-3,4-dihydro-2H-benzo[b][1,4]oxazin-8-yl)acetate: To a flask charged with NaH (60% in mineral oil, 79 mg, 1.97 mmol) was added a solution of ethyl 2-(3-amino-2-hydroxyphenyl)acetate (240 mg, 0.98 mmol) in DMF (4 mL). The solution was stirred at RT for 10 min, then methyl 2-bromo-2-(3-bromo-5-isopropylphenyl)acetate (174 mg, 0.49 mmol) in DMF (6 mL) was added dropwise and

the reaction mixture was stirred at RT for 2 h. The reaction mixture was quenched with water and extracted with EtOAc (2x). The combined organic layer was washed with brine, dried (phase separator), the solvent evaporated under reduced pressure and the residue was purified by flash column chromatography (100% c-hexane to c-hexane/EtOAc (1:1) in 15 min) to afford the title compound (139 mg, 65%). MS (ESI^+) *m/z* 432/434 (M+1); ^1H NMR (400 MHz, DMSO-d_6) δ 10.98 (s, 1H), 7.46 (m, 1H), 7.32 (t, *J* = 1.7 Hz, 1H), 7.25 (m, 1H), 6.99-6.85 (m, 3H), 5.73 (s, 1H), 4.04-3.95 (m, 2H), 3.63 (d, *J* = 4.0 Hz, 2H), 2.96-2.85 (m, 1H), 1.17 (d, *J* = 6.9 Hz, 6H), 1.09 (t, *J* = 7.1 Hz, 3H).

Methyl 2-bromo-2-(3-bromo-5-isopropylphenyl)acetate*:* To a solution of methyl 2-(3-bromo-5-isopropylphenyl)acetate (500 mg, 1.75 mmol) in THF (9 mL) at -78°C was added dropwise LiHMDS (1M solution in THF, 1.93 mL, 1.93 mmol) under inert atmosphere. The reaction mixture was stirred at -78°C for 15 min. Then, TMSCl (0.425 mL, 3.33 mmol) was added and stirring continued at -78°C for 15 min. Then N-bromosuccinimide (327 mg, 1.84 mmol) was added to the reaction mixture which was subsequently warmed to RT and stirred at RT for 16 h. The reaction mixture was diluted with water and extracted with EtOAc (2x). The combined organic layer was washed with brine, dried (phase separator), the solvent evaporated under reduced pressure and the residue was purified by reversed phase column chromatography (RediSep Rf GOLD 50 g C18 column, Eluent A: H_2O+0.1% TFA, B: CH_3CN, Gradient: 10% to 100% B in 13 min, flow 40 mL/min) to afford the title compound (174 mg, 28%). MS (ESI^+) *m/z* 368/370 (M+18); ^1H NMR (400

MHz, DMSO-d_6) δ 7.56 (t, J = 1.7 Hz, 1H), 7.46 (t, J = 1.7 Hz, 1H), 7.43 (t, J = 1.5 Hz, 1H), 5.93 (s, 1H), 3.73 (s, 3H), 2.91 (hept, J = 7.3 Hz, 1H), 1.19 (d, J = 6.9 Hz, 6H).

Methyl 2-(3-bromo-5-isopropylphenyl)acetate: To a solution of 2-(3-bromo-5-isopropylphenyl)acetic acid (1.48 g, 5.4 mmol) in THF/MeOH (1:1, 44 mL) was added dropwise over 30 min trimethylsilyldiazomethane (2M solution in Et_2O, 5.41 mL, 10.82 mmol) and the reaction mixture was stirred at RT for 4 h. The volatiles were evaporated under reduced pressure and the residue was purified by flash column chromatography (100% c-hexane to c-hexane/EtOAc (1:1) in 20 min) to afford the title compound (1.25 g, 81%). MS (ESI$^+$) *m/z* 288/290 (M+18); ^{1}H NMR (400 MHz, DMSO-d_6) δ 7.33 (t, J = 1.7 Hz, 1H), 7.30 (t, J = 1.6 Hz, 1H), 7.15 (t, J = 1.5 Hz, 1H), 3.69 (s, 2H), 3.62 (s, 3H), 2.87 (hept, J = 6.9 Hz, 1H), 1.18 (d, J = 6.9 Hz, 6H).

2-(3-bromo-5-isopropylphenyl)acetic acid: To a solution of 2-(3-bromo-5-isopropylphenyl)acetonitrile (1.40 g, 5.84 mmol) in EtOH/H_2O (1:1, 22 mL) were added KOH (1.64 g, 29 mmol). The reaction mixture was stirred at 85 °C for 18 h then cooled to RT and the volatiles evaporated under reduced pressure. The residue was taken up in 1N aqueous HCl and extracted with EtOAc (2x). The combined organic layers were washed with brine, dried (phase separator), the solvent evaporated under reduced pressure to provide the title compound which was used without further purification (1.48 g, 93%). MS (ESI$^+$) *m/z* 274/276 (M+18); ^{1}H NMR (400 MHz, DMSO-d_6) δ 12.40 (s, 1H), 7.31 (t, J = 1.7 Hz, 1H), 7.28 (t, J = 1.7 Hz, 1H), 7.14 (t, J = 1.6 Hz, 1H), 3.57 (s, 2H), 2.87 (hept, J = 6.9 Hz, 1H), 1.18 (d, J = 6.9 Hz, 6H).

2-(3-bromo-5-isopropylphenyl)acetonitrile: A solution of (3-bromo-5-isopropylphenyl)methanol (**25,** Supp. Info.) (1.85 g, 7.9 mmol), Et_3N (1.64 ml, 11.9 mmol) and MsCl (0.74 mL, 9.5 mmol) in CH_2Cl_2 (30 mL) was stirred at 0 °C for 30 min. The reaction mixture was diluted with CH_2Cl_2 and washed with H_2O (2x). The organic layer was dried (phase separator), the solvent evaporated under reduced pressure, the crude intermediate was dissolved in dry DMF (30 mL) and sodium cyanide (0.76 g, 15.8 mmol) was added. The reaction mixture was stirred at RT for 56 h. The reaction mixture was diluted with water and extracted with EtOAc (2x). The organic layer was washed with brine, dried (phase separator), the solvent evaporated under reduced pressure and the residue was purified by flash column chromatography (100% c-hexane to c-hexane/EtOAc (4:1) in 15 min) to afford the title compound (1.39 g, 73%). ^{1}H NMR (400 MHz, DMSO-d_6) δ 7.42 (t, J = 1.7 Hz, 1H), 7.38 (t, J = 1.7 Hz, 1H), 7.24 (t, J = 1.4 Hz, 1H), 4.03 (s, 2H), 2.90 (hept, J = 7.0 Hz, 1H), 1.19 (d, J = 6.9 Hz, 6H).

(*S*)-2-(3-(3-Amino-2,3-dihydrobenzofuran-5-yl)-5-isopropylphenethoxy)benzoic acid trifluoroacetate (14): To a solution of (*S*)-2-(3-(3-((*tert*-butoxycarbonyl)amino)-2,3-dihydrobenzofuran-5-yl)-5-isopropylphenethoxy)benzoic acid (35 mg, 0.07 mmol) in CH_2Cl_2 (1 mL) was added TFA (156 µL, 2.03 mmol). The reaction mixture was stirred at RT for 18 h. The reaction mixture was diluted with CH_2Cl_2 and MeOH and then volatiles were evaporated. The reaction mixture was taken up in MeOH and then evaporated. This operation was done twice. The crude mixture was purified by preparative HPLC (column:

Sunfire C18-ODB 5 µm, 30x100 mm, flow: 40 mL/min, eluent: 5-100% CH_3CN/H_2O/20 min, 100% CH_3CN/2 min, CH_3CN and H_2O containing 0.1% TFA). The desired fractions were combined, CH_3CN was evaporated, followed by freeze-drying overnight to obtain the TFA salt of the title compound as a white solid (17 mg, 46%). MS (ESI^+) *m/z* 418.2 (M+1); HPLC t_R: 4.05 min, purity 99% (conditions b); ^1H NMR (400 MHz, DMSO-d_6) δ 12.56 (bs, 1H), 8.43 (s, 3H), 7.83 (d, *J* = 1.9 Hz, 1H), 7.68-7.62 (m, 2H), 7.51-7.44 (m, 1H), 7.38 (d, *J* = 1.8 Hz, 1H), 7.28 (d, *J* = 1.8 Hz, 1H), 7.24 (d, *J* = 1.7 Hz, 1H), 7.14 (d, *J* = 8.4 Hz, 1H), 7.04-6.95 (m, 2H), 5.16 – 5.06 (m, 1H), 4.76 (dd, *J* = 11.0, 8.2 Hz, 1H), 4.53 (dd, *J* = 11.0, 3.5 Hz, 1H), 4.27 (t, *J* = 6.7 Hz, 2H), 3.08 (t, *J* = 6.6 Hz, 2H), 2.98-2.89 (m, 1H), 1.29-1.20 (m, 6H).

(*S*)-2-(3-(3-((*tert*-Butoxycarbonyl)amino)-2,3-dihydrobenzofuran-5-yl)-5-isopropylphenethoxy)benzoic acid: To a solution of (*S*)-methyl 2-(3-(3-((*tert*-butoxycarbonyl)amino)-2,3-dihydrobenzofuran-5-yl)-5-isopropylphenethoxy)benzoate (30 mg, 0.06 mmol) in THF (0.5 mL) and water (0.5 mL) was added $LiOH.H_2O$ (4.74 mg, 0.11 mmol). The reaction mixture was stirred at 60 °C for 18 h. The reaction mixture was acidified to pH=1 with HCl (6N) and was extracted with CH_2Cl_2 (x2). The combined organic layers were dried (phase separator) and evaporated under vacuum to afford the title compound (35 mg, quantitative) as a colorless oil. MS (ESI^+) *m/z* 518.2 (M+1).

(*S*)- methyl 2-(3-(3-((*tert*-butoxycarbonyl)amino)-2,3-dihydrobenzofuran-5-yl)-5-isopropylphenethyl 2-hydroxybenzoate: To an ice cooled solution of (*S*)-*tert*-butyl (5-(3-(2-hydroxyethyl)-5-isopropylphenyl)-2,3-dihydrobenzofuran-3-yl)carbamate (90 mg, 0.23

mmol) in THF (1.5 mL) was added methyl 2-hydroxybenzoate (**32**) (34.4 mg, 0.23 mmol), PPh_3 (71.3 mg, 0.27 mmol) and DIAD (0.05 mL, 0.27 mmol). The reaction mixture was allowed to warm to RT and stirred for 18 h. Volatiles were evaporated, and the residue was taken up EtOAc and then washed with a saturated aqueous NH_4Cl solution (5 mL). The organic phase was dried (phase separator) and evaporated under vacuum. The crude mixture was purified by preparative HPLC (column: Sunfire, C18-ODB 5 µm, 30 x100 mm, flow: 40 mL/min, 40-100% CH_3CN/H_2O/20 min, 100% CH_3CN/2 min, CH_3CN and H_2O containing 0.1% TFA). The desired fractions were combined, CH_3CN was evaporated, followed by freeze-drying overnight to obtain the title compound (30 mg, 24%) as a white solid. MS (ESI^+) *m/z* 532.2 (M+1).

(*S*)-*tert*-Butyl (5-(3-(2-hydroxyethyl)-5-isopropylphenyl)-2,3-dihydrobenzofuran-3-yl)carbamate: In a 10-20 mL microwave reaction vessel, to a solution of 2-(3-bromo-5-isopropylphenyl)ethanol (**28,** Supp. Info.) (100 mg, 0.41 mmol) in CH_3CN (3 mL) was added (*S*)-(3-((*tert*-butoxycarbonyl)amino)-2,3-dihydrobenzofuran-5-yl)boronic acid (**47,** Supp. Info.) (135 mg, 0.41 mmol) and 2M K_3PO_4 (0.62 mL, 1.24 mmol). The reaction mixture was degassed under argon for 2 min and then $PdCl_2(dppf).CH_2Cl_2$ adduct (16.8 mg, 0.02 mmol) was added. The reaction mixture was stirred at 120 °C for 40 min under microwave irradiations (with a Biotage Initiator$^+$ apparatus). The reaction mixture was diluted with AcOEt and then washed with water (10 mL). The organic phase was dried (phase separator) and evaporated under vacuum to afford the title compound (158 mg,

93%) as a brown oil which was used without further purification. MS (ESI$^+$) *m/z* 415.2 (M+18).

(S)-2-(3-(3-Amino-2,3-dihydrobenzofuran-5-yl)-5-isopropylphenethoxy)-3-methoxybenzoic acid trifluoroacetate (15): The TFA salt of the title compound (22 mg, 42%) was prepared from (*S*)-2-(3-(3-((*tert*-butoxycarbonyl)amino)-2,3-dihydrobenzofuran-5-yl)-5-isopropylphenethoxy)-3-methoxybenzoic acid (50 mg, 0.091 mmol) in a similar manner as described for (*S*)-2-(3-(3-amino-2,3-dihydrobenzofuran-5-yl)-5-isopropylphenethoxy)benzoic acid trifluoroacetate (**14**). MS (ESI$^+$) *m/z* 432.3 (M+1); HPLC t_R: 4.12 min, purity 100% (conditions b); ^{1}H NMR (400 MHz, DMSO-d_6) δ 12.84 (s, 1H), 8.41 (s, 3H), 7.83 (d, *J* = 2.0 Hz, 1H), 7.64 (dd, *J* = 8.5, 2.0 Hz, 1H), 7.33-7.27 (m, 2H), 7.22-7.08 (m, 4H), 7.02 (d, *J* = 8.4 Hz, 1H), 5.16-5.07 (m, 1H), 4.76 (dd, *J* = 11.0, 8.2 Hz, 1H), 4.53 (dd, *J* = 11.0, 3.5 Hz, 1H), 4.21 (t, *J* = 7.2 Hz, 2H), 3.77 (s, 3H), 3.06 (t, *J* = 7.2 Hz, 2H), 2.97-2.89 (m, 1H), 1.28-1.21 (m, 6H).

(*S*)-2-(3-(3-((*tert*-Butoxycarbonyl)amino)-2,3-dihydrobenzofuran-5-yl)-5-isopropylphenethoxy)-3-methoxybenzoic acid: The title compound (50 mg, 64%) was prepared from (*S*)-methyl 2-(3-(3-((*tert*-butoxycarbonyl)amino)-2,3-dihydrobenzofuran-5-yl)-5-isopropylphenethoxy)-3-methoxybenzoate in a similar manner as described for (*S*)-methyl 2-(3-(3-((*tert*-butoxycarbonyl)amino)-2,3-dihydrobenzofuran-5-yl)-5-isopropylphenethoxy)benzoic acid (described in the synthesis of compound **14**). MS (ESI$^+$) *m/z* 548.3 (M+1).

(*S*)-Methyl 2-(3-(3-((*tert*-butoxycarbonyl)amino)-2,3-dihydrobenzofuran-5-yl)-5-isopropylphenethoxy)-3-methoxybenzoate: The title compound was prepared from methyl 2-(3-bromo-5-isopropylphenethoxy)-3-methoxybenzoate (**43**) (80 mg, 0.20 mmol) and (*S*)-(3-((*tert*-butoxycarbonyl)amino)-2,3-dihydrobenzofuran-5-yl)boronic acid (**47**, Supp. Info.) (64.5 mg, 0.20 mmol) in a similar manner as described for (*S*)-*tert*-butyl (5-(3-(2-hydroxyethyl)-5-isopropylphenyl)-2,3-dihydrobenzofuran-3-yl)carbamate (described in the synthesis of compound **14**). The crude mixture was purified by preparative HPLC (column: Sunfire, C18-ODB 5 µm, 30 x100 mm; flow: 40 mL/min; gradient: 20-100% CH_3CN/H_2O/20 min, 100% CH_3CN/2 min, CH_3CN and H_2O containing 0.1% TFA). The desired fractions were combined, CH_3CN was evaporated, followed by freeze-drying overnight to obtain the title compound as a colorless oil (60 mg, 43%). MS (ESI^+) *m/z* 562.3 (M+1).

Methyl 2-(3-bromo-5-isopropylphenethoxy)-3-methoxybenzoate (**43**): The title compound (80 mg, 65%) was prepared from 2-(3-bromo-5-isopropylphenyl)ethanol (**28**, Supp. Info.) (70 mg, 0.29 mmol) and methyl 2-hydroxy-3-methoxybenzoate (**33**) (52.4 mg, 0.29 mmol) in a similar manner as described for (*S*)-3-(3-((*tert*-butoxycarbonyl)amino)-2,3-dihydrobenzofuran-5-yl)-5-isopropylphenethyl 2-hydroxybenzoate (described in the synthesis of compound **14**). MS (ESI^+) *m/z* 409.5 (M+1).

(*S*)-2-((3-(3-Amino-2,3-dihydrobenzofuran-5-yl)-5-isopropylphenethyl)amino)benzoic acid hydrochloride (16): To a solution of (*S*)-2-((3-(3-((*tert*-butoxycarbonyl)amino)-2,3-

dihydrobenzofuran-5-yl)-5-isopropylphenethyl)amino)benzoic acid (62.2 mg, 60% pure, 0.07 mmol) in CH_2Cl_2 (1 mL) was added TFA (1.56 mmol). The reaction stirred at RT for 3 h. The reaction was concentrated to a brown film. The crude residue was purified by preparative HPLC (column: Sunfire C18 5 μM 100 x 30 mm; flow: 42 mL/min; 10 to 80% CH_3CN/H_2O/20 min, 80% CH_3CN/2min, CH_3CN and H_2O containing 0.1% TFA). The combined product fractions were lyophilized to afford the TFA salt of the title compound. The TFA salt was converted to the HCl salt by dissolution in 1:1 CH_3CN/H_2O and addition of 1N HCl (0.05 mL, 0.05 mmol, 2 eq) followed by lyophilization. This procedure was repeated 3 times to give the hydrochloride salt of the title compound (9.60 mg, 26%). UPLC/MS (ESI^+) *m/z* 417.3 (M+1), t_R: 2.03 min, purity 95% (conditions e); ^1H NMR (400 MHz, Deuterium Oxide, MeCN-d_3 added to solublize) δ 7.86 (dd, *J* = 8.0, 1.6 Hz, 1H), 7.76 (d, *J* = 1.9 Hz, 1H), 7.63 (dd, *J* = 8.5, 2.0 Hz, 1H), 7.47 – 7.37 (m, 1H), 7.30 (d, *J* = 18.7 Hz, 2H), 7.12 (s, 1H), 7.04 (d, *J* = 8.5 Hz, 1H), 6.91 (d, *J* = 8.4 Hz, 1H), 6.75 (t, *J* = 7.5 Hz, 1H), 5.13 (dd, *J* = 7.5, 2.9 Hz, 1H), 4.81 – 4.65 (m, 2H), 3.55 (t, *J* = 6.5 Hz, 2H), 2.98 (t, *J* = 6.6 Hz, 2H), 2.96 – 2.87 (m, 1H), 1.22 (d, *J* = 6.9 Hz, 6H).

(*S*)-2-((3-(3-((*tert*-Butoxycarbonyl)amino)-2,3-dihydrobenzofuran-5-yl)-5-isopropylphenethyl)amino)benzoic acid: A microwave vial was charged with 2-((3-bromo-5-isopropylphenethyl)amino)benzoic acid (30.8 mg, 0.077 mmol) and (*S*)-*tert*-butyl (5-(4,4,5,5-tetramethyl-1,3,2-dioxaborolan-2-yl)-2,3-dihydrobenzofuran-3-yl)carbamate (**48**, Supp. Info.) (35.0 mg, 0.097 mmol) in 1,4-dioxane (1.5 mL). $PdCl_2$(dppf).CH_2Cl_2 adduct

(3.6 mg, 4.41 μmol) and Na_2CO_3 (2M aqueous, 0.12 mL, 0.24 mmol) was added to the vial. N_2 was bubbled through the reaction mixture for 5 min and the vial was sealed. The reaction was heated at 120 °C under microwave irradiations for 90 min. The reaction mixture was diluted with a pH=7.0 buffer and extracted with EtOAc (x3). The combined organic layers were washed with brine, dried over Na_2SO_4, filtered, and concentrated. The crude residue was taken up in THF (5 mL) and SiliaMetS® Thiol (SiliCycle®; 50 mg, 1.25 mmol/g) was added to scavenge residual palladium. The resulting suspension was stirred for 1 h at 40 °C. The scavenger was filtered and washed with THF (x2). The filtrate was concentrated to afford the title compound as a brown film (62.2 mg, 94%, 60% pure). MS (ESI^+) *m/z* 517.1 (M+1).

2-((3-Bromo-5-isopropylphenethyl)amino)benzoic acid: To a suspension of 2-((3-bromo-5-isopropylphenethyl)amino)benzonitrile (47.9 mg, 0.14 mmol) in ethylene glycol (1.5 mL) was added KOH (70 mg, 1.25 mmol). The reaction mixture was heated to 185 °C and stirred for 16 h. The reaction mixture was cooled to RT, diluted with H_2O and extracted with EtOAc (x3). The combined organic layers were washed with brine, dried over Na_2SO_4, filtered and concentrated. The crude residue was purified by flash column chromatography (Isco RediSep 12 g silica cartridge; gradient: 0-30% EtOAc in n-heptane) to afford the title compound (30.8 mg, 55%). MS (ESI^+) *m/z* 363.9 (M+1).

2-((3-Bromo-5-isopropylphenethyl)amino)benzonitrile: To a suspension of 2-(3-bromo-5-isopropylphenyl)ethanamine (115 mg, 0.475 mmol) and K_2CO_3 (130 mg, 0.94 mmol) in anhydrous DMF (2 mL) was added 2-fluorobenzonitrile (0.10 mL, 0.94 mmol). The

reaction mixture was stirred at 80 °C for 21 h then at 120 °C for 5 h and finally was cooled to 100 °C and stirred for 16 h. After cooling to RT, the reaction mixture was diluted with EtOAc and washed with H_2O. The aqueous layer was extracted with EtOAc (x2) and the combined organic layers were washed with H_2O, with brine, dried over Na_2SO_4, filtered, and concentrated to a yellow oil. This crude residue was purified by flash column chromatography (Isco RediSep 24 g silica cartridge; gradient 0-15% EtOAc in n-heptane) to afford the title compound (169 mg, 72%). MS (ESI^+) *m/z* 344.9 (M+1).

2-(3-Bromo-5-isopropylphenyl)ethanamine: To a solution of 2-(3-bromo-5-isopropylphenyl)acetonitrile (described in the synthesis of compound **13**) (968 mg, 4.07 mmol) in anhydrous THF (12 mL) cooled to 0 °C was slowly added BH_3.THF (1.0 M in THF, 12.0 mL, 12.0 mmol). Upon completion of addition, the ice bath was removed and the reaction mixture warmed to RT while stirring was maintained for 3.5 h. The reaction mixture was cooled to 10 °C and MeOH (1.6 mL) was slowly added to quench the excess borane (gas evolved). The reaction mixture was allowed to warm to RT and stirred for 30 min. The resulting solution was concentrated, taken up in MeOH, and concentrated to a viscous oil, which was taken up in EtOAc and washed with a saturated aquoues solution of $NaHCO_3$. The aqueous layer was extracted with EtOAc (x2) and the combined organic layers were washed with brine, dried over Na_2SO_4, filtered and concentrated. The crude residue was purified by flash column chromatography (Isco Redisep 12 g silica cartridge; gradient 0-20% (10% TEA/MeOH) in CH_2Cl_2) to afford the title compound (115 mg, 12%). MS (ESI^+) *m/z* 243.8 (M+1).

(*S*)-1-(3-(3-Amino-2,3-dihydrobenzofuran-5-yl)-5-isopropylphenethyl)indoline-7-carboxylic acid trifluoroacetate (17): Methyl (*S*)-1-(3-(3-((*tert*-butoxycarbonyl)amino)-2,3-dihydrobenzofuran-5-yl)-5-isopropylphenethyl)indoline-7-carboxylate (14 mg, 0.025 mmol) was dissolved in THF:MeOH:H_2O (0.9 mL, 4:2:1), $LiOH{\cdot}H_2O$ (5.28 mg, 0.126 mmol) was added and the mixture was stirred at 50 °C until consumption of the starting material. The mixture was concentrated under reduced pressure. The residue was co-evaporated with toluene (x2) and dried under high vacuum overnight. The crude residue, (*S*)-1-(3-(3-((*tert*-butoxycarbonyl)amino)-2,3-dihydrobenzofuran-5-yl)-5-isopropylphenethyl)indoline-7-carboxylic acid (10.9 mg), was dissolved in CH_2Cl_2 (1 mL), TFA (0.04 mL, 0.50 mmol) was added and the reaction mixture was stirred at RT. After completion the reaction mixture was concentrated and the crude residue was purified by reverse phase preparative HPLC (prep HPLC conditions k, gradient: 10-80% CH_3CN) to afford the title compound (6 mg, 34%). UPLC/MS (ESI^-) *m/z* 440.9 (M-1), t_R: 1.64 min, purity 100% (condition e); ^1H NMR (400 MHz, DMSO-d_6) δ 8.42 (bs, 3H), 7.83 (d, J = 2.0 Hz, 1H), 7.65-7.60 (m, 1H), 7.37 (d, J = 7.9 Hz, 1H), 7.28-7.21 (m, 2H), 7.16 (d, J = 7.0 Hz, 1H), 7.05-7.00 (m, 2H), 6.62 (t, J = 7.4 Hz, 1H), 5.14-5.07 (m, 1H), 4.79-4.72 (m, 1H), 4.57-4.51 (m, 1H), 2.98-2.87 (m, 3H), 2.83-2.75 (m, 2H), 1.25 (d, J = 6.8 Hz, 6H).

Methyl (*S*)-1-(3-(3-((*tert*-butoxycarbonyl)amino)-2,3-dihydrobenzofuran-5-yl)-5-isopropylphenethyl)indoline-7-carboxylate: The title compound was prepared in a similar manner as described for (*S*)-2-((3-(3-((*tert*-butoxycarbonyl)amino)-2,3-

dihydrobenzofuran-5-yl)-5-isopropylphenethyl)amino)benzoic acid (described in the synthesis of compound **16**) using methyl 1-(3-bromo-5-isopropylphenethyl)indoline-7-carboxylate (24 mg, 0.06 mmol) and *tert*-butyl (S)-(5-(4,4,5,5-tetramethyl-1,3,2-dioxaborolan-2-yl)-2,3-dihydrobenzofuran-3-yl)carbamate (**48**, Supp. Info.) (0.213mmol). The crude residue was purified by flash column chromatography (Isco RediSep 12 g silica cartridge; gradient: 0-15% EtOAc in n-heptane) to afford the title compound (14 mg, 42%). MS (ESI^+) *m/z* 557.1 (M+1).

Methyl 1-(3-bromo-5-isopropylphenethyl)indoline-7-carboxylate: To a solution of 2-(3-bromo-5-isopropylphenyl)acetaldehyde (180 mg, 0.75 mmol) in EtOH (5 mL) was added methyl indoline-7-carboxylate (304 mg, 1.72 mmol) followed by a catalytic amount of AcOH and powdered 4Å molecular sieves. The resulting mixture was stirred at 70 °C for 12 h, cooled to RT, and concentrated under reduced pressure. The resulting residue was diluted with CH_2Cl_2 (5 mL), AcOH (0.064 mL, 1.10 mmol) and $NaBH(OAc)_3$ (633 mg, 3.00 mmol) were added and the reaction mixture was stirred at RT overnight. Then, the reaction mixture was diluted with CH_2Cl_2 and washed with a saturated aqueous solution of $NaHCO_3$, with H_2O, and brine, dried over $MgSO_4$, filtered, and concentrated. The crude residue was purified by preparative reverse phase HPLC (prep. HPLC conditions k; gradient: 10-80% CH_3CN) to afford the title compound (54 mg, 14%) as a TFA salt. MS (ESI^+) *m/z* 402.0 (M+1).

2-(3-Bromo-5-isopropylphenyl)acetaldehyde: To a mixture of lead tetraacetate (591 mg, 1.30 mmol) in TFA (1.10 mL) at 0 °C was added 1-bromo-3-isopropyl-5-vinylbenzene (**51**,

Supp. Info.) (250 mg, 1.10 mmol) in CH_2Cl_2 (1.1 mL) dropwise and the resulting mixture was allowed to warm to RT and stirred at RT for 2 h. The reaction mixture was diluted with CH_2Cl_2 and poured into water. The mixture was vigorously stirred and filtered through a plug of Celite®. The filter cake was washed with CH_2Cl_2 and water. The filtrate was collected and the organic phase was separated. The aueous phase was extracted with CH_2Cl_2 and the combined organic layers were washed with water and a saturated aqueous solution of $NaHCO_3$, dried over $MgSO_4$, filtered, and concentrated under reduced pressure. The crude residue was purified by flash column chromatography (gradient: 0-10% EtOAc in n-heptane) to give the title compound (80 mg, 30%). MS (ESI^-) *m/z* 238.8 (M-1).

(*S*)-2-(3-(3-Amino-2,3-dihydrobenzofuran-5-yl)-5-isopropylphenethoxy)-3-methylbenzoic acid trifluoroacetate (18): The title compound (32 mg, 61%) was prepared in a similar manner as described for (*S*)-2-(3-(3-amino-2,3-dihydrobenzofuran-5-yl)-5-isopropylphenethoxy)-3-methoxybenzoic acid trifluoroacetate (**15**) using methyl 2-hydroxy-3-methylbenzoate (**34**) (47.8 mg, 0.29 mmol) instead of methyl 2-hydroxy-3-methoxybenzoate (**33**). MS (ESI^+) *m/z* 432.3 (M+1); HPLC t_R: 4.35 min, purity 99% (conditions b); ^1H NMR (400 MHz, DMSO-d_6) δ 12.87 (bs, 1H), 8.43 (bs, 3H), 7.84 (d, *J* = 2.0 Hz, 1H), 7.64 (dd, *J* = 8.4, 2.1 Hz, 1H), 7.51 (dd, *J* = 7.7, 1.8 Hz, 1H), 7.38-7.27 (m, 3H), 7.17 (d, *J* = 1.8 Hz, 1H), 7.06 (t, *J* = 7.6 Hz, 1H), 7.01 (d, *J* = 8.4 Hz, 1H), 5.15-5.06

(m, 1H), 4.76 (dd, *J* = 11.0, 8.2 Hz, 1H), 4.53 (dd, *J* = 11.0, 3.6 Hz, 1H), 4.14 (t, *J* = 6.9 Hz, 2H), 3.08 (t, *J* = 6.9 Hz, 2H), 2.98-2.89 (m, 1H), 2.08 (s, 3H), 1.29-1.21 (m, 6H).

(*S*)-2-(3-(3-Amino-2,3-dihydrobenzofuran-5-yl)-5-isopropylphenethoxy)-3-chlorobenzoic acid trifluoroacetate (19): The title compound (32 mg, 68%) was prepared in a similar manner as described for (*S*)-2-(3-(3-amino-2,3-dihydrobenzofuran-5-yl)-5-isopropylphenethoxy)benzoic acid trifluoroacetate (**14**) using methyl 3-chloro-2-hydroxybenzoate (**35**) (32.9 mg, 0.18 mmol) instead of methyl 2-hydroxybenzoate (**32**). MS (ESI$^+$) *m/z* 452.2 (M+1); HPLC t_R: 4.50 min, purity 100% (conditions b); ^{1}H NMR (400 MHz, DMSO-d_6) δ 8.42 (s, 3H), 7.83 (d, *J* = 2.0 Hz, 1H), 7.69-7.61 (m, 3H), 7.32 (s, 1H), 7.29 (s, 1H), 7.22 (t, *J* = 7.9 Hz, 1H), 7.17 (s, 1H), 7.02 (d, *J* = 8.4 Hz, 1H), 5.15-5.06 (m, 1H), 4.76 (dd, *J* = 11.0, 8.2 Hz, 1H), 4.53 (dd, *J* = 11.0, 3.6 Hz, 1H), 4.26 (t, *J* = 7.0 Hz, 2H), 3.13 (t, *J* = 7.1 Hz, 2H), 2.98-2.89 (m, 1H), 1.25 (d, *J* = 6.9 Hz, 6H).

2-(2-(3-((*S*)-3-Amino-2,3-dihydrobenzofuran-5-yl)-5-isopropylphenyl)-2-hydroxyethoxy)-3-methoxybenzoic acid (20): To a solution of methyl 2-(2-(3-((*S*)-3-amino-2,3-dihydrobenzofuran-5-yl)-5-isopropylphenyl)-2-hydroxyethoxy)-3-methoxybenzoate (45 mg, 0.094 mmol) in THF/MeOH/H_2O (7:2:1, 2.5 mL) cooled to 0 °C was slowly added a solution of LiOH·H_2O (0.28 mmol) in THF/MeOH/H_2O (7:2:1, 2.5 mL). The reaction mixture was stirred at RT for 6 h. The reaction mixture was acidified with 1N HCl and partitioned between water and EtOAc. The organic layer was separated, dried over

Na_2SO_4 and concentrated under reduced pressure to afford the title compound (13 mg, 30%). MS (ESI^-) *m/z* 462.05 (M-1); HPLC (ZORBAX Eclipse C18 5 µm, 4.6 x 150 mm; gradient: 5% (1:1 CH_3CN:MeOH) in H_2O (containing 0.1% TFA)/1 min, 5-100% (1:1 CH_3CN:MeOH)/ in H_2O (containing 0.1% TFA)/5 min, 100% (1:1 CH_3CN:MeOH)/2 min.; flow rate: 1.0 mL/min; column temperature: 40 °C); t_R: 6.68 min, purity 99%; ^1H NMR (300 MHz, CD_3OD) δ ppm 7.93 (s, 1H), 7.73 (s, 1H), 7.64 (m, 2H), 7.33 (s, 1H), 7.20 (m, 1H), 7.01 (m, 3H), 5.10 (m, 1H), 4.90 (m,1H), 4.80 (m, 1H), 4.60 (m, 1H), 4.38 (m, 1H), 4.22 (m, 1H), 4.12 (m, 1H), 3.82 (d, *J*=2.1 Hz, 3H), 2.96 (m, 1H), 1.28 (d, *J*=6.8 Hz, 6H).

Methyl 2-(2-(3-((*S*)-3-amino-2,3-dihydrobenzofuran-5-yl)-5-isopropylphenyl)-2-hydroxyethoxy)-3-methoxybenzoate: To a solution of methyl 2-(2-(3-((*S*)-3-((*tert*-butoxycarbonyl)amino)-2,3-dihydrobenzofuran-5-yl)-5-isopropylphenyl)-2-hydroxyethoxy)-3-methoxybenzoate (65 mg, 0.11 mmol) in 1,4-dioxane (0.5 mL) was added HCl (4N in 1,4-dioxane, 3.0 mL, 12.0 mmol). The reaction mixture was stirred at RT for 6 h, then was concentrated under reduced pressure to give the title compound as a HCl salt (45 mg, 64%). ^1H NMR (300 MHz, DMSO-d_6) δ ppm 8.48 (bs, 3H), 7.87 (s, 1H), 7.64 (m, 1H), 7.45 (m, 1H), 7.35 (m, 1H), 7.2 (m, 4H), 7.03 (m, 1H), 5.57 (d, *J*=3.9 Hz, 1H), 5.1 (m, 1H), 4.9 (m, 1H), 4.79 (m, 1H), 4.55 (m, 1H), 4.2 (m, 2H), 3.8 (s, 3H), 3.75 (s, 3H), 2.96 (m, 1H), 1.25 (d, *J*=6.9 Hz, 6H).

Methyl 2-(2-(3-((*S*)-3-((*tert*-butoxycarbonyl)amino)-2,3-dihydrobenzofuran-5-yl)-5-isopropylphenyl)-2-hydroxyethoxy)-3-methoxybenzoate: To a solution of methyl 2-(2-(3-bromo-5-isopropylphenyl)-2-hydroxyethoxy)-3-methoxybenzoate (75 mg, 0.18 mmol)

and *tert*-butyl (*S*)-(5-(4,4,5,5-tetramethyl-1,3,2-dioxaborolan-2-yl)-2,3-dihydrobenzofuran-3-yl)carbamate (**48**, Supp. Info.) (76.1 mg, 0.21 mmol) in 1,4-dioxane (4.0 mL) was added Na_2CO_3 (2N aqueous, 0.4 ml, 0.40 mmol). The suspension was degassed with argon for 10 min. and $PdCl_2(dppf).CH_2Cl_2$ adduct (7.8 mg, 0.008 mmol) was added. The reaction mixture was further degassed with argon for 5 min. and then heated to 80 °C and stirred for 16 h. The reaction mixture was partitioned between water and EtOAc. The organic layer was separated, dried over Na_2SO_4 and concentrated under reduced pressure. The crude residue was purified by flash column chromatography (gradient: 0-20% EtOAc in hexane) to give the title compound (65 mg, 64%). ^{1}H NMR (300 MHz, $CDCl_3$) δ ppm 7.56 (s, 1H), 7.46 (m, 3H), 7.3 (m, 2H), 7.10 (m, 2H), 6.88 (m, 1H), 5.51(m, 1H), 5.38 (m, 1H), 5.13 (m, 1H), 4.92 (m, 1H), 4.69 (m, 2H), 3.92 (s, 3H), 3.86 (s, 3H), 2.96 (m, 1H), 1.46 (s, 9H), 1.28 (d, J = 6.9 Hz, 6H).

Methyl 2-(2-(3-bromo-5-isopropylphenyl)-2-hydroxyethoxy)-3-methoxybenzoate: To a solution of methyl 2-(2-(3-bromo-5-isopropylphenyl)-2-oxoethoxy)-3-methoxybenzoate (100 mg, 0.24 mmol) in THF/MeOH (1:1, 5.0 mL) cooled to 0 °C was added $NaBH_4$ (18.1 mg, 0.48 mmol) under inert atmosphere. The reaction mixture was stirred at RT for 4 h. The reaction mixture was diluted with water and extracted with EtOAc. The organic layer was washed with brine, dried over Na_2SO_4, and concentrated under reduced pressure. The crude residue was purified by flash column chromatography (gradient: 0-15% EtOAc in hexane) to give the title compound (75 mg, 78%). ^{1}H NMR (300 MHz, $CDCl_3$) δ ppm 7.43 (m, 2H), 7.25 (m, 2H), 7.10 (d, J = 5.4 Hz, 2H), 5.52 (s, 1H), 5.03 (d, J = 9.3 Hz, 1H),

4.6 (d, *J* = 9.4 Hz, 1H), 3.93 (s, 3H), 3.87 (s, 3H), 3.81 (m, 1H), 2.87 (m, 1H), 1.23 (d, *J* = 6.9 Hz, 6H).

Methyl 2-(2-(3-bromo-5-isopropylphenyl)-2-oxoethoxy)-3-methoxybenzoate: To a solution of methyl 2-hydroxy-3-methoxybenzoate (**33**) (100 mg, 0.55 mmol) in anhydrous acetone (5 mL) cooled to 0 °C was added 2-bromo-1-(3-bromo-5-isopropylphenyl)ethan-1-one (226 mg, 0.71 mmol) followed by Cs_2CO_3 (267 mg, 0.82 mmol). The reaction mixture was stirred at 0 °C for 2 h. Then was diluted with water and extracted with EtOAc. The organic layer was washed with brine, dried over Na_2SO_4, and concentrated under reduced pressure. The crude residue was purified by flash column chromatography (gradient: 0-10% EtOAc in hexane) to give the title compound (50 mg, 65%). ^{1}H NMR (300 MHz, $CDCl_3$) δ ppm 7.99 (m, 1H), 7.81 (m, 1H), 7.57 (m, 1H), 7.36 (m, 1H), 7.12 (m, 2H), 5.25 (s, 2H), 3.80 (s, 6H), 2.95 (m, 1 H), 1.26 (d, J = 6.9 Hz, 6H).

1-(2-(3-((*S*)-3-Amino-2,3-dihydrobenzofuran-5-yl)-5-isopropylphenyl)-2-hydroxyethyl)indoline-7-carboxylic acid trifluoroacetate (21): The title compound (5 mg, 16%) was prepared as a mixture of diastereomers in a similar manner as describe for (*S*)-1-(3-(3-amino-2,3-dihydrobenzofuran-5-yl)-5-isopropylphenethyl)indoline-7-carboxylic acid trifluoroacetate (**17**) from methyl 1-(2-(3-((*S*)-3-((*tert*-butoxycarbonyl)amino)-2,3-dihydrobenzofuran-5-yl)-5-isopropylphenyl)-2-hydroxyethyl)indoline-7-carboxylate (25 mg, 0.44 mmol). UPLC/MS (ESI$^+$) *m/z* 459.3 (M+1), t_R: 1.60 min, purity 96% (conditions e); ^{1}H NMR (400 MHz, Acetonitrile-d_3) δ 7.82 (bs, 1H), 7.57 (br d, *J* = 8.31 Hz, 1H), 7.48-

7.35 (m, 2H), 7.27 (br s, 1H), 7.20-7.14 (m, 2H), 6.89 (m, 1H), 6.82-6.72 (m, 1H), 5.13-5.09 (m, 1H), 5.02-4.94 (m, 1H), 4.69-4.57 (m, 2H), 3.79-3.65 (m, 2H), 3.39-3.31 (m, 1H), 3.06-2.85 (m, 4H), 1.19 (m, 6H).

Methyl 1-(2-(3-((*S*)-3-((*tert*-butoxycarbonyl)amino)-2,3-dihydrobenzofuran-5-yl)-5-isopropylphenyl)-2-hydroxyethyl)indoline-7-carboxylate: A solution of *tert*-butyl ((3*S*)-5-(3-isopropyl-5-(oxiran-2-yl)phenyl)-2,3-dihydrobenzofuran-3-yl)carbamate (62 mg, 0.16 mmol) and methyl indoline-7-carboxylate (30.6 mg, 0.17 mmol) in *t*-BuOH (0.3 mL) was stirred at 90 °C for 3 days. The reaction mixture was cooled to RT and purified directly by flash column chromatography (gradient: 0-20% EtOAc in n-heptane) to give the title compound as a mixture of diastereomers (40 mg, 45%). MS (ESI$^+$) *m/z* 573.4 (M+1).

tert-Butyl ((3*S*)-5-(3-isopropyl-5-(oxiran-2-yl)phenyl)-2,3-dihydrobenzofuran-3-yl)carbamate: Saturated aqueous $NaHCO_3$ (2 mL) was added to a solution of *tert*-butyl (*S*)-(5-(3-isopropyl-5-vinylphenyl)-2,3-dihydrobenzofuran-3-yl)carbamate (65 mg, 0.17 mmol) in CH_3CN/acetone (2:1, 3 mL), followed by oxone (316 mg, 0.51 mmol). The reaction mixture was stirred at RT for 2 h and then diluted with H_2O and extracted with EtOAc. The combined organic layers were washed with brine, dried over Na_2SO_4, filtered, and concentrated to give the title compound (65 mg, 96%) which was used in the next step without purification. ^{1}H NMR (400 MHz, Chloroform-*d*) δ 7.59-7.56 (m, 1H), 7.51-7.46 (m, 1H), 7.35-7.32 (m, 1H), 7.27-7.26 (m, 1H), 7.13 (s, 1H), 6.92 (d, *J* = 8.3 Hz, 1H), 5.43 (s, 1H), 4.79-4.71 (m, 1H), 4.46-4.40 (m, 1H), 3.96-3.91 (m, 1H), 3.19 (dd, *J* = 5.5, 4.1 Hz, 1H), 3.03-2.94 (m, 1H), 2.89-2.85 (m, 1H), 1.50 (s, 9H), 1.32 (d, *J* = 6.9 Hz, 6H).

tert-Butyl (*S*)-(5-(3-isopropyl-5-vinylphenyl)-2,3-dihydrobenzofuran-3-yl)carbamate: A mixture of (*S*)-3-(3-((*tert*-butoxycarbonyl)amino)-2,3-dihydrobenzofuran-5-yl)-5-isopropylphenyl trifluoromethanesulfonate (200 mg, 0.40 mmol), 4,4,5,5-tetramethyl-2-vinyl-1,3,2-dioxaborolane (76 mg, 0.47 mmol), and 2M aqueous Na_2CO_3 (0.60 mL, 1.20 mmol) in DME (4 mL) was sparged with nitrogen for 5 min. $Pd(PPh_3)_2Cl_2$ (15 mg, 0.02 mmol) was then added and resulting mixture was stirred at 70 °C for 16 h. The reaction mixture was cooled to RT, diluted with H_2O, and extracted with EtOAc. The aqueous layer was back extracted with EtOAc, and the combined organic layers were washed with brine, dried over Na_2SO_4, filtered, and concentrated. The residue was dissolved in THF (5 mL) and SiliaMetS® Thiol (SiliCycle®; 100mg, 1.25 mmol/g) was added. The resulting suspension was stirred at 40 °C for 1 h, and then filtered. The filter cake was washed with THF. The filtrate was concentrated, and the crude residue was purified by flash column chromatography (gradient: 0-15% EtOAc in n-heptane) to give the title compound (145 mg, 96%). MS (ESI^+) *m/z* 380.5 (M+1).

(*S*)-3-(3-((*tert*-Butoxycarbonyl)amino)-2,3-dihydrobenzofuran-5-yl)-5-isopropylphenyl trifluoromethanesulfonate: To a solution of *tert*-butyl (*S*)-(5-(3-hydroxy-5-isopropylphenyl)-2,3-dihydrobenzofuran-3-yl)carbamate (100 mg, 0.22 mmol) and pyridine (254 mg, 0.62 mmol) in CH_2Cl_2 (2.0 mL) cooled to 0 °C was slowly added Tf_2O (100 mg, 0.30 mmol). Upon completion of the addition, the reaction mixture was stirred at RT for 1 h and then diluted with CH_2Cl_2 and poured into ice cold sat. aq. $NaHCO_3$. The layers were separated and the aqueous layer was back extracted with CH_2Cl_2. The

combined organic layers were washed with brine, dried over Na_2SO_4, filtered, and concentrated. The residue was purified by flash column chromatography (gradient: 0-30% EtOAc in n-heptane) to afford the title compound (126 mg, 93%). ^{1}H NMR (400 MHz, Chloroform-*d*) δ 7.55 (d, *J* = 1.9 Hz, 1H), 7.45 (dd, *J* = 8.4, 1.9 Hz, 1H), 7.40 (t, *J* = 1.3 Hz, 1H), 7.25-7.21 (m, 1H), 7.09-7.05 (m, 1H), 6.94 (d, *J* = 8.4 Hz, 1H), 5.45 (s, 1H), 4.93 (d, *J* = 6.6 Hz, 1H), 4.77 (dd, *J* = 10.0, 8.0 Hz, 1H), 4.44 (dd, *J* = 10.1, 4.1 Hz, 1H), 3.02 (m, 1H), 1.50 (s, 9H), 1.33 (d, *J* = 6.9 Hz, 6H).

tert-Butyl (*S*)-(5-(3-hydroxy-5-isopropylphenyl)-2,3-dihydrobenzofuran-3-yl)carbamate: TBAF (1.0 M in THF, 1.40 mL, 1.40 mmol) was added to a solution of *tert*-butyl (*S*)-(5-(3-((*tert*-butyldimethylsilyl)oxy)-5-isopropylphenyl)-2,3-dihydrobenzofuran-3-yl)carbamate (534 mg, 1.10 mmol) in THF (10 mL). The resulting mixture was stirred at RT for 2 h and then was diluted with H_2O and extracted with EtOAc. The aqueous layer was back extracted with EtOAc and the combined organic layers were washed with brine, dried over Na_2SO_4, filtered, and concentrated. The crude residue was purified by flash column chromatography (gradient: 0-50% EtOAc in n-heptane) to afford the title compound (259 mg, 63%). MS (ESI$^-$) *m/z* 367.9 (M-1).

tert-Butyl (*S*)-(5-(3-((*tert*-butyldimethylsilyl)oxy)-5-isopropylphenyl)-2,3-dihydrobenzofuran-3-yl)carbamate: The title compound was prepared in a similar manner as described for (*S*)-2-((3-(3-((*tert*-butoxycarbonyl)amino)-2,3-dihydrobenzofuran-5-yl)-5-isopropylphenethyl)amino)benzoic acid (described in the synthesis of compound **16**) using *tert*-butyl (3-isopropyl-5-(4,4,5,5-tetramethyl-1,3,2-dioxaborolan-2-

yl)phenoxy)dimethylsilane (473 mg, 1.26 mmol) and (*S*)-*tert*-butyl (5-bromo-2,3-dihydrobenzofuran-3-yl)carbamate (425 mg, 1.35 mmol). The crude residue was purified by flash column chromatography (gradient: 0-30% EtOAc in n-heptane) to afford the title compound (534 mg, 88%). MS (ESI$^+$) *m/z* 484.0 (M+1).

tert-Butyl (3-isopropyl-5-(4,4,5,5-tetramethyl-1,3,2-dioxaborolan-2-yl)phenoxy)dimethylsilane: Nitrogen gas was bubbled through a solution of *tert*-butyl (3-isopropylphenoxy)dimethylsilane (50 mg, 0.20 mmol) in c-hexane (2.0 mL) for ~5 min. The solution was then added to a microwave vial containing bis(pinacoloto)diboron (55 mg, 0.22 mmol), $[Ir(cod)(OMe)]_2$ (5.0 mg, 7.5 μmol), and 4,4′-di-tert-butyl-2,2′-dipyridyl (4.3 mg, 0.02 mmol). The resulting mixture was heated at 80 °C for 8 h under microwave irradiations and then cooled to RT and concentrated. The crude residue was purified by flash column chromatography (gradient: 0-100% CH_2Cl_2 in n-heptane) to afford the title compound (25 mg, 33%). ^{1}H NMR (400 MHz, Chloroform-*d*) δ 7.26 (s, 1H), 7.09 (dd, *J* = 2.4, 0.8 Hz, 1H), 6.79 (t, *J* = 2.0 Hz, 1H), 2.97-2.75 (m, 1H), 1.33 (s, 12H), 1.23 (d, *J* = 6.9 Hz, 6H), 0.99 (s, 9H), 0.19 (s, 6H).

tert-Butyl (3-isopropylphenoxy)dimethylsilane: To a solution of 3-isopropylphenol (5.0 g, 36.7 mmol) in DMF (100 mL) was added imidazole (5.0 g, 73.4 mmol) followed by TBSCl (8.5 g, 56.4 mmol). The reaction mixture was stirred at RT for 2.5 days and then diluted with 1:1 EtOAc/heptane and washed with saturated aqueous $NaHCO_3$. After separation of the organic layer, the aqueous layer was back extracted with 1:1 EtOAc/heptane. The combined organic layers were washed with brine, dried over $MgSO_4$, filtered, and

concentrated. The crude residue was purified by flash column chromatography (gradient: 0-10% EtOAc in heptane) to afford the title compound (9.27 g, quantitative). ^{1}H NMR (400 MHz, Chloroform-*d*) δ 7.13 (t, *J* = 7.8 Hz, 1H), 6.85-6.77 (m, 1H), 6.73-6.68 (m, 1H), 6.65 (m, 1H), 2.84 (m, 1H), 1.22 (d, *J* = 6.9 Hz, 6H), 0.98 (s, 9H), 0.19 (s, 6H).

1-(2-(3-((S)-3-Amino-2,3-dihydrobenzofuran-5-yl)-5-isopropylphenyl)-2-hydroxyethyl)-1H-indole-7-carboxylic acid (22): TFA (0.09 mL, 1.2 mmol) was added to a solution of 1-(2-(3-((*S*)-3-((*tert*-butoxycarbonyl)amino)-2,3-dihydrobenzofuran-5-yl)-5-isopropylphenyl)-2-hydroxyethyl)-1*H*-indole-7-carboxylic acid (25 mg, 0.05 mmol) in CH_2Cl_2 (1.0 mL). The reaction mixture was stirred at RT for 2 h and concentrated under reduced pressure. The resulting residue was dissolved in THF (1.0 mL) and 2M aqueous LiOH (0.6 mL, 1.2 mmol) was added. The reaction mixture was stirred at 50 °C for 1 h and then cooled to RT, and purified directly by reverse phase HPLC (prep HPLC conditions i; gradient: 15-40% CH_3CN) to afford the title compound as a mixture of diastereomers (3.0 mg, 13%). UPLC/MS (ESI$^+$) *m/z* 457.1 (M+1), t_R: 1.29 min, purity 92% (conditions f); ^{1}H NMR (400 MHz, Acetonitrile-d_3) δ 8.54-8.45 (m, 1H), 8.19-8.14 (m, 2H), 8.14-8.05 (m, 1H), 7.95-7.91 (m, 1H), 7.88-7.82 (m, 1H), 7.76 (d, *J* = 1.7 Hz, 1H), 7.73 (dd, *J* = 5.7, 3.2 Hz, 1H), 7.59-7.52 (m, 1H), 7.50 (d, *J* = 8.4 Hz, 1H), 7.05-7.00 (m, 1H), 5.67-5.59 (m, 1H), 5.52-5.44 (m, 1H), 5.33-5.22 (m, 1H), 5.13-5.02 (m, 3H), 3.56-3.45 (m, 1H), 1.84-1.79 (m, 6H).

1-(2-(3-((*S*)-3-((*tert*-Butoxycarbonyl)amino)-2,3-dihydrobenzofuran-5-yl)-5-isopropylphenyl)-2-hydroxyethyl)-1*H*-indole-7-carboxylic acid: The title compound was prepared in a similar manner as described for (*S*)-2-((3-(3-((*tert*-butoxycarbonyl)amino)-2,3-dihydrobenzofuran-5-yl)-5-isopropylphenethyl)amino)benzoic acid (described in the synthesis of compound **16**) using 1-(2-(3-bromo-5-isopropylphenyl)-2-hydroxyethyl)-1H-indole-7-carboxylic acid (20 mg, 0.05 mmol) and *tert*-butyl (*S*)-(5-(4,4,5,5-tetramethyl-1,3,2-dioxaborolan-2-yl)-2,3-dihydrobenzofuran-3-yl)carbamate (**48**, Supp. Info.) (20 mg, 0.06 mmol). The crude residue was used in the next step without purification. MS (ESI^+) m/z 557.3 (M+1).

1-(2-(3-Bromo-5-isopropylphenyl)-2-hydroxyethyl)-1*H*-indole-7-carboxylic acid: Methyl 1*H*-indole-7-carboxylate (425 mg, 2.43 mmol) and Cs_2CO_3 (790 mg, 2.43 mmol) were added to a solution of 2-(3-bromo-5-isopropylphenyl)oxirane (195 mg, 0.81 mmol) in DMF (8.0 mL) and the resulting mixture was stirred at 90 °C for 17 h. The reaction mixture was then cooled to RT, filtered, and purified directly by preparative reverse phase HPLC (prep HPLC conditions j; gradient: 10 to 30% CH_3CN) to give the title compound (33 mg, 10%, 70% pure). ^1H NMR (600 MHz, Chloroform-*d*) δ 7.95-7.91 (m, 1H), 7.88-7.85 (m, 1H), 7.39-7.38 (m, 1H), 7.16 (t, *J* = 7.7 Hz, 1H), 7.11-7.08 (m, 2H), 7.05 (d, *J* = 1.6 Hz, 1H), 6.60 (d, *J* = 3.2 Hz, 1H), 5.07-5.02 (m, 1H), 4.80-4.74 (m, 1H), 4.60-4.53 (m, 1H), 2.86-2.76 (m, 1H), 1.18-1.15 (m, 6H).

2-(3-Bromo-5-isopropylphenyl)oxirane: *m*CPBA (1.20 g, 5.33 mmol) was added to a solution of 1-bromo-3-isopropyl-5-vinylbenzene (**51**, Supp. Info.) (1.0 g, 4.40 mmol) in

CH_2Cl_2 (20 mL) at 0 °C. The reaction mixture was stirred at RT for 16 h, washed with sat. aq. $NaHCO_3$ and brine, and then concentrated. The crude residue was purified by flash column chromatography (gradient: 0-10% EtOAc in n-heptane) to afford the title compound as a racemate (420 mg, 39%). ^{1}H NMR (400 MHz, Chloroform-*d*) δ 7.31-7.29 (m, 1H), 7.24-7.22 (m, 1H), 7.07-7.05 (m, 1H), 3.83-3.78 (m, 1H), 3.13 (dd, *J* = 5.5, 4.0 Hz, 1H), 2.92-2.82 (m, 1H), 2.76 (dd, *J* = 5.5, 2.5 Hz, 1H), 1.23 (d, *J* = 6.9 Hz, 6H).

1-((*S*)-2-(3-((S)-3-Amino-2,3-dihydrobenzofuran-5-yl)-5-isopropylphenyl)-2-hydroxyethyl)-1H-indole-7-carboxylic acid (23): A mixture of 1-((*S*)-2-hydroxy-2-(3-isopropyl-5-((*S*)-3-(2,2,2-trifluoroacetamido)-2,3-dihydrobenzofuran-5-yl)phenyl)ethyl)-1H-indole-7-carboxylic acid (**59**) and 2,2,2-trifluoro-N-((*S*)-5-(3-isopropyl-5-((S)-1-oxo-3,4-dihydro-1H-[1,4]oxazepino[6,5,4-hi]indol-3-yl)phenyl)-2,3-dihydrobenzofuran-3-yl)acetamide (**60**) (2.00 g, 3.62 mmol) was dissolved in MeOH (24.1 mL) and 2M aqueous NaOH (7.24 mL, 18.1 mmol) was added. The reaction mixture was heated at 60 °C for 90 min and then MeOH was removed under reduced pressure. The resulting aqueous residue was dissolved by the addition of CH_3CN and DMSO. The solution was partially purified by reverse phase flash column chromatography (gradient: 10-60% CH_3CN (containing 0.1% NH_4OH) in Water (containing 0.1% NH_4OH)). The resulting residue was further purified by SFC (Chiralpak IG 4.6 x 100 mm 5µm, 5-55% MeOH w/ 10 mM NH_4OH/CO_2) to give the title compound (562 mg, 32%). UPLC/MS (ESI^-) *m/z* 455.0 (M-1), t_R: 1.63 min, purity 100% (conditions e); ^{1}H NMR (DMSO-d_6) δ: 7.83 (d, *J* = 2.0 Hz,

1H), 7.56-7.61 (m, 2H), 7.52 (dd, *J* = 8.3, 2.0 Hz, 1H), 7.30-7.40 (m, 3H), 7.19 (s, 1H), 6.99 (t, *J* = 7.6 Hz, 1H), 6.91 (d, *J* = 8.8 Hz, 1H), 6.47 (d, *J* = 3.4 Hz, 1H), 4.76-4.83 (m, 2H), 4.69 (dd, *J* = 14.2, 3.4 Hz, 1H), 4.59-4.66 (m, 1H), 4.44 (dd, *J* = 14.2, 9.3 Hz, 1H), 4.29 (dd, *J* = 10.3, 4.9 Hz, 1H), 2.89-2.96 (m, 1H), 1.34 (d, *J* = 6.9 Hz, 3H), 1.25 (d, *J* = 6.9 Hz, 3H); HRMS *m/z* (ESI^+) calcd for $C_{28}H_{28}N_2O_4$ (2M+1) 913.4176; found, 913.4174.

1-((*S*)-2-Hydroxy-2-(3-isopropyl-5-((*S*)-3-(2,2,2-trifluoroacetamido)-2,3-dihydrobenzofuran-5-yl)phenyl)ethyl)-1H-indole-7-carboxylic acid (**59**) and 2,2,2-trifluoro-N-((S)-5-(3-isopropyl-5-((S)-1-oxo-3,4-dihydro-1H-[1,4]oxazepino[6,5,4-hi]indol-3-yl)phenyl)-2,3-dihydrobenzofuran-3-yl)acetamide (**60**): To a mixture of (*S*)-1-(2-(3-bromo-5-isopropylphenyl)-2-hydroxyethyl)-1H-indole-7-carboxylic acid (**57**) (365 mg, 1.02 mmol), (*S*)-2,2,2-Trifluoro-N-(5-(4,4,5,5-tetramethyl-1,3,2-dioxaborolan-2-yl)-2,3-dihydrobenzofuran-3-yl)acetamide (**58**, Supp. Info.) (337 mg, 0.84 mmol) and $PdCl_2$(dppf).CH_2Cl_2 adduct (82 mg, 0.10 mmol) in 1,4-dioxane (8 mL) was added 2M aq. Na_2CO_3 (1.26 mL 2.52 mmol) and the resulting mixture was sparged with N_2 gas for 5 min. The reaction mixture was then stirred at 70 °C for 4.25 h, cooled to RT, and diluted with EtOAc. The mixture was further diluted with pH 7 buffer and the layers were separated. The aqueous layer was back extracted twice with EtOAc and the combined organic layers were washed with brine, dried over sodium sulfate, filtered, and concentrated under reduced pressure. The resulting residue was passed through a plug of silica gel eluting with EtOAc to afford a mixture of the title compounds **59** (MS (ESI^-)

m/z 551.3 (M-1)) and the corresponding lactone **60** (MS (ESI$^+$) *m/z* 534.2 (M+1)) which was carried on to the next step without further purification.

(*S*)-1-(2-(3-Bromo-5-isopropylphenyl)-2-hydroxyethyl)-1H-indole-7-carboxylic acid (**57**): To (*S*)-1-(2-(3-bromo-5-isopropylphenyl)-2-hydroxyethyl)-1H-indole-7-carbonitrile (**56**) (785 mg, 2.05 mmol) dissolved in EtOH (12 mL) and cooled to 0 °C was added KOH (8.2 mL, 20.5 mmol) and the resulting mixture was heated under microwave irradiations at 100 °C for 8 h. The reaction mixture was then diluted with 1M aq. HCl and EtOAc and extracted with EtOAc. The combined organic layers were dried over magnesium sulfate, filtered, and concentrated to afford the title compound (867 mg, 100%). MS (ESI$^+$) *m/z* 402.2 (M+1).

(*S*)-1-(2-(3-Bromo-5-isopropylphenyl)-2-hydroxyethyl)-1H-indole-7-carbonitrile (**56**): To a solution of 1*H*-indole-7-carbonitrile (**55**) (295 mg, 2.07 mmol) in DMF (10 mL) at RT was added K_2CO_3 (574 mg, 4.15 mmol) and the resulting mixture was stirred for 5 min. (*S*)-2-(3-Bromo-5-isopropylphenyl)oxirane (**54**) (550 mg, 2.28 mmol) in DMF (10 mL) was then added and the reaction mixture was heated to 80 °C and stirred for 16 h. The reaction mixture was then diluted with water and extracted with EtOAc. The combined organic layers were washed with brine, dried over magnesium sulfate, filtered, and concentrated. The crude residue was purified by flash column chromatography (gradient: 0-50% EtOAc in n-heptane) to give the title compound (685 mg, 86%). ^{1}H NMR (400 MHz, DMSO-d_6) δ 7.84-8.00 (m, 1H), 7.57 (dd, *J* = 7.4, 1.1 Hz, 1H), 7.52 (d, *J* = 3.0 Hz, 1H), 7.43 (t, *J* = 1.7 Hz, 1H), 7.30 (t, *J* = 1.9 Hz, 1H), 7.20-7.27 (m, 1H), 7.09-7.18 (m, 1H), 6.63 (d, *J* = 2.9

Hz, 1H), 5.76 (d, *J* = 4.4 Hz, 1H), 4.97 (dt, *J* = 8.7, 4.3 Hz, 1H), 4.65 (dd, *J* = 14.5, 4.1 Hz, 1H), 4.51 (dd, *J* = 14.6, 8.8 Hz, 1H), 2.81 (hept, *J* = 6.9 Hz, 1H), 1.13 (d, *J* = 7.3 Hz, 6H).

(*S*)-2-(3-Bromo-5-isopropylphenyl)oxirane (**54**): To a solution of (*S*)-2-(3-Bromo-5-isopropylphenyl)-2-hydroxyethyl 2,4,6-trimethylbenzenesulfonate (**53**) (1.86 g, 4.21 mmol) in toluene (64 mL) cooled to 0°C was added 10% NaOH (aq.) (32 mL, 4.21 mmol). The reaction was then warmed to RT and stirred for 16 h. The reaction mixture was diluted with water and extracted with EtOAc (x3). The combined organic layers were washed with brine, dried over magnesium sulfate, filtered, and concentrated. The crude residue was purified by flash column chromatography (gradient: 0-50% EtOAc in n-heptane) to give the title compound (265 mg, 26%). ^{1}H NMR (400 MHz, DMSO-d_6) δ 7.38 (t, *J* = 1.7 Hz, 1H), 7.27 (t, *J* = 1.7 Hz, 1H), 7.20 (t, *J* = 1.6 Hz, 1H), 3.93 (dd, *J* = 4.0, 2.5 Hz, 1H), 3.10 (dd, *J* = 5.4, 4.0 Hz, 1H), 2.95 – 2.83 (m, 2H), 1.19 (d, *J* = 6.9 Hz, 6H).

(*S*)-2-(3-Bromo-5-isopropylphenyl)-2-hydroxyethyl 2,4,6-trimethylbenzenesulfonate (**53**): 2,4,6-Trimethylbenzene-1-sulfonyl chloride (1.92 g, 8.80 mmol) was added to a solution of (*S*)-1-(3-bromo-5-isopropylphenyl)ethane-1,2-diol (**52**) (1.52 g, 5.87 mmol), pyridine (0.95 mL, 11.7 mmol), and DMAP (0.05 g, 0.411 mmol) in CH_2Cl_2 (50 mL). The reaction mixture was stirred at RT for about 60 h. The reaction mixture was then concentrated, and the residue was purified by flash column chromatography (gradient: 0-60% EtOAc in n-heptane) to give the title compound (1.86 g, 72%). ^{1}H NMR (400 MHz, DMSO-d_6) δ 7.30 (t, *J* = 1.6 Hz, 1H), 7.27-7.24 (m, 1H), 7.10 (s, 1H), 6.98-6.96 (m, 2H), 4.95 (dd, *J* =

8.2, 3.4 Hz, 1H), 4.09 (dd, *J* = 10.5, 3.4 Hz, 1H), 3.98 (dd, *J* = 10.5, 8.2 Hz, 1H), 2.85 (hept, *J* = 6.7 Hz, 1H), 2.59 (s, 6H), 2.32 (s, 3H), 1.21 (d, *J* = 6.9 Hz, 6H).

(*S*)-1-(3-Bromo-5-isopropylphenyl)ethane-1,2-diol (**52**): AD-mix-α (23.0 g, 15.5 mmol) was added to a mixture of *t*-BuOH (100 mL) and H_2O (100 mL) and the reaction mixture was stirred at RT until both phases were clear. The reaction mixture was then cooled to -10 °C and 1-bromo-3-isopropyl-5-vinylbenzene (**51**, Supp. Info.) (3.50 g, 15.5 mmol) was added. The resulting slurry was stirred vigorously at 0 °C for 1 h, and then warmed to RT for 16 h. Sodium sulfite (9.80 g, 78 mmol) was added and the mixture was stirred at RT for 30 min, diluted with water, and extracted with EtOAc. The organic layer was concentrated and the residue was purified by flash column chromatography (gradient: 0-60% EtOAc in n-heptane) to provide the title compound (1.52 g, 38%). ^{1}H NMR (400 MHz, Chloroform-*d*) δ 7.36 (t, *J* = 1.4 Hz, 1H), 7.32 (t, *J* = 1.5 Hz, 1H), 7.16 (s, 1H), 4.79 (dd, *J* = 8.1, 3.5 Hz, 1H), 3.78 (dd, *J* = 11.3, 3.5 Hz, 1H), 3.65 (dd, *J* = 11.3, 7.9 Hz, 1H), 2.89 (h, *J* = 7.0 Hz, 1H), 1.26 (d, *J* = 6.9 Hz, 6H).

2. Biological and *in vivo* experiments

Protocols, handling and care of animals were in accordance with the policy of the NIBR Cambridge Animal Care and Use Committee.

2.1 Human FXIa assay

The activity of human FXIa (Kordia Life Science NL, catalogue number HFXIa 1111a) was determined by monitoring the cleavage of a fluorescently labelled peptide

with the sequence D-Leu-Pro-Arg*Rh110-D-Pro (product number BS-2494.P2; Biosyntan GmbH, Berlin, Germany), where * indicates the scissile bond, D-Leu: D-leucine, Pro: proline, Arg: arginine, Rh110: rhodamine 110, D-Pro: D-proline. FXIa-mediated cleavage of the scissile bond of the peptide substrate leads to an increase of fluorescence intensity of the rhodamine 110 when using excitation and emission wavelengths of 485 nm and 535 nm, respectively. Fluorescence intensity one hour after addition of substrate was measured using the Synergy Neo2 (BioTek, Winooski, VT) 384-well microtiter plate reader at room temperature. The assay buffer contained 50 mM HEPES at pH 7.4, 125 mM NaCl, 5 mM $CaCl_2$ and 0.05% (w/v) CHAPS. Human FXIa was used at a final concentration of 0.1-0.4 nM (depending on enzyme batch activity) and the substrate BS-2494 concentration was 0.5 μM, which was much below its measured Km of 171 +/- 14 μM. Under these conditions, the increase of fluorescence intensity over time is linear for at least 60 minutes.

For testing the inhibitory activity of molecules, serial dilutions of compounds were prepared in 100% DMSO, and then diluted into 50 mM HEPES (2-[4-(2-

hydroxyethyl)piperazin-1-yl]ethanesulfonic acid) buffer pH 7.4 with 125 mM NaCl, and 0.05% (w/v) CHAPS (3-[(3-Cholamidopropyl)dimethylammonio]-1-propanesulfonate hydrate), with final DMSO concentrations not to exceed 1%. One µL of compound solution was pre-incubated with 11.5 µL FXIa solution in assay buffer (50 mM HEPES buffer pH7.4 with 125 mM NaCl, 5 mM $CaCl_2$, and 0.05% (w/v) CHAPS) for 60 minutes at room temperature. After the pre-incubation step, 12.5 µL of substrate BS-2494.P2 (diluted in assay buffer) was added and the enzymatic reaction was allowed to proceed for 60 minutes before measuring fluorescence intensity.

2.2 Human FXIa assay in plasma

In order to measure the activity of human FXIa in the presence of plasma, the catalytic domain fragment of the enzyme was used in order to prevent activation of the entire coagulation pathway (the catalytic domain fragment is incapable of activating Factor IX). A catalytic domain fragment containing a C500S mutation was added to 50% normal human plasma control obtained as a lyophilized powder 'Coagulation Control N' (reference no 5020050) purchased from Technoclone GmbH (Vienna, Austria). It was pooled from citrated plasma of selected healthy donors. The lyophilized plasma was

stored at 4 °C. Prior to its use the plasma was re-suspended in 1 mL of distilled water by carefully rotating the vial and then keeping it for 10 minutes at room temperature.

The catalytic domain fragment of FXIa (FXIa_cd_C500s) was produced in e.coli strain BL21(DE3) using the following synthetic DNA fragment:

MGSS**DDDDK**IVGGTASVRGEWPWQVTLHTTSPTQRHLCGGSIIGNQWILTAAHCFYG
VESPKILRVYSGILNQSEIKEDTSFFGVQEIIIHDQYKMAESGYDIALLKLETTVNYTDS
QRPISLPSKGDRNVIYTDCWVTGWGYRKLRDKIQNTLQKAKIPLVTNEECQKRYRGH
KITHKMICAGYREGGKDACKGDSGGPLSCKHNEVWHLVGITSWGEGCAQRERPGVY
TNVVEYVDWILEKTQAV

The underlined N-terminal extension was removed following enterokinase cleavage (recognition

sequence in red).

To measure the inhibitory activity of molecules in this system, serial dilutions of compounds were prepared in 100% DMSO, and then diluted into 50 mM HEPES (2-[4-(2-hydroxyethyl)piperazin-1-yl]ethanesulfonic acid) buffer pH 7.4 with 125 mM NaCl, and 0.05% (w/v) CHAPS (3-[(3-Cholamidopropyl)dimethylammonio]-1-propanesulfonate hydrate), with final DMSO concentrations not to exceed 1%. One µL of compound solution was pre-incubated with 11.5 µL FXIa_cd_C500S in 100% normal human control plasma

for 60 minutes at room temperature. After the pre-incubation step, 12.5 µL of substrate BS-2494.P2 in assay buffer (50 mM HEPES buffer pH 7.4 with 125 mM NaCl, 5 mM $CaCl_2$, and 0.05% (w/v) CHAPS) was added, and the enzymatic reaction was allowed to proceed for 60 minutes before measuring fluorescence intensity as described above for the biochemical assay without plasma. Final enzyme concentration in this system was 30 nM FXIa_cd_C500S, and final substrate concentration was 0.5 µM.

2.3 Protease panel: FXIa

To determine biochemical selectivity, a panel of related protease activities was profiled using a similar assay setup to that described above for human FXIa. Factor D was assessed using a TR-FRET-based assay as described in Ref. 26. The relevant conditions for each of the protease selectivity assays delineated in text, including enzyme source, fluorogenic peptide sequence and buffer modifications are described in the supporting information.

2.4 Plasma coagulation assays

The antithrombotic activity of compounds were tested using the activated partial thromboplastin time (aPTT) assay performed using in an Amelung ball coagulometer model KC4A (purchased through SYCOmed, Lemgo, Germany) or MC-10 (Merlin Medical, Lemgo, Germany). Compounds were diluted to 4x final concentration into

dilution buffer containing 80 mM Tris/HCl at pH 7.5 (Invitrogen, 15567-027) and 0.05% (w/v) CHAPS (Calbiochem, 220201). Assay reagents were added into a special cuvette containing a stainless ball (Merlin medical, Germany, Z05100) at 12 o'clock position. 50 µl of 4x compound solution was added to 50 µl of pre-warmed (37 °C) normal human plasma ("Coagulation Control N" reference no 5020050) and 50 µl of pre-warmed aPTT-s reagent (reference no TE0350 purchased from SYCOmed Lemgo, Germany) and incubated for 3 minutes at 37°C under rotation. The coagulation reaction was triggered by addition of 50 µl of 25 mM Calcium Chloride with an automatic handystep pipette supplied with the Coagulometer in order to start recording automatically upon reagent addition. Time until clotting was measured and plotted as a function of compound concentration to determine the potency of intrinsic pathway inhibition (reported as the concentration required to double the clotting time measured without compound present).

In order to measure any off-target coagulation activity, compounds were profiled in the prothrombin time (PT) assay to assess extrinsic coagulation cascade activity. Theoretically, compounds that selectively inhibit FXIa alone in the coagulation cascade should not modulate the prothrombin time assay. For measurement of the prothrombin time, compounds were tested at 1:3 serial dilutions starting from 100 µM top concentration.

Compounds were prepared as a 5x concentrate in dilution buffer containing 80 mM Tris/HCl at pH 7.5 (Invitrogen, 15567-027) and 0.05% (w/v) CHAPS (Calbiochem, 220201). 60 µl of compound (5X of final concentration) was placed into the coagulometer cuvette containing a stainless ball (Merlin medical, Germany, Z05100) at 12 o'clock position and 40 µl of pre-warmed (37 °C) normal human plasma was placed at the 9 o'clock position. The reaction was started by addition of 200 µl of Thromboplastin-DS reagent using the automatic handystep pipette supplied with the Coagulometer in order to start recording automatically upon reagent addition. Time until clotting was measured and plotted as a function of compound concentration to determine the potency of extrinsic pathway inhibition.

2.5 Plasma pharmacokinetic studies in mice.

The pharmacokinetics of compounds **1**, **6**, **7**, **8**, **11,** and **17** were determined in C57BL/6 mice and pharmacokinetics of compound **23** were determined in CD1 mice. Blood concentration versus time profiles were obtained from 2 groups of 3 male mice except for compound **17** where 2 male mice were used for intravenous PK study. In the intravenous PK group, the compound was administered intravenously (i.v.) by bolus injection (5 mL/kg) at a dose of 1 mg/kg (compounds **1**, **6**, **7**, **8**, **11**, **23**) or 0.4 mg/kg (compound **17**), solubilized in N-Methyl-2-pyrrolidone (10%) and blank plasma (90%) (compounds **6**, **7**, **11**) or 10% propyleneglycol and 25% of Solutol™(20%), dissolved in

PBS (compounds **1** and **8**) or 20% captisol in water (compound **17**) or 10% propyleneglycol and 10% of Solutol™, dissolved in PBS (compound **23**).

For oral PK, in another group of 3 male mice, a dose of 3 mg/kg (additional dose of 100 mg/kg for compound **23**) was orally applied (dosing volume of 10 mL/kg) as a homogenous suspension of water (99%), Tween80 (0.5%) and methylcellulose (0.5%) (compounds **1**, **6**, **7**, **8**, **11**, and **17**) or 20% captisol in water (compound **23**).

For compounds **6**, **7**, **11**, **17**, and **23**, blood (10 µL/time point, without anticoagulant) was collected by puncture of the lateral saphenous vein at different time points from the same animal (n=3 mice per route). The awake mice were restrained in a plastic tube for blood sampling. At the last time point, the animals were sacrificed. Analyses of parent compound concentrations were carried out in blood using LC-MS/MS. An aliquot of 10 µL was taken and 200 µL acetonitrile (including Glyburide (c = 50 ng/ml) as internal standard) was added for protein precipitation. Sample analysis was performed on a LC–MS/MS system.

In case of compounds **1** and **8**, approximately 50 µL of whole blood was collected from the tails at 5 min (IV dose only), 15 min (PO dose only), 0.5, 1, 2, 4, and 7 hours post-

dose and was transferred to EDTA tubes. Blood was centrifuged at 3,000 rpm and the resultant plasma was transferred to a capped PCR 96-well plate, and frozen at –20 °C until subsequent analysis by high performance liquid chromatography coupled with tandem mass spectrometry (HPLC-MS/MS). Similarly, the relevant pharmacokinetic parameters were estimated using non-compartmental methods using WinNonlin (Enterprise, Version 5.2) purchased from Pharsight Corporation (St. Louis, MO) or Watson LIMS (Thermo, Waltham, MA). Other relevant calculations were performed in Microsoft Excel.

2.6 Plasma pharmacokinetic studies in rats

The pharmacokinetics of compound **23** was determined in Sprague Dawley rats. The compound was dosed intravenously (IV, via injection into the jugular vein catheter; 1 mg/kg, n=3 animals) and orally (PO, via oral gavage; at 3, 30, and 100 mg/kg, n=3 animals). The IV solution was prepared as a 1 mg/mL formulation of 10% hydroxypropyl-β-cyclodextrin (HP-β-CD) and 20% polyethylene glycol 300 in water. The PO solution formulations were prepared at concentrations of 0.3, 3 and 10 mg/mL for the 3, 30, and 100 mg/kg doses, respectively and were prepared with 10% hydroxypropyl-β-cyclodextrin

(HP-β-CD) and 20% polyethylene glycol 300 in water. Approximately 200 μL of whole blood was collected from the tails at 5 min (IV dose only), 15 min, 0.5, 1, 2, 4, 7, and 24 hours post-dose and was transferred to EDTA tubes. Blood was centrifuged at 3,000 rpm and the resultant plasma was transferred to a capped PCR 96-well plate, and frozen at –20 °C until subsequent analysis by HPLC-MS/MS. The relevant pharmacokinetic parameters were estimated using non-compartmental methods using WinNonlin (Enterprise, Version 5.2) purchased from Pharsight Corporation (St. Louis, MO) or Watson LIMS (Thermo, Waltham, MA).

2.7 Plasma pharmacokinetic studies in dogs

The pharmacokinetics of compound **23** was determined in beagle dogs. The compound was dosed intravenously (IV, via slow bolus injection via the cephalic vein; 1 mg/kg, n=3 animals) and orally (PO; 10 mg/kg, and 75 mg/kg n=3 animals/compound) by gavage. The IV formulation was a 1 mg/mL solution consisting of 10% hydroxypropyl-β-cyclodextrin (HP-β-CD) and 20% polyethylene glycol 300 in water. The PO solution formulations were prepared at concentrations of 1 and 15 mg/mL for the 10 and 75 mg/kg doses, respectively and were prepared with 10% hydroxypropyl-β-cyclodextrin (HP-β-CD)

and 20% polyethylene glycol 300 in water. Blood was collected at 5 min (IV dose only), 15 min, 0.5, 1, 2, 4, 7, and 24 hours post-dose for the 1 mg/kg IV dose and the 10 mg/kg PO dose. For the 75 mg/kg dose, blood was collected at 0.5, 1, 3, 7, and 24 hours post-dose. Blood was centrifuged at 3,000 rpm and the resultant plasma was transferred for subsequent analysis by HPLC-MS/MS. Similarly, the relevant pharmacokinetic parameters were estimated using non-compartmental methods using WinNonlin (Enterprise, Version 5.2) purchased from Pharsight Corporation (St. Louis, MO) or Watson LIMS (Thermo, Waltham, MA). Other relevant calculations were performed in Microsoft Excel.

ASSOCIATED CONTENT

Supporting Information

The Supporting Information is available free of charge on the ACS Publication website at DOI:

Synthesis and characterization of compounds **4, 25, 26, 28, 29, 40, 41, 47, 48, 51, and 58.** Crystallographic structure determination of PKL in complex with **4** and of fXIa in complex with compounds **2**, **3, 7, 15** and **23**.

Molecular formula string (CSV)

Accession Codes

Atomic coordinates and structure factors for the crystal structures of PKL with compound **4** and of FXIa with compounds **2**, **3**, **7**, **15** and **23** can be accessed using PDB codes 6T7P, 6TS4, 6TS7, 6TS6, 6TS5, and 6USY, respectively.

AUTHOR INFORMATION

Corresponding Author

* Edwige Lorthiois: Tel: +41616961955. E-mail: edwige.lorthiois@novartis.com
* James Roache: Tel: +16178717539. E-mail: james.roache@novartis.com

ORCID

Edwige Lorthiois: 0000-0002-6147-9321
James Roache: 0000-0002-9515-2394
Gordon Turner: 0000-0001-9156-7499

Rajeshri G. Karki: 0000-0003-2210-5789
Martin Renatus: 0000-0002-7348-2915
Richard Sedrani: 0000-0001-7759-5856
Christopher M. Adams: 0000-0002-5246-884X

Present Addresses

¶Merck KGaA, Frankfurter Str. 250, D-64293 Darmstadt, Germany.
$DMPK Modelling & Simulation, AstraZeneca, Oncology R&D, DMPK, Hodgkin Building (B900), Chesterford Research Park, Little Chesterford, Saffron Walden, CB10 1XL.
%Biomolecular NMR platform, ETH Zurich, HPP L 25.2, Hönggerbergring 64, 8093 Zürich, Switzerland.
!National Kidney Foundation, 30 East 33rd Street, New York, NY 10016, USA.
ʃCedilla Therapeutics, 38 Sidney Street, Cambridge, MA 02139.
⌇Molecular Templates, Inc., 9301 Amberglen Blvd., Ste. 100, Austin, TX 78729.
tDepartment of Medicinal Chemistry, Relay Therapeutics, 399 Binney Street, Cambridge, MA 02138.

Author Contributions

The manuscript was written through contributions of all authors. All authors have given approval to the final version of the manuscript.

Funding Sources

The authors declare no competing financial interest beyond their employment by Novartis Institutes for BioMedical Research Inc. which funded all work described in the manuscript.

ACKNOWLEDGMENT

The authors would like to thank Prasad Appukuttan, Sangamesh Badiger, Ramalinga Vara Prasad and their team at Aurigene Discovery Technologies Limited (www.aurigene.com) and James Powers for the synthesis of select compounds for this project. Arnaud Decock is acknowledged for the crystallization of compound **4** with PKL.

ABBREVIATIONS

aPTT, activated partial thromboplastin time; BEI, binding efficiency index; BSEP, bile salt export pump; cd, catalytic domain; cLogD, calculated LogD; COX1, cyclooxygenase-1; DDI, drug-drug interaction; D.N., dose normalized; FII, Factor II; FVIIa, Factor VIIa; FIX, Factor IX; FXa, Factor Xa; FXI, Factor XI; FXIa, Factor XIa; FD, Factor D; FBS, fragment based screening; LLE, lipophilic ligand efficiency; MDCK, Madin–Darby canine kidney;

MDR1, multi-drug resistance gene 1; NOACs, non-vitamin K anti-coagulants; PBPK, physiologically based pharmacokinetic; PDE4d, phosphodiesterase 4d; PK, prekallikrein; PKL, plasma kallikrein; PPAR, peroxisome proliferator-activated receptors; PT, prothrombin time; SAR, structure activity relationship; SSAO, semicarbazide-sensitive amine oxidase; tPa, tissue plasminogen activator; uPA, urokinase-type plasminogen activator; VMAT2, vesicular monoamine transporter 2.

REFERENCES

1 Wardroop, D.; Keeling, D. The story of the discovery of heparin and warfarin. *British Journal of Haematology*, **2008**, *141*, 757-763.

2 Kirley, K.; Qato, D. M.; Kornfield, R.; Stafford, R. S.; Alexander, G. C. National trends in oral anticoagulant use in the United States 2007-2011. *Circ Cardiovasc Qual Outcomes,* **2012**, *5*, 615-621.

3 Ageno, W.; Gallus, A.S.; Wittkowsky, A.; Crowther, M.; Hylek, E.M.; Palareti, G. Oral anticoagulant therapy: antithrombotic therapy and prevention of thrombosis, 9th ed:

American College of Chest Physicians Evidence Based-Based Clinical Practice Guidelines. *Chest.*, **2012**, *141,* e44S-e88S.

4 Meurer, L. N.; Jamieson, B. What is the interval for monitoring warfarin therapy once therapeutic levels are achieved? *J. Fam. Pract.,* **2005**, *54*, 156-178.

5 Roehrig, S.; Straub, a.; Pohlmann, J.; Lampe, T.; Pernerstorfer, J.; Schlemmer, K.-H.; Reinemer, P.; Perzborn, E. Discovery of the novel antithrombotic agent 5-chloro-N-({(5S)-2-oxo-3- [4-(3-oxomorpholin-4-yl)phenyl]-1,3-oxazolidin-5-yl}methyl)thiophene-2-carboxamide (BAY 59-7939): an oral, direct factor Xa inhibitor. *J. Med. Chem.*, **2005**, *48*, 5900-5908.

6 Pinto, D. J. P.; Orwat, M. J.; Koch, S.; Rossi, K. A.; Alexander, R. A.; Smallwood, A.; Wong, P. C.; Rendina, A. R.; Luettgen, J. M.; Knabb, R. M.; He, K.; Xin, B.; Wexler, R. R.; Lam, P. Y. S. Discovery of 1-(4-methoxyphenyl)-7-oxo-6-(4-(2-oxopiperidin-1-yl)phenyl)-4,5,6,7-tetrahydro-1H-pyrazolo[3,4-c]pyridine-3-carboxamide (Apixaban, BMS-562247), a highly potent, selective, efficacious, and orally bioavailable inhibitor of blood coagulation factor Xa. *J. Med. Chem.*, **2007**, *50*, 5339-5356.

7 Hauel, N. H.; Nar, H.; Priepke, H.; Ries, U.; Stassen, J.-M.; Wienen, W. Structure-based design of novel potent nonpeptide thrombin inhibitors. *J. Med. Chem.*, **2002**, *45*, 1757-1766.

8 Briere, J. B.; Bowrin, K.; Coleman, C.; Fauchier, L.; Levy, P.; Folkerts, K.; Toumi, M.; Taieb, V.; Millier, A.; Wu, O. Real-world clinical evidence on rivaroxaban, dabigatran, and apixaban compared with vitamin K antagonists in patients with nonvalvular atrial fibrillation: a systematic literature review. *Expert Rev. Pharmacoecon Outcomes Res.,* **2018**, *19*, 27-36.

9 Yao, X.; Abraham, N. S.; Sangaralingham, L. R.; Bellolio, M. F.; McBane, R. D.; Shah, N. D. Noseworthy P. A. Effectiveness and safety of dabigatran, rivaroxaban, and apixaban versus warfarin in nonvalvular atrial fibrillation. *J. Am. Heart Assoc.*, **2016**, *5*, e003725.

10 Friberg, L.; Rosenqvist M.; Lip, G. Y. Net clinical benefit of warfarin in patients with atrial fibrillation: a report from the Swedish atrial fibrillation cohort study. *Circulation*, **2012**, *125*, 2298-2307.

11 Bassand, J. P.; Accetta, G.; Camm, A. J.; Cools, F.; Fitzmaurice, D. A.; Fox, K. A.; Goldhaber S. Z.; Goto, S.; Haas, S.; Hacke, W.; Kayani, G.; Mantovani, L. G.; Misselwitz, F.; Ten Cate, H.; Turpie, A. G.; Verheugt, F. W.; Kakkar, A. K. Two-year outcomes of patients with newly diagnosed atrial fibrillation: results from GARFIELD-AF. *Eur. Heart J.*, **2016**, *37*, 2882-2889.

12 Gailani, D.; Bane, C. E.; Gruberm, A. Factor XI and contact activation as targets for antithrombotic therapy. *J. Thromb. Haemost.*, **2015**, *13*, 1383-1395.

13 a) Chen, Z.; Seiffert, D.; Hawes, B. Inhibition of factor XI activity as a promising antithrombotic strategy. *Drug Discov. Today*, **2014**, *19*, 1435-1439. b) Bane, C. E.; Gailani, D. Factor XI as a target for antithrombotic therapy. *Drug Discov. Today*, **2014**, *19*, 1454-1458.

14 Duga, S.; Salomon, O. Congenital factor XI deficiency: an update. *Seminars in Thrombosis & Hemostasis*, **2013**, *39*, 621-631.

15 Büller, H. R.; Bethune, C.; Bhanot, S.; Gailani, D.; Monia, B. P.; Raskob, G. E.; Segers, A.; Verhamme, P.; Weitz, J. I. Factor XI antisense oligonucleotide for prevention of venous thrombosis. *N. Engl. J. Med.*, **2015**, *372*, 232-240.

16 Quan, M. L.; Pinto, D. J. P.; Smallheer, J. M.; Ewing, W. R.; Rossi, K. A.; Luettgen J. M.; Seiffert, D. A.; Wexler, R. R. Factor XIa inhibitors as new anticoagulants. *J. Med. Chem.*, **2018**, *61*, 7425-7447.

17 Al-Horani, R. A.; Desai, U. R. Factor XIa inhibitors: a review of patent literature. *Expert Opin. Ther. Pat.*, **2016**, *26*, 323-345.

18 a) Thomas, D.; Thelen, K.; van der Mey, D.; Schwers, S.; Schiffer, S.; Unger, J.; Heubach, A.; Yassen, A.; Boxnick, S. First evaluation of the safety, pharmacokinetics and pharmacodynamics of BAY1213790, a full human IgG1 antibody targeting coagulation factor XIa, in healthy young men. *Res. Pract. Thromb. Haemostasis* **2017**, *1 (Suppl. 1)*, 392 (Abstract PB 834), b) Koch, A. W.; Schiering N.; Melkko S.; Ewert S.; Salter J.; Zhang Y.; McCormack P.; Yu J.; Huang X.; Chiu Y. H.; Chen Z.; Schleeger S.; Horny G.; DiPetrillo K.; Muller L.; Hein A.; Villard F.; Scharenberg M.; Ramage P.; Hassiepen U.;

Côté S.; DeGagne J.; Krantz C.; Eder J.; Stoll B.; Kulmatycki K.; Feldman D. L.; Hoffmann P.; Basson C. T.; Frost R. J. A.; Khder Y. MAA868, a novel FXI antibody with a unique binding mode, shows durable effects on markers of anticoagulation in humans. *Blood* **2019**, *133*, 1507-1516.

19 Corte, J. R.; Pinto, D. J. P.; Fang, T.; Osuna, H.; Yang, W.; Wang, Y.; Lai, A.; Clark, C. G.; Sun, J.-H.; Rampulla, R.; Mathur, A.; Kaspady, M.; Neithnadka, P. R.; Li, Y.-X. C.; Rossi, K. A.; Myers Jr., J. E.; Sheriff, S.; Lou, Z.; Harper, T. W.; Huang, C.; Zheng, J. J.; Bozarth, J. M.; Wu, Y.; Wong, P. C.; Crain, E. J.; Seiffert, D. A.; Luettgen, J. M.; Lam, P. Y. S.; Wexler, R. R.; Ewing, W. R. Potent, orally bioavailable, and efficacious macrocyclic inhibitors of factor XIa. Discovery of pyridine-based macrocycles possessing phenylazole carboxamide P1 groups. *J. Med. Chem.,* **2020**, *63*, 784-803.

20 Pinto, D. J. P.; Orwat, M. J.; Smith II, L. M.; Quan, M. L.; Lam, P. Y. S.; Rossi, K. A.; Apedo, A.; Bozarth, J. M.; Wu, Y.; Zheng, J. J.; Xin, B.; Toussaint, N.; Stetsko, P.; Gudmundsson, O.; Maxwell, B.; Crain, E. J.; Wong, P. C.; Lou, Z.; Harper, T. W.; Chacko, S. A.; Myers Jr., J. E.; Sheriff, S.; Zhang, H.; Hou, X.; Mathur, A.; Seiffert, D. A.; Wexler,

R. R.; Luettgen, J. M.; Ewing, W. R. Discovery of a parenteral small molecule coagulation factor XIa inhibitor clinical candidate (BMS-962212). *J. Med. Chem.*, **2017**, *60*, 9703-9723.

21 Perera, V.; Luettgen, J. M.; Wang, Z.; Frost, C. E.; Yones, C.; Russo, C.; Lee, J.; Zhao, Y.; LaCreta, F. P.; Ma, X.; Knabb, R. M.; Seiffert, D.; DeSouza, M.; Mugnier, P.; Cirincione, B.; Ueno, T.; Frost, R. J. A. First in human study to assess safety, pharmacokinetics and pharmacodynamics of BMS-962212, a direct, reversible, small molecule factor XIa inhibitor in non-Japanese and Japanese healthy subjects. *Br. J. Clin. Pharmacol.* **2018**, *84*, 876.

22 Oral factor XIa inhibitor for the prevention of new ischemic stroke in patients receiving aspirin and clopidogrel following acute ischemic stroke or transient ischemic attack (TIA): https://clinicaltrials.gov/ct2/show/NCT03766581 (accessed Apr 26, 2019).

23 Hayward, N. J.; Goldberg, D. I.; Morrel, E. M.; Friden, P. M.; Bokesch, P. M. *Abstract 13747*: Phase 1a/1b study of EP-7041: a novel, potent, selective, small molecule FXIa inhibitor. *Circulation* **2017**, *136*, A13747.

24 Sedrani, R.; Hommel, U.; Eder, J. Protease-Directed Drug Discovery. In *Gene Family Targeted Molecular Design*; Lackey, K.E., Ed.; John Wiley and Sons: New York, 2008; Chapter 6, 159-197.

25 Long, A. T.; Kenne, E.; Jung, R.; Fuchs, T. A.; Renné, T. Human deficiencies in intrinsic cascade proteases FXII and plasma kallikrein (PKL) have not been strongly associated with antithrombotic protection or enhanced bleeding risk, see: Contact system revisited: an interface between inflammation, coagulation, and innate immunity. *J. Thromb. Haemost.*, **2016**, *14*, 427-437.

26 a) Bates, S. M.; Weitz, J. I. Coagulation Assays. *Circulation* **2005**, *112,* e53-e60. b) Kitchen, S.; McCraw, A.; Echenagucia, M. Diagnosis of Hemophilia and Other Bleeding Disorders, A Laboratory Manual (second edition, **2010**). World Federation of Hemophilia http://www1.wfh.org/publication/files/pdf-1283.pdf (accessed Apr 3, 2020).

27 Karki, R. G.; Powers, J.; Mainolfi, N.; Anderson, K.; Belanger, D. B.; Liu, D.; Ji, N.; Jendza, K.; Gelin, C. F.; Mac Sweeney, A.; Solovay, C.; Delgado, O.; Crowley, M.; Liao, S.-M.; Argikar, U. A.; Flohr, S.; La Bonte, L. R.; Lorthiois, E.; Vulpetti, A.; Brown, A.; Long,

D.; Prentiss, M.; Gradoux, N.; de Erkenez, A.; Cumin, F.; Adams, C.; Jaffee, B.; Mogi, M. Design, synthesis, and preclinical characterization of selective factor D inhibitors targeting the alternative complement pathway. *J. Med. Chem.* **2019**, *62*, 4656-4668.

28 Vulpetti, V.; Randl, R.; Rüdisser, S.; Ostermann, N.; Erbel, P.; Mac Sweeney, A.; Zoller, T.; Salem, B.; Gerhartz, B.; Cumin, F.; Hommel, U.; Dalvit, C.; Lorthiois, E.; Maibaum, J. Structure-based library design and fragment screening for the identification of reversible complement factor D protease inhibitors. *J. Med. Chem.* **2017**, *60*, 1946-1958.

29 Vulpetti, V.; Ostermann, N.; Randl, S.; Yoon, T.; Mac Sweeney, A.; Cumin, F.; Lorthiois, E.; Rüdisser, S.; Erbel, P.; Maibaum, J. Discovery and design of first benzylamine-based ligands binding to an unlocked conformation of the complement factor D. *ACS Med. Chem. Lett.,* **2018**, *9*, 490-495.

30 Volanakis, J. E.; Narayana, S. V. Complement factor D, a novel serine protease. *Protein Sci.,* **1996**, *5*, 553-564.

31 Fischer, P. M. Design of small-molecule active-site inhibitors of the S1A family proteases as procoagulant and anticoagulant drugs. *J. Med. Chem.*, **2018**, *61*, 3799-3822.

32 a) Pinto, D. J.; Smallheer, J. M.; Corte, J. R.; Austin, E. J.; Wang, C.; Fang, T.; Smith, L. M., 2nd; Rossi, K. A.; Rendina, A. R.; Bozarth, J. M.; Zhang, G.; Wei, A.; Ramamurthy, V.; Sheriff, S.; Myers, J. E., Jr.; Morin, P. E.; Luettgen, J. M.; Seiffert, D. A.; Quan, M. L.; Wexler, R. R. Structure-based design of inhibitors of coagulation factor XIa with novel P1 moieties. *Bioorg. Med. Chem. Lett.,* **2015**, *25*, 1635-1642; b) Quan, M. L.; Lam, P. Y. S.; Han, Q.; Pinto, D. J. P.; He, M. Y.; Li, R.; Ellis, C. D.; Clark, C. G.; Teleha, C. A.; Sun, J. H.; Alexander, R. S.; Bai, S.; Luettgen, J. M.; Knabb, R. M.; Wong, P. C.; Wexler, R. R. Discovery of 1-(3‘-aminobenzisoxazol-5‘-yl)-3-trifluoromethyl-N-[2-fluoro-4-[(2‘-dimethylaminomethyl)imidazol-1-yl]phenyl]-1H-pyrazole-5-carboxyamide hydrochloride (Razaxaban), a highly potent, selective, and orally bioavailable factor Xa inhibitor. *J. Med. Chem.,* **2005**, *48*, 1729-1744.

33 Katz, B. A.; Sprengeler, P. A.; Luong, C.; Verner, E.; Elrod, K.; Kirtley, M.; Janc, J.; Spencer, J. R.; Breitenbucher, J. G.; Hui, H.; McGee, D.; Allen, D.; Martelli, A.; Mackman, R. L. Engineering inhibitors highly selective for the S1 sites of Ser190 trypsin-like serine protease drug targets. *Chem. Biol.,* **2001**, *8*, 1107-1121.

34 Wendt, M. D.; Geyer, A.; McClellan, W. J.; Rockway, T. W.; Weitzberg, M.; Zhao, X.; Mantei, R.; Stewart, K.; Nienaber, V.; Klinghofer, V.; Giranda, V. L. Interaction with the S1 beta-pocket of urokinase: 8-heterocycle substituted and 6,8-disubstituted 2-naphthamidine urokinase inhibitors. *Bioorg. Med. Chem. Lett.,* **2004**, *14*, 3063-3068.

35 Mackman, R. L.; Katz, B. A.; Breitenbucher, J. G.; Hui, H. C.; Verner, E.; Luong, C.; Liu, L.; Sprengeler, P. A. Exploiting subsite S1 of trypsin-like serine proteases for selectivity: potent and selective inhibitors of urokinase-type plasminogen activator. *J. Med. Chem.* **2001**, *44*, 3856-3871.

36 Our subsequent efforts to target the S2' pocket will be reported in due course.

37 For examples of S1 serine protease inhibitors with acid-like motif interacting in the oxyanion hole: a) Kohrt, J. T.; Filipski, K. J.; Cody, W. L.; Cai, C.; Dudley, D. A.; Van Huis,

C. A.; Willardsen, A.; Rapundalo, S. T.; Saiya-Cork, K.; Leadley, R. J.; Narasimhan, L.; Zhang, E.; Witlow, M.; Adler, M.; McLean, K.; Chou, Y.-L.; mcKnight, C.; Arnaiz, D. O.; Shaw, K. J.; light, D. R.; Edmunds, J. J. The discovery of fluoropyridine-based inhibitors of the factor VIIa/TF complex. *Bioorg. Med. Chem. Lett.*, **2005**, *15*, 4752-4756. b) West, C. W.; Adler, M.; Arnaiz, D.; Chen, D.; Chu, K.; Gualtieri, G.; Ho, E.; Huwe, C.; Light, D.; Phillips, G.; Pulk, R.; Sukovich, D.; Wiltlow, M.; Yuan, S.; Bryant, J. Identification of orally bioavailable, non-amidine inhibitors of urokinase plasminogen activator (uPA). *Bioorg. Med. Chem. Lett.*, **2009**, *19*, 5712-5715, c) Greco, M. N.; Hawkins, M. J.; Powell, E. T.; Almond, H. R.; de Garavilla, L.; Hall, J.; Minor, L. K.; Wang, Y. P.; Corcoran, T. W.; Di Cera, E.; Cantwell, A. M.; Savvides, S. N.; Damiano, B. P.; Maryanoff, B. E. Discovery of potent, selective, orally active, nonpeptide inhibitors of human mast cell chymase. *J. Med. Chem.,* **2007**, *50*, 1727-1730.

38 Decock A.; Renatus, M. Unpublished results.

39 The assignment of the (*S)*-configured absolute stereochemistry was not entirely unambiguous.

40 Liang, G.; Choi-Sledeski, Y. M.; Poli, G. B.; Chen, X.; Minnich, A. ; Wang, Q. ; Tsay, J.; Sides, K. Vaz, R. J. Structure-based design, synthesis and profiling of a β-tryptase inhibitor with a spiro-piperidineamide scaffold, benzylamnine P1 group, and a substituted indole P4 group. *Med. Chem. Commun.*, **2011**, *2*, 794-798.

41 a) Mutlib, A. E.; Dickenson, P.; Chen, S.-Y.; Espina, R. J.; Daniels, J. S.; Gan, L.-S. Bioactivation of benzylamine to reactive intermediates in rodents: formation of glutathione, glutamate, and peptide conjugates. *Chem. Res. Toxicol.*, **2002**, *15*, 1190-1207, b) Mutlib, A. E.; Chen, S.-Y.; Espina, R. J.; Shockcor, J.; Prakash, S. R.; Gan, L.-S. P450-mediated metabolism of 1-[3-(aminomethyl)phenyl]-N-[3-fluoro-2'-(methylsulfonyl)- [1,1'-biphenyl]-4-yl]-3-(trifluoromethyl)-1H-pyrazole- 5-carboxamide (DPC 423) and its analogues to aldoximes. Characterization of glutathione conjugates of postulated intermediates derived from aldoximes. *Chem. Res. Toxicol.*, **2002**, *15*, 63-75.

42 Belanger, D.; Flohr, S.; Gelin, C. F.; Jendza, K.; Ji, N.; Karki, R. G.; Liu, D.; Lorthiois, E.; Mainolfi, N.; Powers, J. J.; Vulpetti, A. Amidomethyl-biaryl Derivatives Complement Factor D Inhibitors and Uses Thereof. PCT Int. Appl. WO/2016/088082, 2016.

43 The enantiomer of **6** with (*R*)-2,3-dihydrobenzofuranyl-3-amine P1 moiety was found significantly less potent with an IC_{50} of 1.90 μM against FXIa.

44 Of note, for the assessment of FXIa inhibition in human plasma we chose to use only the catalytic domain of FXIa to prevent FXIa activation of endogenous substrates present in the plasma (e.g FIX) which could lead to unintended activation of the fluorescent peptide substrates used in the assay. Based on crystallographic data of the delineated inhibitors in this manuscript we do not expect substantial differences in potency would arise due to differences between full length and catalytic domain variants.

45 Veloso, D.; Shilling, J.; Shine, J.; Fitch, W. M.; Colman, R. W. Recent evolutionary divergence of plasma prekallikrein and factor XI. *Thrombosis Research*, **1986**, *43*, 153-160.

46 Girolami, A.; Scarparo, P.; Candeo, N.; Lombardi, A. M. Congenital prekallikrein deficiency. *Expert Rev. Hematol.* **2010**, *3*, 685- 695.

47 The correlation of FXI activity to 2xaPTT was determined via a calibration curve using FXI depleted plasma. Please see the supporting information for details.

48 One advantage of employing the PT assay is that it provides a more comprehensive assessment of off-target coagulation modulation by compounds, in particular those which may inhibit more than one proteases in the cascade, which would be challenging to asses by individual biochemical selectivity values alone.

49 a) Kuntz, I. D.; Chen, K.; Sharp, K. A.; Kollman, P. A. The maximal affinity of ligands. *Proc.Natl. Acad. Sci. USA,* **1999**, *96*, 9997-10002, b) Hopkins, A. L.; Groom, C. R.; Alex, A. Ligand efficiency: a useful metric for lead selection. *Drug Discov. Today,* **2004**, *9*, 430-431, c) Abad-Zapatero, C.; Metz, J. T. Ligand efficiency indices as guideposts for drug discovery. *Drug Discov. Today,* **2005**, *10*, 464-469, d) Reynolds, C. H.; Bembenek, S. D.; Tounge, B. A. The role of molecular size in ligand efficiency. *Bioorg. Med. Chem. Lett.,* **2007**, *17*, 4258-4261.

50 a) Leeson; P. D., Springthorpe; B. The influence of drug like concepts on decision-making in medicinal chemistry. *Nat. Rev. Drug Discov.,* **2007**, *6*, 881-890, b) Perola, E. An analysis of binding efficiencies of drugs and their leads in successful drug discovery programs. *J. Med. Chem.,* **2010**, *53*, 2986-2997, c) Ryckmans, T.; Edwards, M. P.; Horne,

V. A.; Correia, A. M.; Owen, D. R.; Thompson, L. R.; Tran, I.; Tutt, M. F.; Young, T. Rapid assessment of a novel series of selective CB2 agonists using parallel synthesis protocols: a lipophilic efficiency (LipE) analysis. *Bioorg. Med. Chem. Lett.,* **2009**, *19*, 4406-4409, d) Schultz, M. D. The thermodynamic basis for the use of lipophilic efficiency in enthalpic optimization. *Bioorg. Med. Chem. Lett.,* **2013**, *23*, 5992-6000. e) Scott, J. S.; Waring, M. J. Practical application of ligand efficiency metrics in lead optimisation. *Bioorg. Med. Chem.*, **2018**, *26*, 3006-3015.

51 The absolute stereochemistry was confirmed by chemical correlation via asymmetric synthesis and via X-ray co-crystal structure of **13** and FXIa (not shown).

52 The (*R*)-isomer, proved to be the less active isomer with a FXIa IC_{50} of 0.005 μM and and IC_{50} in the presence of plasma of 0.42 μM.

53 Structurally, the activity of the (*S*)-isomer correlated well with the active (*R*) conformation of the fused 3,4-dihydro-2H-benzo[b][1,4]oxazine **13**, described earlier with the S benzylic hydroxyl group of **23** lying in the same trajectory as the C3 carbon of the 3,4-dihydro-2H-benzo[b][1,4]oxazine.

54 A strategy focused on molecules with a low Vdss has previously been successful for the development of FXa inhibitors, see: Pinto, D. J.; Orwat, M. J.; Koch, S.; Rossi, K. A.; Alexander, R. S.; Smallwood, A.; Wong, P. C.; Rendina, A. R.; Luettgen, J. M.; Knabb, R. M.; He, K.; Xin, B.; Wexler, R. R.; Lam, P. Y. Discovery of 1-(4-methoxyphenyl)-7-oxo-6-(4-(2-oxopiperidin-1-yl)phenyl)-4,5,6,7-tetrahydro-1H-pyrazolo[3,4-c]pyridine-3-carboxamide (apixaban, BMS-562247), a highly potent, selective, efficacious, and orally bioavailable inhibitor of blood coagulation factor Xa. *J. Med. Chem*. **2007**, *50*, 5339-5356.

55 Gobeau, N.; Stringer, R.; De Buck, S.; Faller, B. Evaluation of the GastroPlus™ Advanced Compartmental and Transit (ACAT) model in early discovery. *Pharm Res.* **2016**, *33*, 216-2139.

56 Molander, G. A.; Trice, S. L. J.; Kennedy, S. M. Scope of the two-step, one-pot palladium-catalyzed borylation/Suzuki cross-coupling reaction utilizing bis-boronic acid. *J. Org. Chem.*, **2012**, *77*, 8678-8688.

Structure-based design and pre-clinical characterization of selective and orally bioavailable Factor XIa inhibitors: Demonstrating the power of an integrated S1 protease family approach.

ABSTRACT:

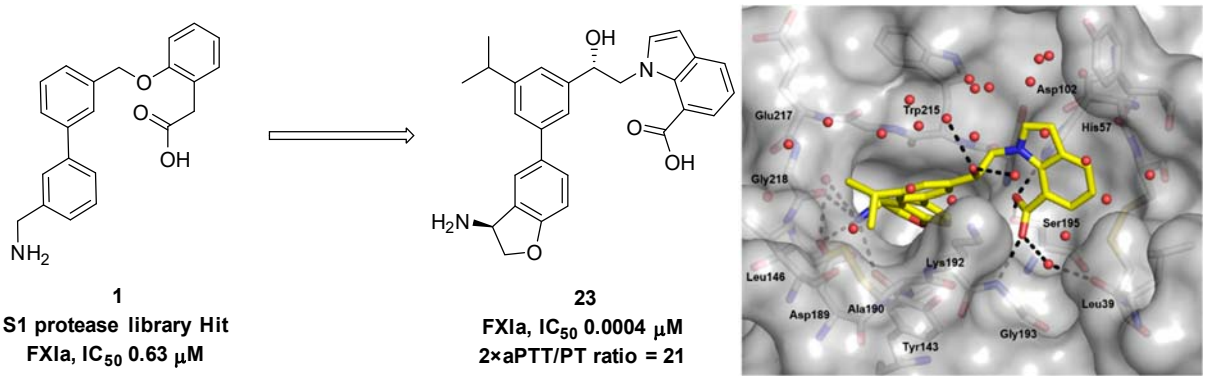

1
S1 protease library Hit
FXIa, IC_{50} 0.63 μM

23
FXIa, IC_{50} 0.0004 μM
2×aPTT/PT ratio = 21

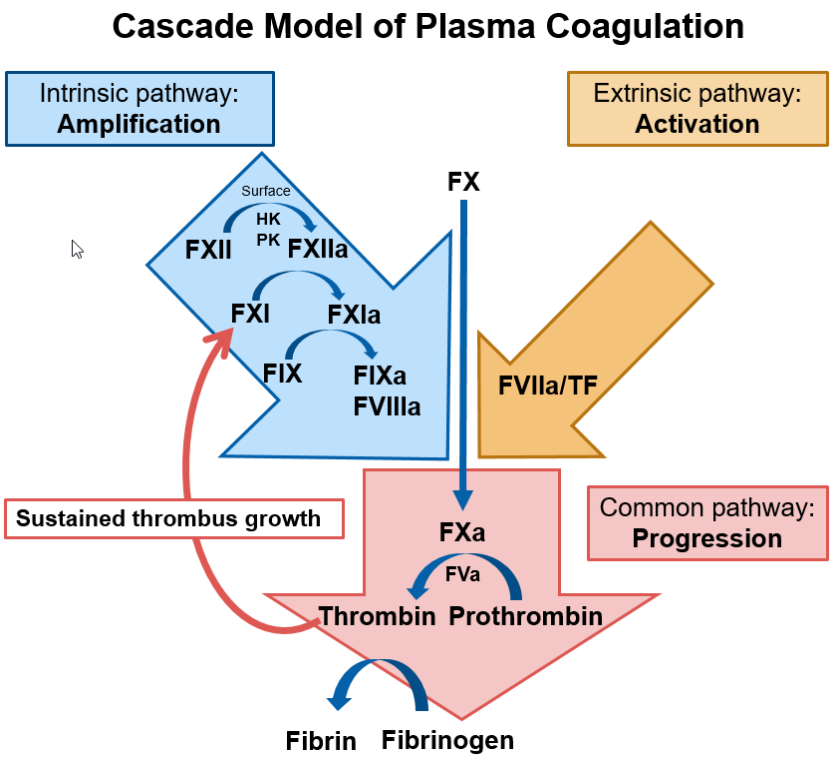

Figure 1: Schematic representation of the coagulation cascade. The aPTT assay assesses inhibition of the intrinsic (blue) and progression (red) components of the pathway, while the PT assay assesses the extrinsic (orange) and progression components.

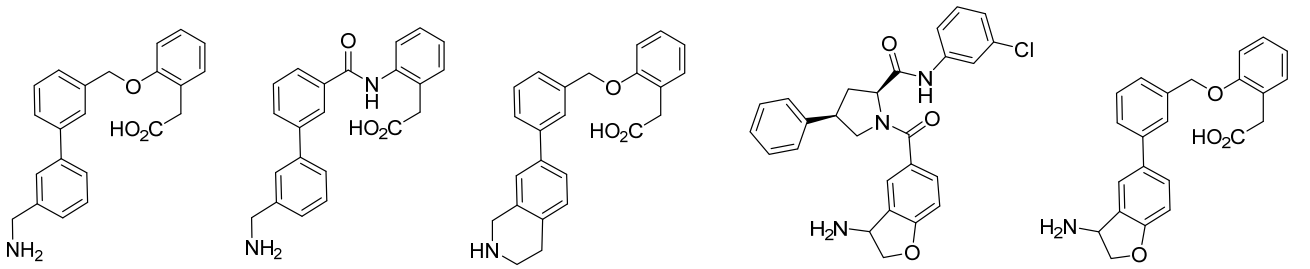

1
FXIa, IC_{50}: 0.63 μM
FD, IC_{50}: 0.008 μM

2
FXIa, IC_{50}: 2.8 μM
FD, IC_{50}: 0.12 μM

3
FXIa, IC_{50}: 0.40 μM
FD, IC_{50}: 0.80 μM

4 (dia. mix.)
FXIa, IC_{50}: 0.97 μM
PKL, IC_{50}: 1.2 μM

5 (rac.)
FXIa, IC_{50}: 0.20 μM
FD, IC_{50}: 0.34 μM
PKL, IC_{50}: 1.3 μM

Figure 2. Chemical structures of early-stage S1-benzylamine-based FXIa inhibitors.

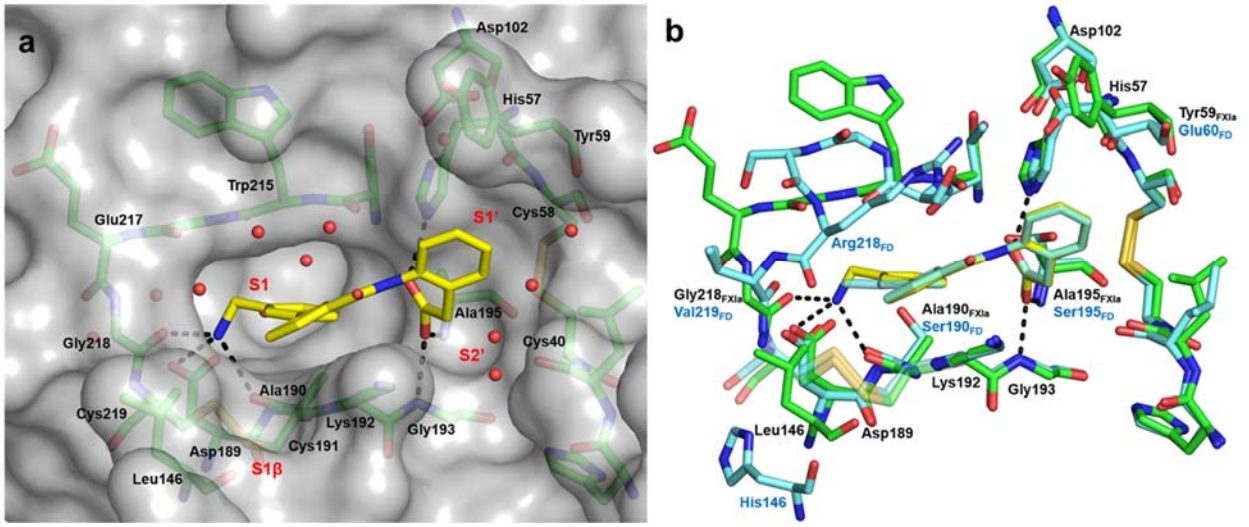

Figure 3. Binding mode of compound **2**: (**a**) Crystal structure of **2** (yellow, PDB code 6TS4) with FXIa $S_{195}A$ mutant (green). The surface of the protein is shown in gray and oxygen atoms of crystallographic water molecules are shown as red spheres. (**b**) Comparison of the crystal structures of compound **2** with FXIa (yellow and green carbons) and FD (pale blue, PDB code 6QMT).[27] Only selected residues in the ligand-binding pocket are shown. FXIa and FD residues are labeled in black and in blue, respectively. H-bonding interactions are shown as black dotted lines.

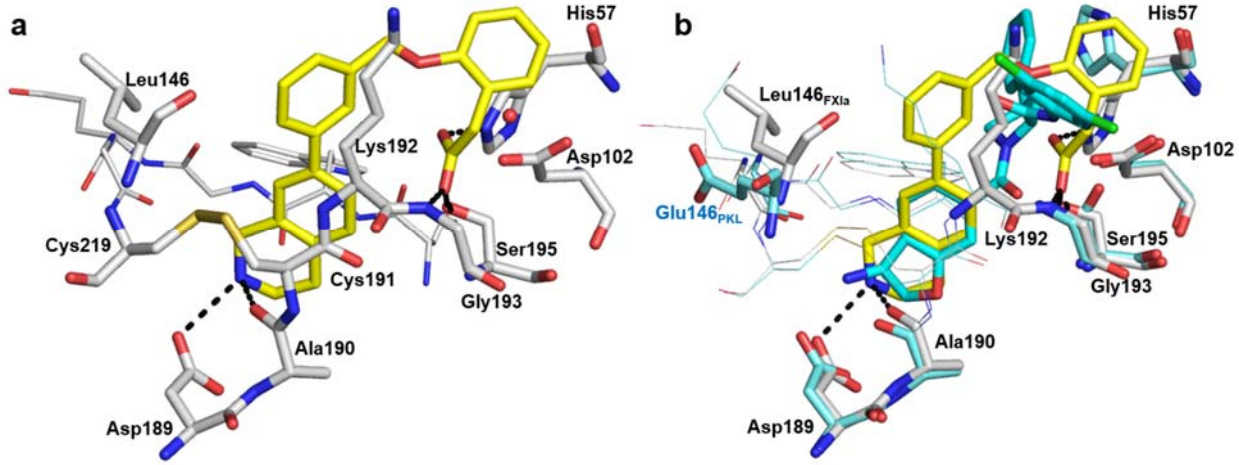

Figure 4. (**a**) Crystal structure of compound **3** (yellow) complexed with FXIa (white, PDB code 6TS7) (**b**) Overlay of the crystal structure of compound **3** (yellow) complexed with FXIa (white) on compound **4** (cyan) complexed with PKL (pale blue, PDB code 6T7P). Only selected residues in the ligand-binding pocket are shown. H-bonding interactions are shown as black dotted lines.

Table 1. *In vitro* FXIa potency (IC_{50}), selectivity data *versus* FD and PKL and *in vitro* profiles.

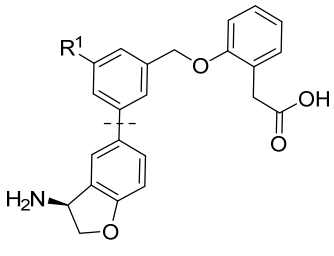

6 (R^1= $CH(CH_3)_2$)
7 (R^1= $C(CH_3)_2CN$)
8 (R^1= $C(CH_3)_2OH$)
9 (R^1= $C(CH_3)_2CONH_2$)

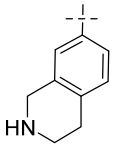

10 (R^1= $C(CH_3)_2OH$)

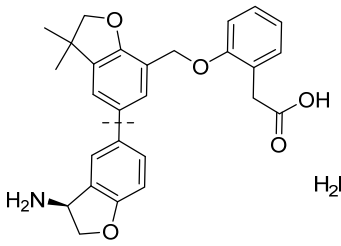

11

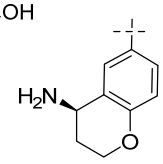

12

Compounds	FXIa IC_{50} [µM][a]	cdFXIa plasma IC_{50} [µM][b]	FD IC_{50} [µM][c]	PKL IC_{50} [µM][d]	Caco-2 P_{app}(AB)/(BA) x10^{-6} (cm/s) (ratio (BA)/(AB))	HT-eq solubility pH 6.8 (mM)[e]
6	0.003	0.12	0.04	0.003	7/ 17 (2.3)	0.008
7	0.004	0.05	0.04	0.002	1.4/ 41 (30)	0.06
8	0.004	0.17	0.32	0.006	BLQ[f]/ 19 (-)	>1
9	0.009	0.067	0.32	0.011	BLQ[f]/ 4 (-)	0.78
10	0.10	0.43	0.23	0.33	ND[g]	ND[g]
11	0.003	0.085	0.05	0.007	12/ 12 (1)	<0.004
12	0.006	0.26	15	0.004	ND[g]	ND[g]

Half-maximal inhibition of [a]purified human FXIa and [b] recombinant catalytic domain of human FXIa as determined in a fluorogenic rhodamine-110 based peptide cleavage assay. [c]Half-maximal inhibition of recombinant human complement FD as determined in a TR-FRET assay. [d]Half-maximal inhibition of PKL as determined in a fluorogenic rhodamine-110-based peptide cleavage assay. Data represent geometric mean values of multiple measurements (n≥2). [e]Equilibrium high throughput solubility in aqueous buffer (pH 6.8). [f]BLQ = below limit of quantitation. [g]ND = not determined.

Table 2. *In vivo* mouse pharmacokinetic profiles for compounds **1**,**Error! Bookmark not defined.** **6**, **7**, **8** and **11**.

Compounds	**1**[a]	**6**[a]	**7**[a]	**8**[a]	**11**[a]
CL (mL·min^{-1}·kg^{-1})	14[b]	1 ± 0	55 ± 4	19 ± 2	4 ± 1
V_{SS} (L/kg)	0.7[b]	0.4 ± 0.1	0.7 ± 0.1	0.4 ± 0.1	1 ± 0.1
$t_{1/2term}$ (h)	1.6[b]	5.5 ± 0.2	0.3 ± 0.0	1.7 ± 0.2	6.4 ± 3.4
AUC p.o. d.n. (nM·h)	3284 ± 138	48927[b]	171 ± 146	186 ± 26	6525 ± 1508
%F	100 ± 17	100[b]	25 ± 21	3 ± 0	61 ± 14
C_{max} d.n. (nM)	2591 ± 36	5263[b]	137 ± 111	99 ± 10	1126 ± 320

[a]Discrete PK profiles, male mice (C57BL/6), dose i.v. 1.0 mg·kg^{-1}, dose p.o. 3.0 mg·kg^{-1}, except for compound **1** dosed po at 10 mg·kg^{-1}; [b]No SD calculated as one animal was excluded from the dosing group due to experimental issues.

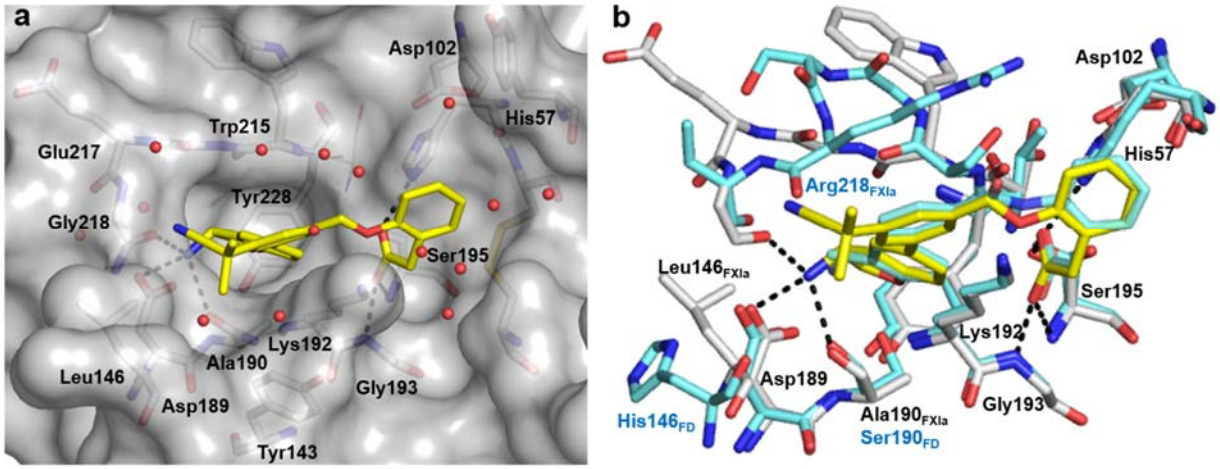

Figure 5. (**a**) Crystal structure of compound **7** (yellow, PDB code 6TS6) in complex with FXIa (white). The surface of the protein is shown in gray and oxygen atoms of crystallographic water molecules are shown as red spheres. (**b**) Comparison of the co-crystal structure of compound **7** (yellow) complexed with FXIa (white) and compound **2** (pale blue) complexed with FD (pale blue, PDB code 6QMT).[27] Only selected residues in the ligand-binding pocket are shown. H-bonding interactions are shown as black dotted lines. FXIa residues are labeled in black and FD residues are labeled in blue.

Table 3. *In vitro* S1 protease selectivity data for selected FXIa inhibitors.

Compounds	**6**	**11**	**12**
FVIIa IC_{50} (μM)[a]	5.10	7.1	75
FIXa IC_{50} (μM)[a]	0.17	0.21	1.6
FXa IC_{50} (μM)[a]	0.50	0.84	4.3
Thrombin IC_{50} (μM)[a]	0.090	0.13	0.86
tPa IC_{50} (μM)[a]	0.090	0.10	0.19
Plasmin IC_{50} (μM)[a]	2.60	6.3	14
Urokinase IC_{50} (μM)[a]	0.047	0.016	0.95

[a]Half-maximal inhibition of selected proteases as determined in biochemical activity assays using quenched fluorescent peptide substrates. Data represent mean values of duplicate measurements.

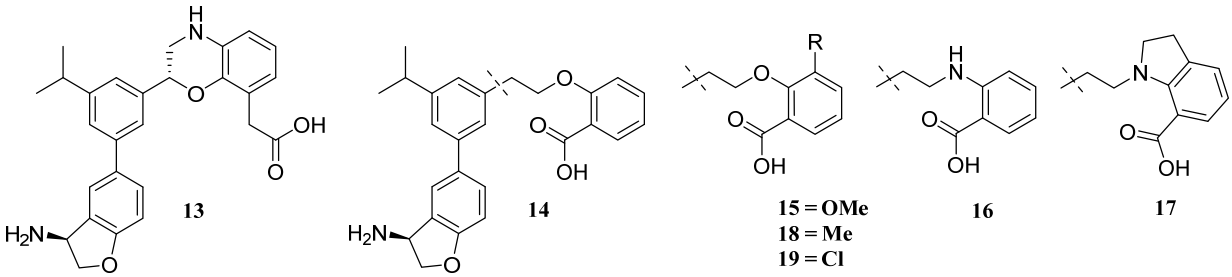

Figure 6. Structure of the fused 3,4-dihydro-2H-benzo[b][1,4]oxazine (**13)** and benzoic acids (**14**-**19**).

Table 4. *In vitro* potency and selectivity data: **IC_{50} (μM)**[a]:

Compound	6	13	14	15	16	17	18	19	20*	21*	22*	23
FXIa	0.003	<0.0007	0.012	0.003	2.52	0.006	0.017	0.015	0.04	0.002	<0.0007	0.0004
cd-FXIa plasma	0.12	0.01	1.19	0.24	ND[b]	0.22	6.62	5.49	8.11	0.17	0.045	0.01
FVIIa	5.10	2.00	3.27	28.3	ND[b]	6.23	45.1	20.5	12.5	8.75	16.7	3.65
FIXa	0.17	0.03	0.04	10.2	ND[b]	3.30	11.3	9.60	15.5	7.86	13.4	1.92
FXa	0.50	0.22	0.24	6.21	ND[b]	1.83	12.5	11.1	16.3	1.71	11.2	1.05
Thrombin	0.090	0.03	0.05	9.09	ND[b]	3.08	9.82	6.22	7.43	6.14	7.21	2.57
PKL	0.003	0.001	0.025	0.009	ND[b]	0.058	0.041	0.021	0.16	0.002	0.016	0.001
tPA	0.090	0.05	0.09	2.20	ND[b]	0.66	4.13	3.67	6.68	0.49	3.70	0.25
Plasmin	2.60	0.69	0.59	30.8	ND[b]	2.56	>100	34.0	46.2	9.58	17.4	1.89
uPA	0.047	0.02	0.02	0.40	ND[b]	0.52	2.48	0.93	1.13	0.25	1.42	0.17
FD	0.04	0.06	1.32	17.5	ND[b]	4.41	>100	34.2	27.2	73.6	8.92	ND[b]

[a]All values are geometric means of ≥2 replicates; [*]Diastereomeric mixture. [b]ND = not determined.

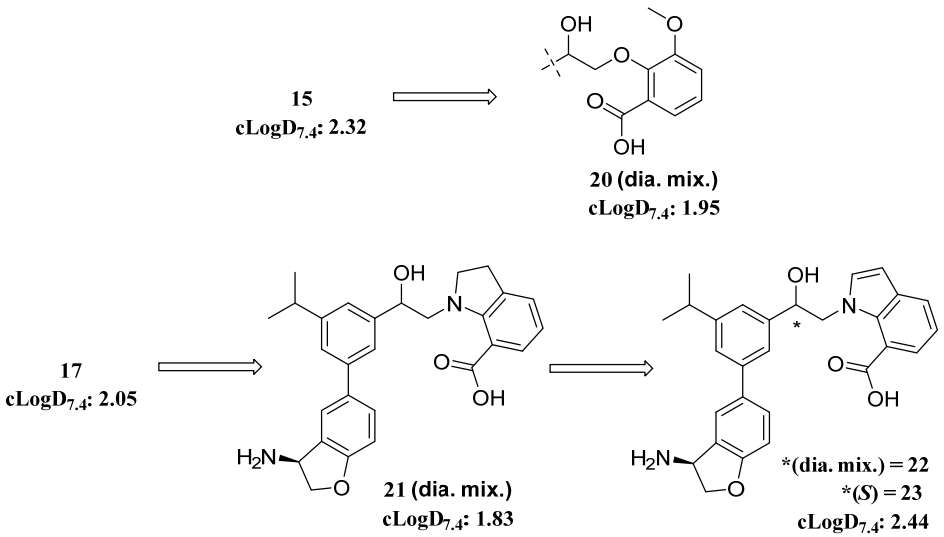

Figure 7. Exploration of addition of a hydroxyl to the linker between the S1β and S1' sites.

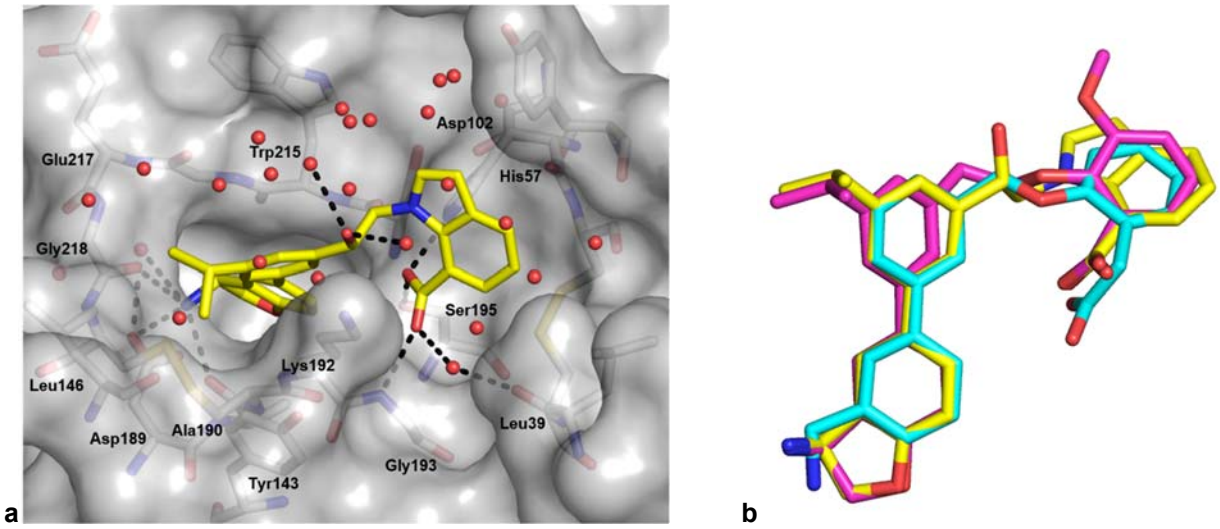

Figure 8. (a) Crystal structure of **23** (yellow) in complex with FXIa (white, PDB code 6USY). The surface of the protein is shown in gray and oxygen atoms of crystallographic water molecules are shown as red spheres. Only selected residues in the ligand-binding pocket are shown. H-bonding interactions are shown as black dotted lines. **(b)** Overlay of compound **1** (cyan) bound to FD, **15** bound to FXIa (magenta, PDB code 6TS5), and **23** (yellow) bound to FXIa.

Table 5. *In vivo* mouse pharmacokinetic profiles of indoline and indole FXIa inhibitors.

	17	**23**	**23**
Dose [i.v. / p.o.] (mg/kg)	0.4 / 3.0	1.0 / 3.0	100 (p.o.)
CL ($mL \cdot min^{-1} \cdot kg^{-1}$)	1	11.01	-
V_{SS} (L/kg)	0.4	0.57	-
$t_{1/2term}$ (h)	9.2	3.73	-
AUC i.v. d.n. (nM·h)	38652	3264 ± 35	-
AUC p.o. d.n. (nM·h)	14041 ± 1090	1297 ± 112	260215 ± 8503
%F	36 ± 3	16	100%
C_{max} d.n. (nM)	1'495 ± 158	494 ± 52	26795 ± 144
T_{max} (h)	0.7 ± 0.3	1	4.0

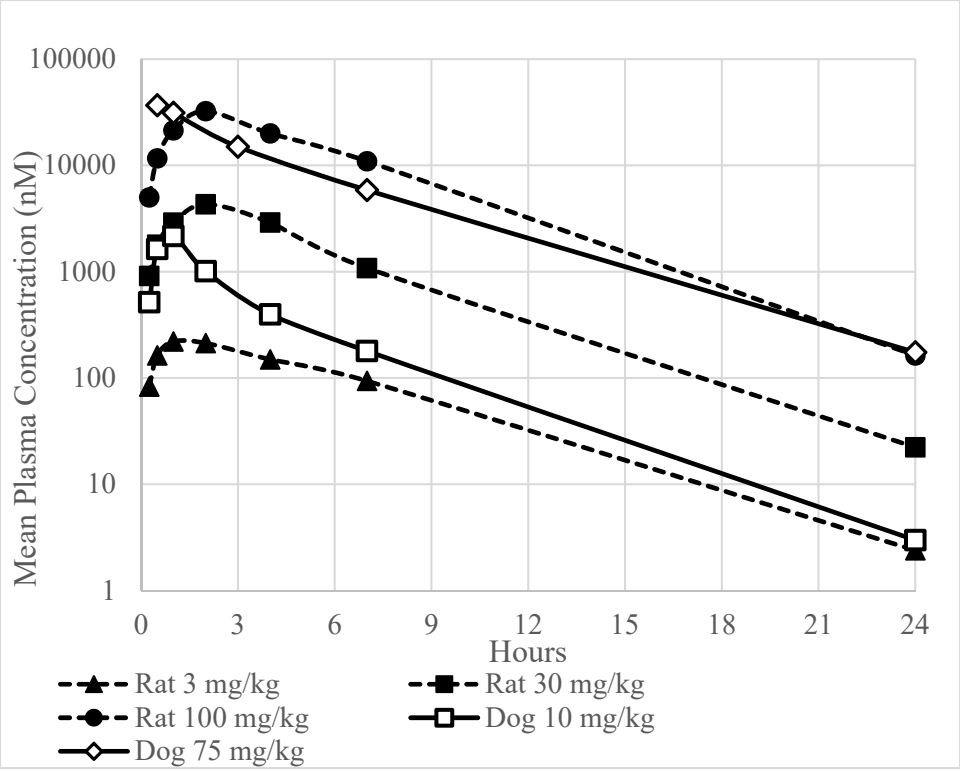

Species	PO Dose (mg/kg)	D.N. Cmax (nM)	D.N. AUC_{0-t} (nM*h)	%F
Rat	3	77 ± 4	382 ± 71	10 ± 2
	30	143 ± 39	621 ± 169	19 ± 5
	100	323 ± 64	1770 ± 439	45 ± 11
Dog	10	217 ± 57	560 ± 254	5 ± 2
	75	504 ± 171	2200 ± 620	21 ± 6
IV parameters (1mg/kg)	Cl (ml/min/kg)	AUC0-t (nM*h)	Vdss (L/kg)	T½ (h)
Rat	9.4 ± 1.0	3330 ± 370	1.3 ± 0.2	6.4 ± 0.1
Dog	4.4 ± 0.4	10660 ± 960	0.3 ± 0.0	2.8 ± 0.1

Figure 9. *In Vivo* Rat and Dog mean plasma pharmacokinetic parameters for **23**. D.N. = dose normalized.

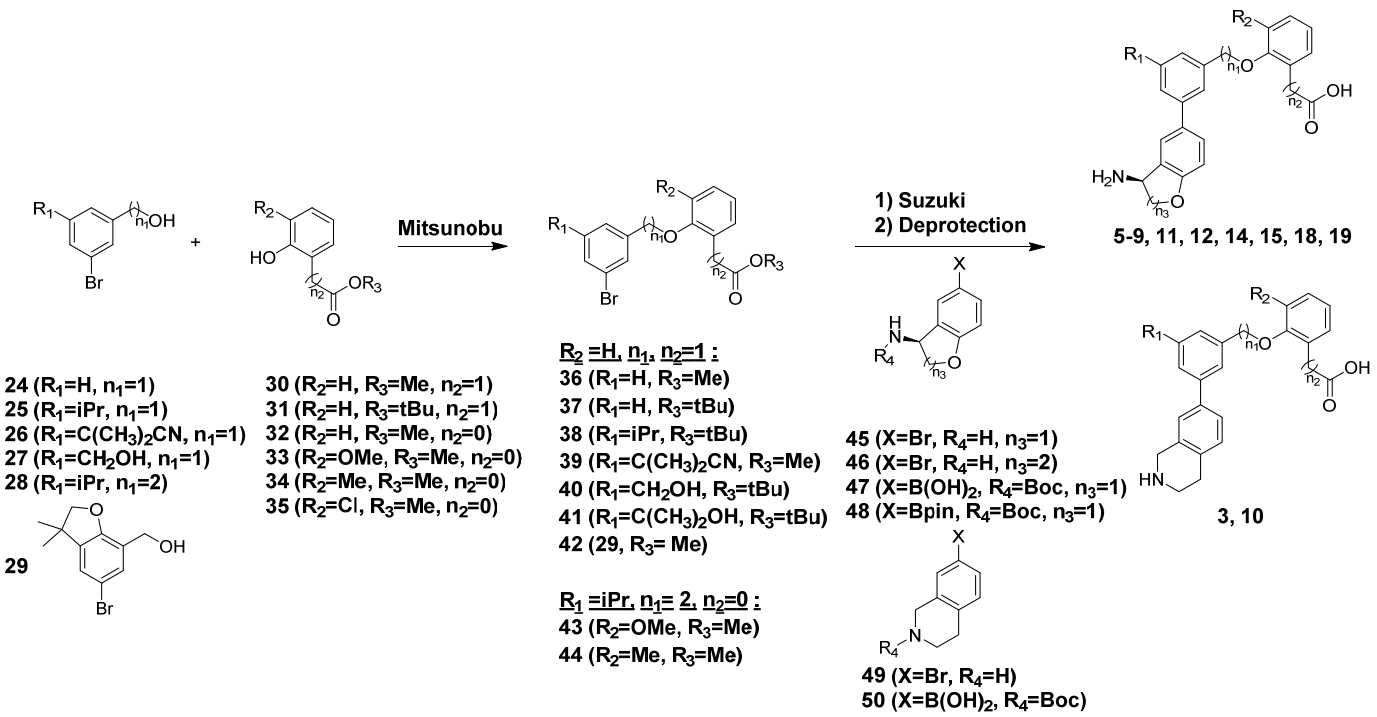

Scheme 1. General synthetic route to aryl acetic acid and benzoic acid FXIa inhibitors.

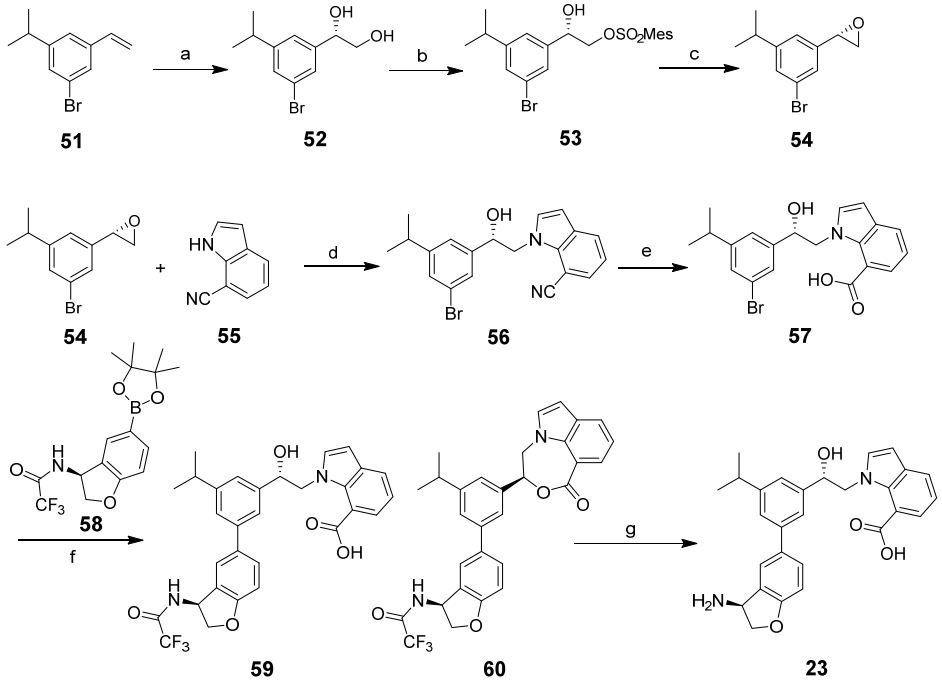

Scheme 2. a) AD-mix-α, tBuOH/H_2O, -10°C-25°C, 38%; b) mesityl-Cl, pyridine, DMAP, CH_2Cl_2, 72%; c) Cs_2CO_3, DMF, 82%; d) K_2CO_3, DMF, 80°C, 86%; e) KOH, EtOH, 0-100°C, 100%; f) $PdCl_2(dppf)\cdot CH_2Cl_2$, 2M Na_2CO_3, 1,4-dioxane, 70°C; g) 3N NaOH, MeOH, 60°C, 32%.